The Conserved MAP Kinase SWIP-13/ERK8 Regulates Dopamine Signaling Through Control of the Presynaptic Dopamine Transporter

By

Daniel Patrick Bermingham

Dissertation

Submitted to the Faculty of the

Graduate School of Vanderbilt University

in partial fulfillment of the requirements

for the degree of

DOCTOR OF PHILOSOPHY

in

Neuroscience

August, 2016

Nashville, Tennessee

Approved:

Roger D. Cone, Ph.D

Roger J. Colbran, Ph.D

David M. Miller, III, Ph.D

Randy D. Blakely, Ph.D

To my parents, who have been an incredible source of

love and support all of my life

ACKNOWLEDGEMENTS

This work would not have been possible without the grant support of the National Institute of Mental Health (NIMH) and the National Institute on Drug Abuse (NIDA), as well as the Vanderbilt Brain Institute Training Grant. I am also grateful to the Neuroscience Graduate Program for an excellent academic program that provided me with critical background in key neuroscience concepts that helped guide my research. I would also like to thank the very supportive staff at Vanderbilt and in the VBI, especially Roz Johnson, Beth Sims, and Mary Michael-Woolman who all helped me successfully navigate the administrative red tape throughout my graduate career.

I would also like to acknowledge the support of my labmates who have helped me along the way. In particular, I would like to thank my fellow Teamatode graduate students Andrew Hardaway and Chelsea Snarrenberg for providing assistance with experiments and for their helpful advice and moral support. I am also grateful to Sarah Sturgeon and Tracy Moore-Jarrett for their technical support, and the rest of Teamatode and the Blakely lab for the various ways that they have helped me throughout the years. My committee has also been incredibly helpful in providing support and guidance, and for this I am eternally grateful. Each and every member of my committee has helped me grow as a scientist, and I would like to thank you all for always being enthusiastic about my work and for pushing me to aim high and to advocate for myself. The advice and guidance of each one of you has been invaluable to me for helping me navigate graduate school and the path ahead. I would particularly like to thank my mentor Randy Blakely, whose eternal enthusiasm for science has made my graduate career a fun and exciting ride.

Lastly, I would like to thank my family, in particular my parents who have been incredibly supportive of me and without whom none of this would have been possible. Your love and guidance have given me the drive to be the best that I can be, and I hope that you know that it is because of you that I was able to accomplish what I have.

Table of Contents

LIST OF FIGURES

ABBREVIATIONS

3MT	3-methoxytyrosine
5-HT	5-hydroxytryptamine (serotonin)
6-OHDA	6-hydroxydopamine
AADC	Aromatic Amino Acid Decarboxylase
ACh	Acetylcholine
AChE	Acetylcholinesterase
ADE	Anterior Deirid
ADHD	Attention Deficit Hyperactivity Disorder
AMPH	Amphetamine
ARS	Area Restricted Search
BDNF	Brain Derived Neurotrophic Factor
BSR	Basal Slowing Response
CaMKII	Ca^{2+}/Calmodulin-Dependent Kinase II
cAMP	Cyclic Adenosine Monophosphate
CEP	Cephalic Neuron
CNS	Central Nervous System
COMT	Catechol O-methyltransferase
DA	Dopamine
DAT	Dopamine Transporter
DMEM	Dulbecco's Modified Eagle Medium
Dyf	Dye-filling (Defect)
EMS	Ethylmethanesulfonate

EPI	Epinephrine
ERK	Extracellular Signal-Related Kinase
ESR	Enhanced Slowing Response
FIF	Formaldehyde-Induced Fluorescence
FRAP	Fluorescence Recovery After Photobleaching
GABA	Gamma-aminobutyric Acid
GAT	GABA Transporter
GDNF	Glial Derived Neurotrophic Factor
GFP	Green Fluorescent Protein
GPCR	G Protein-Coupled Receptor
GST	Glutathione-S-Transferase
HRP	Horseradish Peroxidase
HVA	Homovanillic Acid
ICE	Interleukin-1β-converting Enzyme
KOR	Kappa Opioid Receptor
L-DOPA	L-dihydroxyphenylalanine
MA	Monoamine
MAO	Monoamine Oxidase
MBP	Myelin Basic Protein
MPH	Methylphenidate
NAc	Nucleus Accumbens
NE	Norepinephrine
NET	Norepinephrine Transporter

NGF	Nerve Growth Factor
NIS	Nisoxetine
PBS	Phosphate-Buffered Saline
PCR	Polymerase Chain Reaction
PD	Parkinson's Disease
PDE	Posterior Deirid
PI3K	Phosphoinositide 3-kinase
PKA	Protein Kinase A
PKC	Protein Kinase C
RFP	Red Fluorescent Protein
RTK	Receptor Tyrosine Kinase
RT-PCR	Reverse Transcriptase Polymerase Chain Reaction
SERT	Serotonin Transporter
SNc	Substantia Nigra Pars Compacta
SNP	Single Nucleotide Polymorphism
Swip	Swimming-induced paralysis
SV	Synaptic Vesicle
TBS	Tris-Buffered Saline
TH	Tyrosine Hydroxylase
TK	Tyrosine Kinase
VMAT	Vesicular Monoamine Transporter
VTA	Ventral Tegmental Area

CHAPTER I

DOPAMINERGIC NEUROTRANSMISSION IN THE CENTRAL NERVOUS SYSTEM

INTRODUCTION

The modulation of behavior by the neurotransmitter dopamine (DA) is evolutionarily conserved, evident in animals that range by orders of magnitude in complexity, from humans to the soil-dwelling nematode *Caenorhabditis elegans*. In humans, DA is a critical neuromodulator that regulates circuits supporting reward, attention, and movement, with perturbed DA signaling associated with disorders including addiction, attention-deficit hyperactivity disorder (ADHD), schizophrenia, and Parkinson's disease. Animal models have been critical in developing our understanding of how these central DA circuits operate, and in helping understand these DA-related disease states in order to generate therapeutic interventions to help patients afflicted with these disorders. In this section, I will briefly discuss some of the history behind the study of DA neurotransmission using primarily mammalian animal models, and introduce some current knowledge of how DA signaling is regulated, with an emphasis on the study of the dopamine transporter (DAT).

THE IDENTIFICATION OF DOPAMINE AS A NEUROTRANSMITTER

Though the catecholamine 3-hydroxytyramine or dopamine (DA) was first synthesized in 1910, it wasn't until the 1950's that the first suggestion of its potential role in the brain was proposed. Montagu first indicated that DA might be present in rat

brain (Montagu, 1957), but it was Carlsson and colleagues who later developed a spectrophotofluorometric method that was able to discriminate between the closely related compounds DA, epinephrine (EPI) and norepinephrine (NE) and verified the presence of DA in the brain (Carlsson et al., 1958; Carlsson and Waldeck, 1958). Whether DA acted as a central nervous system (CNS) agonist in its own right, or if DA was simply present in the brain due to its role as an intermediate for NE and EPI synthesis was unclear at the time, however. Importantly, Bertler and Rosengren first observed high levels of DA in the striatum where NE levels were low, suggesting a role independent from being a precursor to NE (Bertler and Rosengren, 1959). One of the first indications of DA's importance in CNS neurotransmission came from the finding that treatment of mice and rabbits with reserpine, an antagonist of the vesicular monoamine transporter (VMAT) later shown to be required for storing DA in synaptic vesicles (SVs), resulted in a depletion of brain DA levels. Additionally, treatment with L-DOPA, a precursor of DA, NE, and EPI, reversed the behavioral effects of reserpine, including rigidity and tremor (Carlsson et al., 1957). Initially, researchers suspected loss of CNS NE and/or EPI was responsible for these effects of reserpine, but they found that L-DOPA had very little effect on brain NE and EPI levels following reserpine, despite a robust reversal of behavioral deficits. CNS DA, on the other hand, was found to be restored by L-DOPA following reserpine treatment, and this DA accumulation coincided with the reversal of the reserpine response.

Though the suggestion of DA acting as a neurotransmitter was met with skepticism, the ensuing years saw numerous findings related to CNS DA that strongly supported this possibility. The finding of low DA levels in the basal ganglia of patients

with Parkinson's disease (PD), and the reversal of PD symptoms with L-DOPA treatment generated great interest in the potential role of DA in the CNS (Birkmayer and Hornykiewicz, 1961). Importantly, new techniques were being developed around this time to visualize catecholamines in order to localize their expression in the brain. Using a formaldehyde-induced fluorescence (FIF)-based approach developed by Carlsson and colleagues, Anden et al. performed the first lesion studies that showed a loss of DA-related fluorescence in the striatum following lesion of the substantia nigra, leading to the first description of a nigrostriatal DA pathway (Anden et al., 1964). Further work revealed other sites of DA presence in the brain, including the mesolimbic and mesocortical DA pathways, and altogether these studies established that DA is present in the presynaptic region of the synapse, further supporting its role as a neurotransmitter.

The first demonstration of activity-dependent DA release from terminals came later from Portig and colleagues, who showed that electrical stimulation of the cat substantia nigra caused an increase in DA collected from the caudate nucleus via superfusion (Portig and Vogt, 1969). This result again suggested the existence of a nigrostriatal pathway of DA-releasing neurons projecting from the substantia nigra to the striatum. Later, electrochemical techniques were developed that would allow for rapid detection of DA (Adams et al., 1972). These methods utilized electrodes held at a potential that causes oxidation of DA to dopamine-o-quinone, which leads to the generation of a current that is proportional to the concentration of DA at the electrode. Using such techniques, multiple studies demonstrated rapid release of DA *in vivo* and *ex vivo* in brain slices in response to electrical stimulation (Adams et al., 1978; Conti et

al., 1978; Gonon et al., 1978). This work helped establish the status of DA as a CNS neurotransmitter, and so began an era of research focusing on understanding the regulation of DA signaling and the role DA plays in the brain to regulate behavior.

DOPAMINE PATHWAYS IN THE MAMMALIAN BRAIN

In the CNS of humans and other mammals, there are two major DAergic nuclei: the substantia nigra pars compacta (SNc) and the ventral tegmental area (VTA), both located in the midbrain (Fig. 1). These nuclei can be identified by the presence of melanin, which is produced naturally by DA neurons in these nuclei, or by *in situ* hybridization and/or immunohistochemical staining for DA-specific genes such as the gene encoding the dopamine transporter (DAT) (Ciliax et al., 1999; Hornykiewicz, 1966). The neurons of the substantia nigra project primarily to the dorsal striatum (subdivided into the caudate nucleus and putamen in humans), and this projection is known as the nigrostriatal pathway (Roeper, 2013). This pathway is critical for control of movement, and degeneration of these neurons is primarily responsible for the motor symptoms observed in Parkinson's disease. Additionally, there are two major projections from the VTA that compose the mesolimbic and mesocortical pathways. The mesolimbic pathway consists of projections to limbic regions of the brain, including primarily the ventral striatum, or nucleus accumbens (NAc), with additional projections to the amygdala, hippocampus, and limbic cortex. This pathway is generally thought of as the "reward pathway", as it is critical for reward-related behaviors and is particularly relevant for the generation of addiction behaviors. The mesocortical pathway projects from the VTA to the prefrontal cortex, and is associated with control of normal cognitive

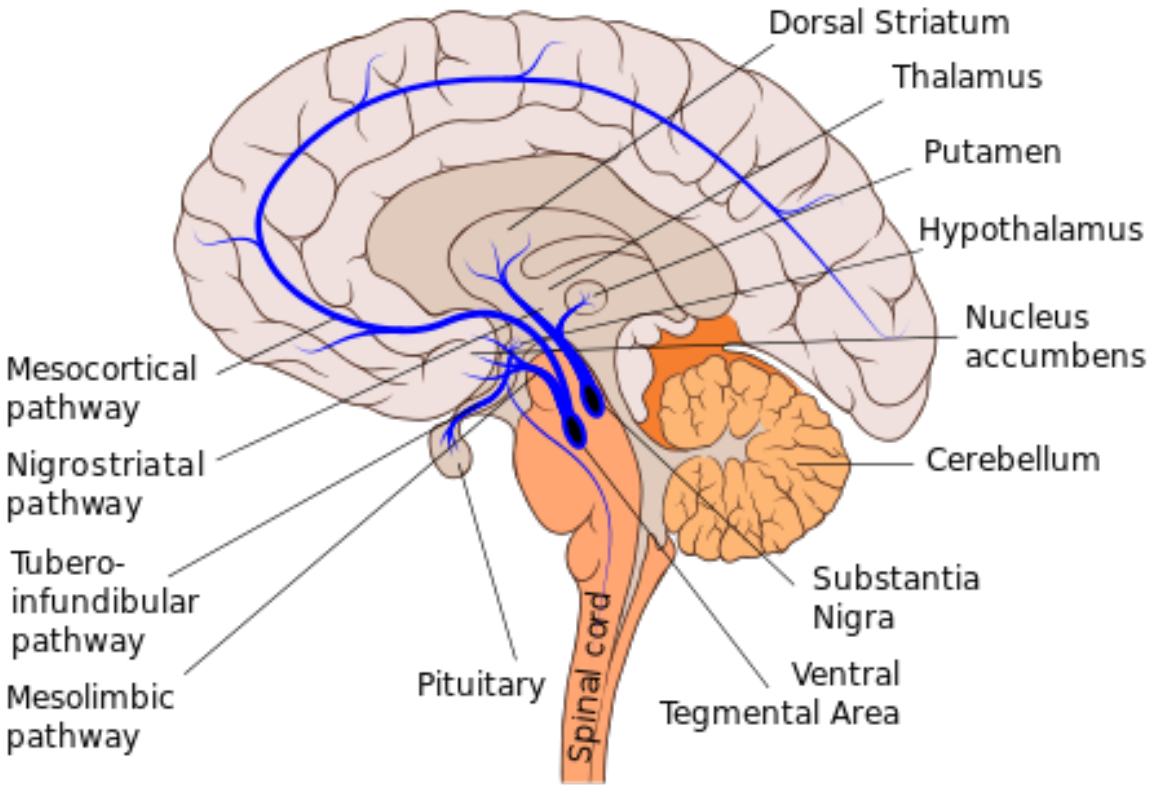

Figure 1 - DA projections in the human brain. The substantia nigra projects to the dorsal striatum in the nigrostriatal pathway. The ventral tegmental area projects to the nucleus accumbens to form the mesolimbic pathway and to the prefrontal cortex to form the mesocortical pathway. Projections from the arcuate nucleaus of the hypothalamus to the pituitary compose the tuberoinfundibular pathway. Image freely available on Wikipedia.

function and motivation. A third, smaller site of DA neurons in the mammalian brain is the arcuate nucleus that projects to the median eminence, composing the tubuloinfundibular pathway (Hu et al., 2004). DA released from these neurons regulates prolactin release from the anterior pituitary gland.

MOLECULAR COMPONENTS OF DOPAMINE SIGNALING

Biosynthesis and Storage

DA is synthesized from the amino acid tyrosine by the actions of tyrosine hydroxylase (TH) (Nagatsu et al., 1964). This enzymatic reaction generates L-dihydroxyphenylalanine (L-DOPA), and is the rate-limiting step in DA biosynthesis. L-DOPA is then converted to DA by the enzyme aromatic amino acid decarboxylase (AADC) (Fig. 2). Importantly, the activity of TH can be regulated by a number of signaling pathways, allowing for control of DA levels at the level of synthesis. DA is packaged into SVs by vesicular monoamine transporters (VMAT). There are two types of VMAT proteins in mammals, VMAT1 and VMAT2, with VMAT1 primarily expressed in peripheral neuroendocrine cells, and VMAT2 expressed in neurons of the CNS and sympathetic nervous system (Peter et al., 1995). These transporters are antiporters that utilize the pH gradient generated by vesicular ATP-dependent proton pumps to exchange one molecule of DA into the SV for each H^+ molecule pumped out. As mentioned earlier, VMATs are the target of reserpine, which blocks loading of DA into SVs, causing eventual depletion of tissue DA levels (Erickson et al., 1992). VMATs also control vesicular serotonin (5-HT) and NE/EPI levels; 5-HT due to its being a direct

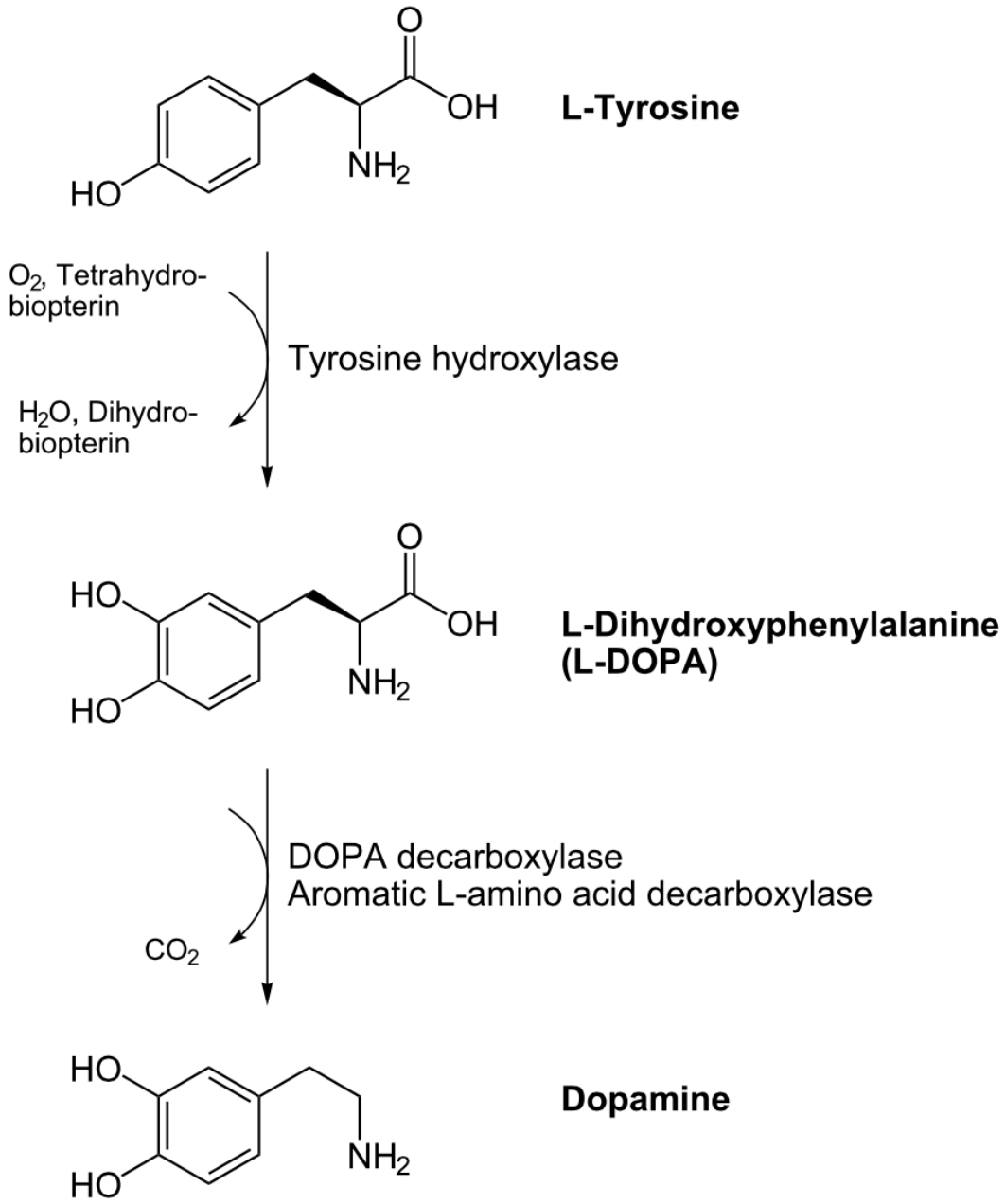

Figure 2 - Biosynthesis of DA. Image freely available on Wikimedia commons.

substrate of VMAT2 in 5-HT neurons, and NE/EPI due to the fact that they are synthesized from DA in SVs (Erickson et al., 1992).

Release

Once DA is loaded into SVs, it can only be released upon fusion of the SVs with the plasma membrane. SV fusion is mediated by the interaction of SNARE proteins, which consist of vesicle-associated v-SNAREs (eg. SNAP-25) and plasma membrane-associated t-SNARE proteins (eg. Syntaxin) (For review, see (Rizo and Xu, 2015). The protein Synaptotagmin prevents the full interaction between these proteins until Ca^{2+} is bound and full fusion is facilitated. This mechanism underlies the triggering of synchronous neurotransmitter release by depolarization-dependent Ca^{2+} influx through voltage-gated Ca^{2+} channels. Importantly, DA SV fusion can be regulated via a number of mechanisms, including through activation of D2 autoreceptors, which can exert multiple modes of regulation of SV release including inhibition of of N- and P/Q-type Ca^{2+} channels on rat midbrain DA neurons, as well as activation of inwardly rectifying K^{+} channels (Cardozo and Bean, 1995; Lacey et al., 1987).

Reuptake

The recapturing of DA from the extracellular space to return it to the DA-releasing neuron is a critical step in the termination of the DA signal. This process is catalyzed by the actions of DAT, which is a member of the SLC6 family of $Na^{+/}Cl^{-}$-dependent transporters (Bannon et al., 1990). Members of this familiy of transporters are proteins that are composed of 12 transmembrane domains, and utilize cotransport of Na^{+} as the driving force for translocation of substrates against their concentration gradients (Chen

et al., 2004). The DAT cDNA was initially isolated from rat brain by Kilty et al., and heterologous expression of this cDNA in HeLa cells resulted in high affinity uptake of exogenously-applied DA, which could be blocked by treatment with the pyschostimulant cocaine (Kilty et al., 1991). Around this same time, other groups also cloned the bovine (Usdin et al., 1991) and human (Shimada et al., 1991) DAT cDNAs and showed similar results, and Caron and colleagues eventually generated a DAT knockout mouse. Studies of these mice demonstrated a loss of striatal DA clearance, as measured by fast-scan cyclic voltammetry, and a dramatic increase in spontaneous locomotor behavior (Giros et al., 1996; Jaber et al., 1997). These experiments and others established DAT as the primary mechanism for DA clearance, and due to its critical role in regulating DA signaling, much effort has been directed towards understanding how this protein is regulated (see subsequent section on DAT Regulation).

Metabolism

DA is metabolized primarily by the actions of two classes of enzymes: the monoamine oxidases MAOA and MAOB and catechol-o-methyltransferase (COMT) (Kopin, 1985). The MAO enzymes are primarily expressed on the outer mitochondrial membrane, and metabolize cytosolic DA via a deamination reaction to form 3,4-dihydroxyphenylacetic acid (DOPAC). COMT metabolizes DA via the transfer of a methyl group to the 3' carbon of DA to form 3-methoxytyramine (3MT). Both DOPAC and 3MT can then be metabolized to homovanillic acid (HVA) via the actions COMT and MAO, respectively.

REGULATION OF DAT

DAT has received much attention from DA researchers due to its apparent importance in multiple DA-associated disease states. Promoter, intronic and exonic polymorphisms in the DAT gene locus have been associated with multiple disorders including bipolar disorder, ADHD, autism, and juvenile dystonia (Hahn and Blakely, 2007) (Kurian et al., 2011). Additionally, the connection of DAT to disease processes is supported by the actions of drugs that block its function, such as the highly addictive pyschostimulant cocaine or the ADHD therapeutic agent methylphenidate, as well as those that induce transport reversal, such as D-amphetamine (AMPH), which is also used to treat ADHD. These observations have inspired researchers investigate how DAT is regulated in the hopes of better understanding these diseases with the belief that this knowledge will help lead to the generation of better therapeutics.

Over the past two decades, researchers have demonstrated multiple levels regulation of DAT and related monoamine (MA) transporters, including modulation by gene transcription (Baudry et al., 2010; Harikrishnan et al., 2010; Sacchetti et al., 2001; Tsao et al., 2008), the control of of protein trafficking to terminals (Bjerggaard et al., 2004; Sucic et al., 2011; Torres et al., 2003), recruitment of transporters to the plasma membrane (Carvelli et al., 2002; Zhu et al., 2004), localization of transporters to and mobility within membrane microdomains (Foster et al., 2008; Navaroli et al., 2011; Sakrikar et al., 2012), and internalization/recycling (Huff et al., 1997; Jayanthi et al., 2004; Loder and Melikian, 2003; Samuvel et al., 2005), along with modulation of substrate recognition and transport capacity (Foster et al., 2008; Steiner et al., 2009; Zhu et al., 2005). These studies have been pursued with the conviction that a better

understanding of transporter regulatory mechanisms may elucidate a broader network of genes and proteins that support risk for DAT-associated brain disorders, as well as novel opportunities to modulate DA clearance without a directly targeting the transporters themselves. In many cases, DAT regulatory processes involve the actions of protein kinases, which may act directly via phosphorylation of transporter cytoplasmic domains, or indirectly by targeting transporter-associated proteins. Potential phosphorylation sites in DAT are shown in Figure 3. Some kinases that appear to regulate DAT function include the serine/threonine kinases Protein Kinase A (PKA), Protein Kinase C (PKC), Extracellular Signal-Related Kinase 1/2 (ERK1/2), Ca^{2+}/Calmodulin-Dependent Kinase II (CaMKII), p38 MAP kinase, and Phosphatidylinositol 3-kinase (PI3K)/Akt, as well as multiple tyrosine kinases. What is known about DAT regulation by these kinases will be discussed in detail in the following sections.

DAT Regulation by PKC

Among the studies of DAT regulation by protein kinases, the most robust and reproducible finding is that of the effects of PKC activation on DAT activity by the phorbol ester β-PMA. Treatment with β-PMA in multiple native and non-native preparations has been found to consistently lead to a significant decrease in DA transport capacity, detected in kinetic studies as a decrease in the maximal velocity of DA transport (V_{max}) (Chang et al., 2001; Copeland et al., 1996; Granas et al., 2003; Huff et al., 1997; Kitayama et al., 1994). These phorbol ester-induced transport capacity changes are paralleled in dose and time by a decrease in steady-state surface DAT

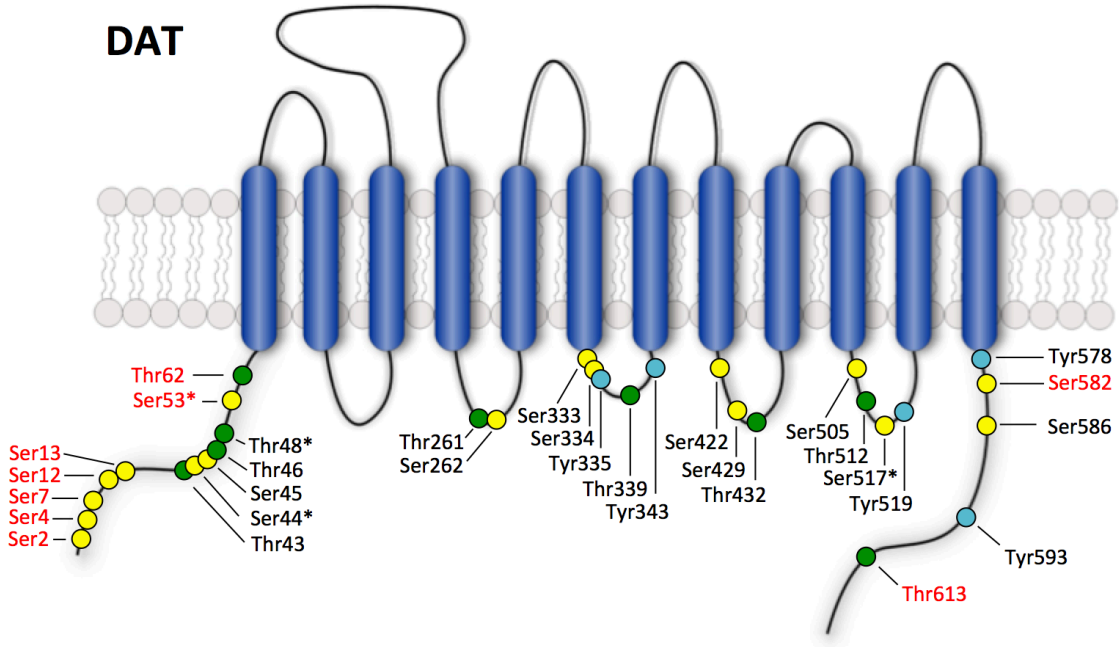

Figure 3: Potential phosphorylation sites in DAT. Model shows intracellular serine (yellow), threonine (green), and tyrosine (cyan) residues in the human DAT protein. Residue names in red are supported by the literature to be phosphorylated based on in vitro kinase assays with purified proteins, mutagenesis studies, phospho-specific antibodies, and/or mass spectrometry analysis. Sites that show species variation between human, mouse, and rat are marked with an asterisk (*).

levels (Boudanova et al., 2008; Daniels and Amara, 1999; Holton et al., 2005; Melikian and Buckley, 1999; Pristupa et al., 1998). Kinetic trafficking studies indicate that these reductions in DAT surface expression derive from increased rates of endocytosis (Loder and Melikian, 2003). Along with producing changes in DA transport and/or DAT internalization, PKC activation also leads to increased transporter phosphorylation. Elevated DAT phosphorylation has been observed in heterologous (Chang et al., 2001; Foster et al., 2012; Gorentla and Vaughan, 2005; Granas et al., 2003; Huff et al., 1997) and native (Cowell et al., 2000; Foster et al., 2012) preparations, though evidence suggests that transporter phosphorylation is not required for changes in DAT trafficking or activity. Thus, truncation of the DAT N-terminus, which results in a significant loss of DAT phosphorylation following phorbol ester treatment, did not affect β-PMA-induced reductions in DAT activity in transfected cells (Granas et al., 2003; Khoshbouei et al., 2004). Additionally, Chang et al. demonstrated that mutation of PKC consensus sites on DAT that prevent β-PMA-induced increases in DAT phosphorylation do not prevent reduction in transport or DAT surface levels, effects similar to those observed by Granas et al. (Chang et al., 2001; Granas et al., 2003).

Due the apparent lack of direct phosphorylation-dependent effects of PKC on DAT, it is possible that PKC exerts its regulatory effects through actions at one or more DAT interacting proteins. Members of the “DAT interactome” include PICK-1 (Torres et al., 2000), PP2Ac (Bauman et al., 2000), a-synuclein (Lee et al., 2001), Hic-5 (Carneiro et al., 2002), syntaxin 1A (Lee et al., 2004), RACK (Lee et al., 2004), CaMKII (Fog et al., 2006), Nedd4-2 (Sorkina et al., 2006), D2 DA receptors (Bolan et al., 2007), Flotillin-1 (Cremona et al., 2011), Rin (Navaroli et al., 2011), and the κ-opioid receptor (Kivell et

al., 2014). A few of these proteins have been implicated in the PKC regulation of DAT, including Flottilin-1, a membrane raft-associated protein linked to PKC-dependent trafficking and AMPH actions (Cremona et al., 2011). Additionally, the E3 ubiquitin ligase Nedd4-2 has also been shown to be necessary for DAT internalization in response to β-PMA, likely through ubiquitination of lysine residues in the DAT N-terminus (Sorkina et al., 2006). The small GTPase Rin also appears to play a critical role in regulating β-PMA-induced DAT trafficking (Navaroli et al., 2011). Interestingly, several DAT-associated proteins have historical associations to PKC pathways (e.g. RACK1, PICK-1) in other systems (Arstikaitis and Gauthier-Campbell, 2006; Battaini et al., 1997), but have yet to be linked to PKC-dependent DAT regulation, and several others (e.g. Hic-5) have been implicated in PKC-dependent regulation of other MA transporters (Carneiro and Blakely, 2004; Carneiro and Blakely, 2006), and thus are likely also to participate in PKC regulation of DAT.

There are many different isoforms of PKC, and phorbol esters like β-PMA do not discriminate between isoforms, so this strategy to activate PKC does not allow for determination of which isoforms are responsible for any observed effects on DAT. Interestingly, studies conducted with the PKCβ specific inhibitor, LY279196, as well as PKCβ knock-out mice, support a role for PKCβ in DAT regulation, though in the direction opposite of that seen with phorbol ester stimulation. Chen et al. observed that treatment of mouse striatal synaptosomes with LY279196 blocked the ability of the D2 agonist quinpirole to increase DAT surface levels and DA uptake, suggesting a role for PKCβ in supporting elevated DAT surface expression. LY279196 also blocked quinpirole-induced increases in p-ERK1/2. In striatal synaptosomes from PKCβ knock-

out mice, reduced basal DA uptake and DAT surface levels were observed, as well as a lack of trafficking sensitivity to quinpirole (Chen et al., 2013). These observations argue that PKCβ may lie upstream of ERK1/2 in a D2 receptor-ERK1/2 signaling cascade (discussed below), ultimately positively supporting DAT surface expression.

Much of the work implicating PKC in DAT regulation has relied on unnatural stimuli such as β-PMA to induce PKC activation. The work discussed above by Chen et al. is important as it places PKCβ downstream of a receptor and known activator or DAT (D2R). Additionally, Page and colleagues have reported that an mGluR agonist decreases DA uptake in rat striatal synaptosomes, an effect that can be blocked by the PKC inhibitor Ro-31-8220 (Page et al., 2001). PKC may also be involved in substance P-induced downregulation of DAT, as substance P treatment of HEK-293 cells co-expressing hDAT and the substance P receptor hNK-1 results in a decrease in DA uptake that is partially blocked by the PKC inhibitor staurosporine and is only slightly additive with PMA (Granas et al., 2003). The NK1 isoform is expressed by human midbrain DA neurons (NK-3 is more abundant in rat) where it may act to support substance P modulation of DA signaling (Whitty et al., 1997). NK-1 is a Gαq-coupled G protein coupled receptor, consistent with coupling to PKC signaling pathways, though these have not been studied in the context of DAT regulation. Interestingly, microdialysis studies using local infusion of an NK-1 antagonist points to a capacity for the receptor to modulate cocaine-induced DA clearance (Loonam et al., 2003). PKC may also regulate reverse transport of DA induced by mGluR signaling in the rat substantia nigra (Opazo et al., 2010), by the σ2-receptor activation in rat striatal synaptosomes (Derbez et al., 2002), and by estradiol activation of membrane estrogen

receptors in NGF-differentiated PC12 (Alyea and Watson, 2009), consistent with a suggested role for PKC in regulating AMPH-induced reversal of DA transport.

DAT Regulation by PKA

Far fewer studies have evaluated the role played by PKA in regulation of DAT than for PKC isoforms, and the results have been rather mixed. With respect to DAT activity, PKA has been suggested to have no effect, stimulatory or inhibitory effects. Initially, Tian and colleagues reported that that, in contrast to GABA uptake in rat stratal synaptosomes, DA uptake is insensitive to adenylyl cyclase or PKA activating agents forskolin or 8-Br-cAMP (Tian et al., 1994). Similar conclusions were reached by Copeland and colleagues (Copeland et al., 1996) and Zhu et al (Zhu et al., 1997) as well as Daniels and Amara using transfected MDCK cells (Daniels and Amara, 1999). Using rotating disk voltammetry to achieve higher time resolution for potential DAT modulation, however, Batchelor and Schenk (Batchelor and Schenk, 1998) reported that DA uptake in rat striatal suspensions can be stimulated by 8-Br-cAMP and forskolin at 1 min but not at 12 min, with effects blocked by a PKA inhibitor and attributed to a V_{MAX} elevation. Adding further complication, studies with DAT-transfected Sf9 and COS-7 cells revealed in these models a simulation of DA transport capacity (V_{MAX}) with PKA inhibition by RP-cAMPS but no effect of PKA stimulatory agents – Sp-CAMPS or 8-Br-cGMP (Pristupa et al., 1998), consistent with tonic, PKA-dependent inhibitory control of DAT in these models. However, Page and colleagues found that activation of PKA by 8-Br-cAMP stimulated DA uptake in rat striatal synaptosomes (Page et al., 2004). This increase in uptake was blocked by inhibitors of both PKA and CaMKII, which may

function downstream of PKA in this regulation (further discussion of CaMKII below). These authors also used very brief treatments of pharmacological agents, suggesting effects may be highly time dependent. Overall though, these issues have yet to be resolved and may in part derive from species differences, tissue and cell preparation variations, and mode of drug application. Recent work from the Amara lab has implicated PKA signaling in the regulation of Rho-mediated DAT internalization, specifically in response to AMPH treatment (Wheeler et al., 2015). In both SK-N-SH cells as well as rat primary DA neurons, db-cAMP and the PKA inhibitor KT5720 blocked and enhanced AMPH-stimulated reduction in DA uptake/DAT surface levels, respectively. Additionally, agonism of the Gαs-coupled D1/D5 and β2 receptors, and thereby activation of PKA, also blocked the effects of AMPH on DAT activity/surface levels. Whether this PKA regulation of DAT plays a role in regulating Rho-mediated internalization of DAT apart from these AMPH effects remains to be seen.

With regards to potential direct phosphorylation of DAT by PKA, Vaughan and colleagues (Vaughan et al., 1997) found no ability of forskolin or 8-BrcAMP to elevate basal DAT phosphorylation in metabolically labeled rat striatal synaptosomes (or to modulate DA uptake), whereas as noted above β-PMA treatments caused a robust elevation in phosphorylation. Similarly, the PKA inhibitor H89 had no impact of DA uptake or on basal phosphorylation of rat DAT in metabolically labeled LLC-PK1 cells (Cervinski et al., 2005). Although these studies support a general lack of regulation of DAT by PKA-linked pathways, Vaughan's group reported the ability of the purified DAT N-terminus to be phosphorylated by PKA *in vitro* (Gorentla et al., 2009). Whether this *in*

vitro result is relevant for any actions of PKA on DAT in an *in vivo* context remains unclear, however.

DAT Regulation by PI3K/Akt

With respect to pathways that appear to sustain normal DAT activity, signaling through PI3K/Akt is one of the best characterized, including studies in both transfected cells and native preparations, using both inhibitors and activators. For instance, Carvelli and colleagues observed that acute application of the PI3K inhibitor LY294002 led to a decreased DA uptake V_{MAX} in rat striatal synaptosomes and in human DAT transfected HEK-293 cells, effects accompanied by a reduction in DAT cell surface expression (Carvelli et al., 2002). Conversely, overexpression of a constitutively active PI3K in HEK-293 cells increased both DA uptake and DAT surface levels. In their studies of kinase inhibitors and activators, Lin and colleagues also observed inhibitory actions of LY294002 on rat DAT activity and surface expression in transfected cells, findings accompanied by a reduction in DAT phosphorylation. This decrease was absent in T62A, S581A, and T612A mutants however, suggesting that one or more of these sites may be the target of a kinase downstream of PI3K signaling. Importantly, these mutations also blocked the effect of LY294002 on reducing the V_{max} of DA uptake, suggesting that phosphorylation of one or more of these residues may be required for the effects of PI3K signaling on DAT activity, though indirect structural explanations cannot as yet be ruled out.

Activation of PI3K and production of PIP3 leads to recruitment and activation of Akt, and studies in multiple preparations support a role for Akt in PI3K-dependent

support of basal DAT surface expression and activity. Garcia and colleagues observed that both a pharmacological inhibitor of Akt (ML9) and transfection of a dominant-negative Akt (K179R) reduced DAT surface expression and DA uptake in DAT transfected HEK-293 cells (Garcia et al., 2005). *In vivo*, viral overexpression of the Akt activator IRS2 in the substantia nigra of rats that had been maintained on high-fat diets alleviated some DAT-related deficits seen in these rats (Speed et al., 2011). These included restoration of reduced striatal DAT surface levels and DA uptake. Importantly, this treatment also rescued reduced pAkt levels seen in these rats. Gorentla et al. demonstrated that Akt1 was unable to phosphorylate the DAT N-terminus *in vitro* (Gorentla et al., 2009), suggesting that either another kinase may act downstream of Akt, or the N-terminus is not the target for Akt phosphorylation of DAT. Another possible explanation is that Akt2, rather than Akt1, may function downstream of PI3K to exert its effects on DAT activity and phosphorylation. This is supported by the findings of Speed et al. that showed that inhibition of Akt2, and not Akt1, reduced DAT surface levels in rat striatal tissue (Speed et al., 2010). AMPH-induced reductions in cell surface expression also appear to be mediated via the Akt pathway. Thus, Wei and colleagues found that AMPH produced a time-dependent reduction in activated Akt, with evidence suggesting that AMPH-induced an increase in CamKII activity that led to reduced Akt activity, resulting in reduced DAT surface expression that could be offset with the CamKII inhibitor KN93 (Wei et al., 2007).

DAT Regulation by CaMKII

At present, limited evidence supports a role for CaMKII in regulating DA uptake by DAT. Inhibition of CaMKII has been shown to block the stimulatory effects of extracellular Ca^{2+} on DAT as well as those of a membrane permeant cAMP analog, but Lin and colleagues found that CaMKII inhibition had no effect on DA uptake in transfected COS cells, suggesting that the kinase plays no essential role in sustaining basal DA uptake (Lin et al., 2003). Consistent with this, in studies where CaMKIIα KO and KI mice have been used to assess contributions of CaMKIIα expression/activity to AMPH evoked DA release (see below), no alterations in basal DA uptake, expression or surface trafficking were evident (Steinkellner et al., 2012), though the opportunity for compensations in the context of life-long kinase manipulations must be taken into account.

Whereas little support for CaMKII regulation of DA uptake exists, substantial evidence supports a role for the kinase in DAT dependent DA efflux triggered by AMPH or DAT mutations. Multiple studies have found that CaMKII inhibition can attenuate AMPH-evoked DA release (Fog et al., 2006; Steinkellner et al., 2012; Weatherspoon and Werling, 1999). Fog and colleagues also found that intracellular perfusion of activated CaMKIIα enhances AMPH-induced DA efflux (Fog et al., 2006). Most recently, Steinkellner and colleagues have reported a reduction in AMPH-evoked DA release *in vivo* via microdialysis in CaMKIIa KO mice as well as a blunting of AMPH induced locomotor activation (Steinkellner et al., 2014). Consistent with these findings, transgenic expression of a CaMKII inhibitory peptide blocks the locomotor stimulating actions of AMPH in Drosophila melanogaster (Pizzo et al., 2014).

Currently it remains unclear as to whether the effects CaMKII exerts on DAT may be in part due to direct phosphorylation of the transporter. Fog and colleagues (Fog et al., 2006) demonstrated that N-terminal human DAT peptides can be efficiently phosphorylated by CaMKIIα. Consistent with these findings, Gorentla et al. demonstrated that that the purified rat DAT N-terminus acquires Ser phosphorylation upon incubation with CaMKII (Gorentla et al., 2009). Importantly, Fog et al. have shown that CaMKII can directly interact with DAT, and the site of interaction between kinase and transporter was mapped to the distal C-terminus including residues 612-617. Additionally, peptides containing the last 24 amino acids of DAT (including this interaction site) have been shown to block DAT/CaMKIIα interactions and AMPH-evoked DA efflux both *in vitro* and *in vivo*, and cause a significant blunting of AMPH-induced hyperlocomotion in mice. Together, these studies make a compelling case that CaMKIIα both associates with DAT and can regulate the functional states of the transporter, as manipulated by AMPH.

The functional relevance of DAT/CaMKII interactions is highlighted by studies involving two ADHD-associated DAT variants. The DAT Val559 variant displays an anomalous DAT-dependent DA efflux that can be reversed by CaMKII inhibition (Bowton et al., 2010; Mazei-Robison et al., 2008), mimicking the state of DAT in the presence of AMPH. Importantly, this variant also shows elevated levels of CaMKII interaction. Recently, Mergy and colleagues have provided *in vivo* evidence via microdialysis studies of knock-in mice that the DAT Val559 variant supports a tonic elevation in basal extracellular DA (Mergy et al., 2014), consistent with chronic DAT-mediated DA efflux, though whether CaMKII sustains DAT Val559 efflux activity *in vivo*

has yet to be addressed. The ADHD-associated human DAT variant Cys615 also appears to have abnormal regulation by CaMKII. This variant was reported by Sakrikar and colleagues to have elevated rates of trafficking to and from the plasma membrane, and also displayed a functional inhibition by the CaMKII inhibitor KN-93 that is absent in wild-type DAT (Sakrikar et al., 2012). Though this inhibition was dictated by a reduction in DAT $V_{MAX,}$ biotinylation studies revealed that it was not a result of a change in surface DAT density, but rather indicated a change in DAT conformation leading to functional inactivation. Additionally, whereas wild-type DAT displays a CaMKII-dependent AMPH-stimulated redistribution from the cell surface, the Cys615 variant did not have this trafficking effect. Importantly, like the Val559 variant, Cys615 DAT displayed elevated levels of CaMKII interaction, which may contribute to the enhanced trafficking of this variant that cannot be further stimulated by AMPH treatment. Together, these findings reveal a role for CaMKII activation in surface DAT trafficking, as well as conformations impacting intrinsic DAT functional activity that may have disease relevance as evidenced by these studies of ADHD-associated DAT variants.

DAT Regulation by ERK1/2

Much of the work concerning ERK1/2 regulation of DAT relies on preventing activation of these kinases through inhibition of the upstream activators MEK1/2. Thus, Rothman and colleagues first noted the ability of the MEK1/2 inhibitor PD98059 to reduce DAT surface levels, as assessed by radioligand binding ([125I]RTI-55) in rat striatal synaptosomes (Rothman et al., 2002). Consistent with these findings, multiple studies have demonstrated that MEK1/2 inhibition reduces DA uptake in both *ex vivo*

and *in vitro* preparations, effects attributed to a reduction in DA uptake V_{MAX} (Lin et al., 2003; Moron et al., 2003). Both Moron et al. and Lin et al. provided evidence that DA uptake reductions following MEK1/2 inhibition derive from a clathrin-dependent reduction in DAT cell surface expression (Moron et al., 2003). These results suggest that ERK1/2 activation downstream of MEK1/2 acts to stabilize DAT at the surface and antagonize internalization signals that trigger clathrin-mediated endocytosis of DAT. Providing evidence that ERK1/2 regulation could be bidirectional, Moron et al observed that transfection of a constitutively-active MEK into human DAT-expressing HEK cells increased DA uptake V_{MAX} (Moron et al., 2003). Finally, Owens and coworkers observed that *in vivo* administration of the ERK1/2 inhibitor SL327 to rat striatum reduced the rate of exogenous DA clearance as measured by high-speed chronoamperometry (Owens et al., 2012). Together, these results reveal MEK1/2 signaling, likely through ERK1/2, acts to sustain or elevate DAT surface expression and DA clearance capacity.

The target of ERK1/2 in regulating DAT is unknown at this point, though evidence has been provided to indicate that DAT phosphorylation may contribute. Lin and colleagues, using rat DAT transfected LLC-PK1 cells, observed a reduction in transporter phosphorylation following treatment of cells with the MEK1/2 inhibitor U0126, suggesting that one or more phosphorylation sites on DAT may contribute positively to ERK1/2-dependent surface DAT trafficking (Lin et al., 2003). In an exploration of potential phosphorylation sites that could support changes in DA uptake produced by U0216 treatments, Ala substitutions yielded complex effects, with mutations noted that either augmented, inverted or reversed uptake changes brought

about by MEK inhibition. Although not all mutations were evaluated, substitutions at Ser12, Ser 13, Ser62, Ser581, Thr591 and Thr612 were found to both block the reduction in basal phosphorylation arising from U0126 treatments as well as to diminish the inhibition seen on DA uptake. Gorentla and colleagues, using purified N- and C termini from rat DAT, observed significant phosphorylation of the N-terminus with both ERK1 and 2 *in vitro* (Gorentla et al., 2009), with phosphoamino acid analysis indicating phosphorylation by ERK1 on Thr residues. Studies with mutant N-termini revealed Thr53 as essential for phosphorylation by ERK1, consistent with the location of the residue in a motif for proline-directed protein kinases (PPQTP) that is conserved in human DAT. Importantly, further studies in this and a later report (Foster et al., 2012) provided evidence for the use of Thr53 as a phosphoacceptor site in rat striatum, leading to the development of a P-Thr53 specific antibody that reveals labeling following ERK1 incubations. Interestingly, PMA treatment of rDAT-LLCPK1 cells increased Thr53 phosphorylation, despite the fact that PKC was unable to phosphorylate this residue *in vitro*. This is consistent with the observation described earlier that PKCβ likely activates ERK1/2, and this may be the route through which PMA increases Thr53 phosphorylation. Additionally, mutation of this residue to alanine or aspartate resulted in a significant decrease in surface DAT and DA uptake in rDAT-LLCPK1 cells. Total DAT levels were also reduced to a similar extent as surface DAT, suggesting that this residue is necessary for stabilizing DAT protein levels.

The biological relevance of ERK1/2 regulation of DAT is supported by findings that ERK1/2 signaling appears to be necessary for upregulation of DAT by D2/D3 receptors. Stimulation of DAT activity by activation of these receptors has been

demonstrated both *in vivo* and *in vitro*, and the dependence on ERK1/2 signaling was demonstrated by co-expressing either D2 or D3 with hDAT in EM4 cells, and treating with the D2/3 agonists quinpirole or PD128907 (Bolan et al., 2007; Zapata et al., 2007). These treatments increased uptake of the fluorescent DAT substrate ASP+ (which does not activate DA receptors), and this increase was blocked by PD90859, a MEK1/2 inhibitor. Importantly, inhibition of PI3K by LY294002 also blocked the increase in cells expressing the D3 receptor, suggesting perhaps some crosstalk between these signaling pathways occurs when D3 is activated. Indeed, studies have suggested that activation of ERK1/2 signaling by D3 activation depends on PI3K activation due to its utilization of the βγ pathway of Gi to signal through RTKs such as EGFR, as opposed to D2 receptor signaling which seems to act primarily through the alpha subunit of the Gi protein to activate ERK1/2 signaling (Beom et al., 2004). More recently, Kivell and colleages reported that DAT could be positively regulated by another GPCR, the kappa opiate receptor (KOR), in both cells and rat striatal synaptosomes in a similar ERK1/2-dependent manner (Kivell et al., 2014). Altogether, these studies provide significant evidence that the ERK1/2 pathway regulates DAT in native preparations downstream of GPCR activation, though the mechanism by which ERK1/2 acts to control DAT trafficking following receptor activation is ill-defined.

DAT Regulation by p38 MAPK

Whereas significant evidence implicates ERK1/2 in DAT regulation, little evidence supports a role for p38 MAPK linked pathways. Gorentla and colleagues did find that a rat DAT N-terminal peptide containing Thr53 can be phosphorylated *in vitro*

by purified p38a MAPK (Gorentla et al., 2009), however no evidence exists that this site is targeted by p38 MAPK *in vivo*. Indeed, p38 MAPK inhibition is without effect on KOR-mediated regulation of DAT, which as noted above is likely mediated by an ERK1/2 pathway. Zhu et al found that the p38 MAPK activator anisomycin reduced DA uptake by human DAT in transfected CHO cells, effects suppressed by the p38 MAPK inhibitor SB203580 (Zhu et al., 2005). Interestingly, this effect is in the opposite direction seen for the norepinephrine transporter (NET) or serotonin transporter (SERT) in the same cell host where uptake stimulation is seen (see below). Lin et al found that the p38 MAPK inhibitor SB202190 failed to alter basal DA uptake of rat DAT transfected COS cells (Lin et al., 2003). However, several N-terminal Ala substitutions (Val14, Ser2, Ser4, Ser12, Ser13, Ser21, Ser45), exposed a capacity for SB202190 induced uptake stimulation, driven by an elevation in transport V_{MAX}, suggesting that a DAT-inhibitory p38 MAPK regulatory pathway may be engaged by changes in DAT structure induced by other signals. Interestingly, these substitutions enhanced uptake inhibition by PI3K inhibition. These findings are reminiscent of studies by Prasad et al who found that SERT coding variation can impart opposite effects on p38 MAPK and PKC-dependent 5-HT uptake modulation, suggesting a dynamic interplay between transporter regulatory pathways (Prasad et al., 2005). Such an idea gains additional support from studies of Quick and colleagues on GAT1 GABA transporters where tyrosine kinase modulation of GAT1 is influenced by the state of PKC activation (Quick et al., 2004). Together, these findings warrant further investigation of a role for p38 MAPK in a more physiological context and in relation to other regulatory signals.

DAT Regulation by Tyrosine Kinases

Simon and colleagues first reported pharmacological evidence of a role for tyrosine kinase (TK) signaling with respect to DAT regulation, with findings of reduced DA uptake in mouse striatal homogenates achieved through a reduction in DA transport V_{MAX} (Simon et al., 1997). Similar, though less potent effects were observed with the TK inhibitor Tyrphostin 23. Consistent with these studies, Doolen and Zahniser, studying DAT-expressing *Xenopus laevis* oocytes, observed that genistein, lavendustin A, and tyrphostin 25 reduced both DA uptake, substrate (tyramine)-induced currents, and DAT leak currents that were paralleled by reduced surface hDAT as measured by [^{3}H]WIN35,428 binding (Doolen and Zahniser, 2001). Interestingly, the Src inhibitor PP2 did not replicate these findings, suggesting a role for other, as yet undefined TK-linked pathways. Zahniser's group replicated these findings in rat striatal synaptosomes and primary mesencephalic cultures, again demonstrating a loss of DA uptake and DAT surface density (Hoover et al., 2007). The identities of TKs that mediate these effects are unknown, but one candidate is the Cdc42-activated tyrosine kinase Ack1. Ack1, downstream of Cdc42, has been shown to negatively regulate DAT endocytosis, as inhibition of either Ack1 or Cdc42 resulted in increased clathrin-dependent DAT internalization and reduced surface DAT (Wu et al., 2015b). Importantly, these effects were non-additive with reductions seen with PMA, suggesting that Cdc42/Ack1 normally act to oppose PKC-stimulated DAT internalization.

Though the studies mentioned above involve the use of TK inhibitors to study DAT regulation, multiple observations provide compelling evidence that receptor tyrosine kinase (RTK) activation by endogenous ligands can impact DAT activity. In the

studies of Hoover and colleagues from Zahniser's group where genistein was found to rapidly reduction DAT V_{MAX} and surface expression in rat brain synaptosomes, these authors also reported that DAT activity could be rapidly (30 min) stimulated in primary cultures by BDNF in a TrkB, MAPK and PI3K-dependent manner (Hoover et al., 2007). Kinetic studies indicated enhancement of DA transport V_{MAX} accompanied by an elevation in DA K_M. These studies were conducted with serum-starved preparations and thus the stimulation may reflect restoration of basal activity/trafficking. Other RTKs have also been shown to play a role in regulating DAT, including Ret, a receptor tyrosine kinase that is activated by GDNF, and that has been show to be essential for DA neuron development and survival. Li and colleagues demonstrated that Ret transfection into rat embryonic mesencephalic cultures induced transcription of DAT as measured by RT-PCR (Li et al., 2006a). Also, mice expressing a constitutively-active form of Ret, MEN2B, have elevated levels of DAT and display increased rates of DA uptake as measured by *in vivo* voltammetry (Mijatovic et al., 2008). Interestingly, overexpression of Src, a known downstream effector of Ret signaling, in human placental trophoblast cells increased DA uptake through transiently transfected human DAT (Annamalai et al., 2011), potentially identifying a downstream tyrosine kinase effector for mediating the effects described above. The heterologous nature of DAT expression here indicates that Src effects are not linked to changes in DAT transcription from its endogenous promoter, reminding us of the post-transcriptional mechanisms engaged by Src to modulate SERT in the same study. Recently, Zhu and coworkers identified a GDNF/Ret signaling pathway that influences DAT trafficking in the nucleus accumbens, mediated by the Rho family guanine exchange factor Vav2 (Zhu et al., 2015). GDNF

stimulation of heterologously expressed DAT/Ret (N2A cells) resulted in reduced transporter surface expression, with no change in total DAT levels, and decreased DA uptake. The actions of GDNF to regulate DAT were blocked by treatment of cells with Vav2 shRNA. Using a split ubiquitin system to monitor protein-protein interactions in yeast, evidence was also gained for a physical interaction between Ret and DAT, results confirmed by co-immunoprecipitation methods using striatal and nucleus accumbens extracts. Additionally, activation of Ret lead to enhanced recovery of DAT/Vav2 complexes. Finally, the authors demonstrate that Vav2 KO mice have deficits in cocaine effects on DAT trafficking, DA uptake and locomotor sensitization. Together, these studies provide strong evidence for a functional and structural interactions between DAT and components of the GNDF signaling pathway.

With respect to potential tyrosine phosphorylation of DAT by these TK signaling pathways, Simon and colleagues failed to detect a phosphoprotein of the size of DAT, as probed by phosphotyrosine immunoblotting methods, following genistein treatment of mouse striatal homogenates, though immunoprecipitation to enrich for DAT was not pursued (Simon et al., 1997). Foster and colleagues also found no reduction in DAT basal phosphorylation when metabolically labeled striatal slices were treated with purified Tyr phosphatase in contrast to efficient dephosphorylation evident with the Ser phosphatase PP1 (Foster et al., 2003). Clearly further study is required, however, to determine whether there exists a context in which DAT may be directly phosphorylated by TKs to regulate its activity.

CHAPTER II

DOPAMINE SIGNALING IN *CAENORHABDITIS ELEGANS*

INTRODUCTION

In the previous section, I discussed a body of literature on the study of DA signaling and DAT regulation that was in large part performed in mammalian model systems such as mice and rats. These models are attractive to researchers due to the relatively high level of similarity between mammalian nervous systems, including humans. Unfortunately, scientists are sometimes restricted in the types of questions they can ask in these models due to limitations such as relatively difficult genetic manipulation and an overwhelming complexity of the nervous systems in these animals, as well as long generation times that make some experiments unfeasible. To circumvent these obstacles, many neuroscience researchers turn to model organisms such as *C. elegans* due to their simpler nervous system, ease of genetic manipulation, and shorter generation time. In this section, I will discuss the use of *C. elegans* to study DA signaling and make the case for using this model to ask questions that might be too difficult to ask in more complex organisms, yet retaining the potential to inform future avenues of investigation in higher order species.

C. ELEGANS DOPAMINE NEUROANATOMY

The nervous system of *C. elegans* is relatively simple, consisting of 302 neurons in the hermaphrodite, and 381 neurons in the male. Serial EM reconstruction has led to

a complete wiring diagram of the *C. elegans* nervous system (Hall and Russell, 1991; Ward et al., 1975; White et al., 1986), something not approachable with the more complex nervous system of a mouse or human. The *C. elegans* nervous system uses many of the same neurotransmitters as the human brain, including glutamate, GABA, acetylcholine (ACh), serotonin (5-HT), and, importantly for this review, DA (Horvitz et al., 1982; Koushika and Nonet, 2000; McDonald et al., 2006a; Rand et al., 1998; Sulston et al., 1975). Sulston et al. first reported the existence of *C. elegans* DA neurons using a similar FIF technique to that employed by Carlsson et al. to identify DA neurons in the mammalian brain (Sulston et al., 1975). In the hermaphrodite worm, Sulsten observed 8 DA neurons; 4 cephalic neurons, dubbed CEP neurons, 2 anterior deirid neurons, or ADE neurons, and two posterior deirid neurons, known as PDE neurons (Fig. 4). The CEP neurons are located just posterior to the anterior pharyngeal bulb, and each sends axonal projections to the nerve ring, as well as a single dendritic process anteriorly to the nose of the worm. These dendrite-like processes terminate in a ciliated ending that is ensheathed by glial cells known as CEP sheath (CEPsh) and CEP socket (CEPso) cells (Ward et al., 1975). The ADE neurons lie posteriorly to the pharyngeal bulb and send axonal processes anteriorly to a small ganglion just posteriorly to the nerve ring. These neurons also have dendritic like processes that terminate in sensillar cilia that are again enwrapped by sheath and socket cells. The bilaterally symmetrical PDE neurons are located in the body of the animal, and send out long axonal processes that initially travel ventrally and then extend both anteriorly and

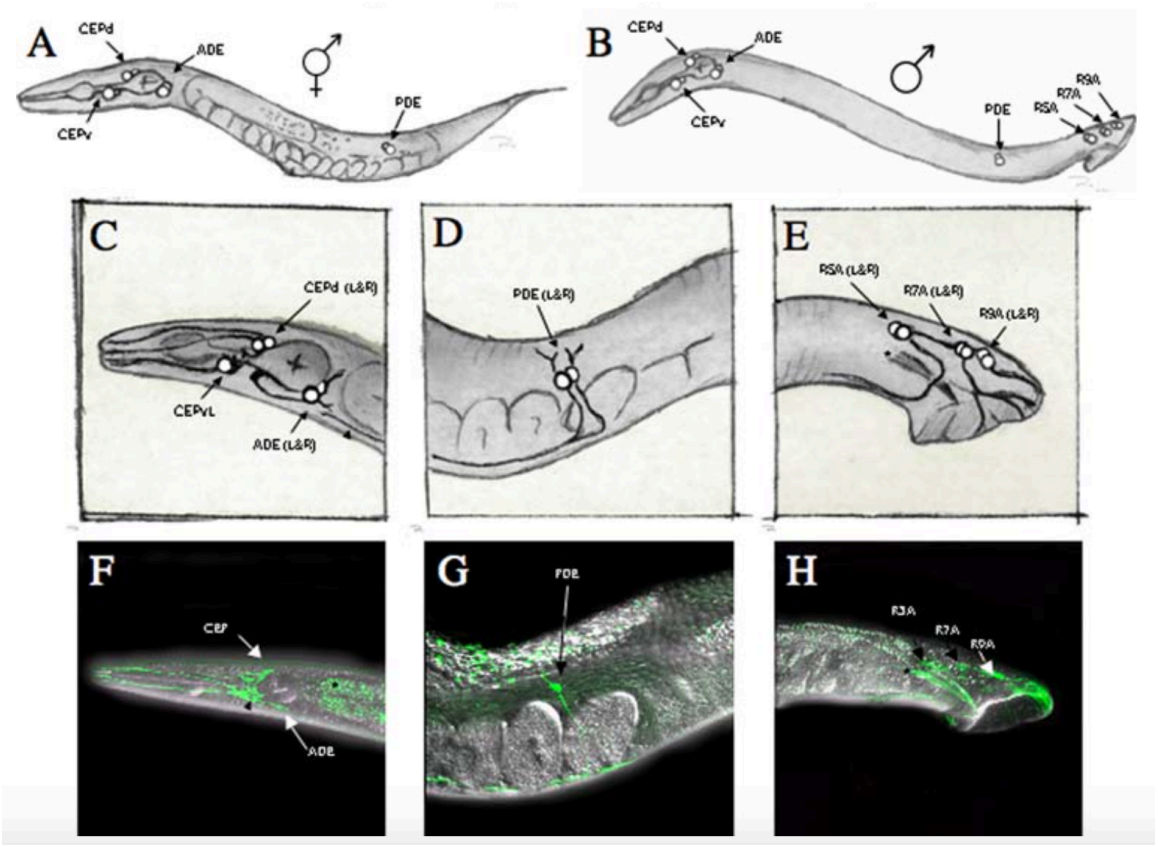

Figure 4 – DA neurons in *C. elegans.* Illustration of DA neurons in hermaphrodite (A) and in male worms (B). (C-D) Schematic showing the locations of the CEP and ADE neurons (C) and PDE neurons (D). (E) Male-specific DA neurons in the male tail, ray neuron pairs R5A, R7A, and R9A. (F-H) Same as in C-E, except neurons shown in worm expressing *pdat-1*::GFP to label DA neurons in green. Figure from (McDonald et al., 2006b)

posteriorly parallel to the ventral nerve cord. These neurons also have short processes that terminate in sensillar cilated endings. Male worms have an additional 6 sensory ray DA neurons (R5A, R7A, R9A) in the tail that also have ciliated endings and are necessary for male mating behavior (Liu and Sternberg, 1995; Loer and Kenyon, 1993).

MOLECULAR COMPONENTS OF *C. ELEGANS* DOPAMINE SIGNALING

The initial identification of genes necessary for normal DA signaling was performed by Sulston et al., who, as noted, used FIF to visualize DA neurons, and who screened for genetic mutations that caused a loss of this FIF signal (Sulston et al., 1975). The first genes identified in this screen were named *cat-1* and *cat-2*, due to their loss of catecholamine signal. These genes were later cloned and identified as orthologs of VMAT (Duerr et al., 1999) and TH (Lints and Emmons, 1999), respectively . With the help of genetic screens like Sulston's, as well as targeted cloning strategies, a fuller picture of the molecular deteminants of DA signaling in *C. elegans* emerged (Fig. 5). Like in humans, DA in the worm is synthesized from tyrosine by the sequential actions of tyrosine hydroxylase (*cat-2* in the worm) and aromatic amino acid carboxylase (*bas-1*) (Hare and Loer, 2004). DA is packaged into vesicles by the action of the vesicular monoamine transporter (*cat-1)* (Duerr et al., 1999) and released using the well-conserved vesicular release machinery, discussed briefly in Chapter I. DA then acts on D1- like (*dop-1, dop-4*), and D2-like (*dop-2, dop-3*) DA receptors (Chase et al., 2004b; Sugiura et al., 2005; Suo et al., 2002, 2003), which can be located presynaptically,

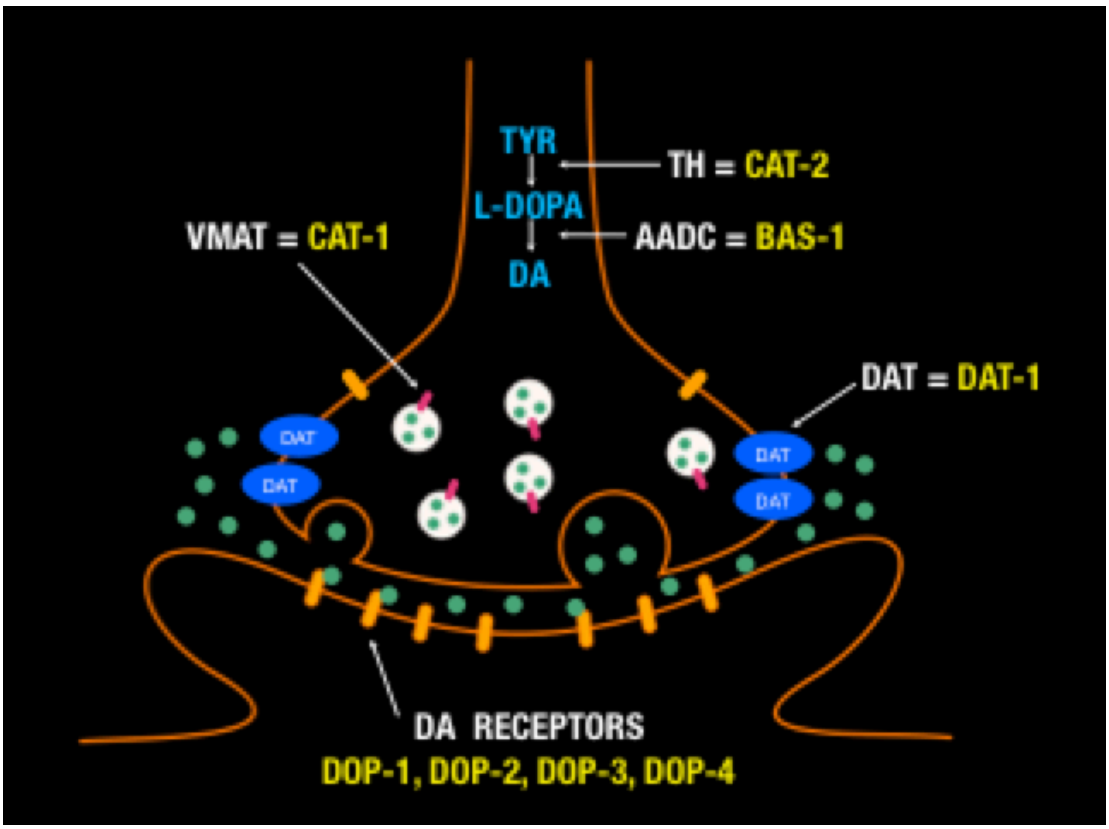

Figure 5 – Molecular components of DA signaling in *C. elegans*. Schematic showing the proteins required for DA biosynthesis, packaging and release, response, and reuptake.

postsynaptically, or extrasynaptically (Bermingham et al., 2016; Chase et al., 2004a; Suo et al., 2003). The *C. elegans* genome also encodes putative orthologs of the DA metabolism genes MAO (amx-1-3) and COMT (comt-1-5) (Wintle and Van Tol, 2001). There is some evidence that *amx-2* has monoamine oxidase activity (Schmid et al., 2015), but little work has been done on these putative MAO genes, and nothing has been published as of this writing on the *C. elegans* COMT genes.

Importantly for this thesis, the worm genome also encodes an ortholog of DAT, identified by Jayanthi and colleagues as the gene T23G5.5 (Jayanthi et al., 1998). This gene was cloned using homology-based oligonucleotide amplification, and expression of this cDNA in cells led to high affinity, saturable DA uptake that could be blocked by inhibitors of DAT and NET. This gene was named *dat-1*, and shares 43% and 47% sequence identity with human DAT and NET, respectively. As worms do not make NE, and uptake of NE in cells expressing *dat-1* was weak, this gene was suspected to be the primary worm ortholog of DAT. Later work by Nass et al. supported this by showing that driving GFP expression by the putative *dat-1* promoter (*pdat-1::GFP)* resulted in labeling of the same neurons identified by Sulston's FIF experiments, and matched the expression of *pcat-2::GFP (Nass et al., 2002).* Additionally, the neurotoxin 6-OHDA, which in mammals is a substrate of DAT that specifically kills DA neurons, led to cell death of *C. elegans* DA neurons, effects that were prevented by genetic ablation of *dat-1* or blockade of DAT-1 using the DAT-1 inhibitor imipramine. Heterologous expression of *dat-1* in non-DA *C. elegans* neurons also led to 6-OHDA-induced cell death, indicating that this transporter is both necessary and sufficient for 6-OHDA

neurotoxicity. Together, these experiments provided compelling evidence that *dat-1* indeed functions as a DA neuron-expressed DA transporter.

DOPAMINE REGULATION OF *C. ELEGANS* BEHAVIOR

Manipulations of DA in the worm have revealed a critical role for this neurotransmitter in regulating a number of behaviors. These experiments have shown that DA is involved in in modulation of egg-laying, defecation, associate and non-associative learning, male mating behavior, habituation to touch, and multiple aspects of movement. Here I will review some of the current evidence for DA modulation of worm behavior, and will highlight the use of analyzing these behaviors to study the molecular determinants of DA signaling in the worm.

Egg-Laying and Defecation

The effects of DA on egg-laying was first reported by Schafer and colleagues, who observed that exposure of wild-type worms to exogenous DA resulted in a reduction in number of eggs laid, as well as a reduced rate of locomotion (discussed in subsequent section) (Schafer and Kenyon, 1995). Interestingly, DA-treated worms displayed adaptation after continuous exposure to DA, with egg-laying and movement returning to normal after prolonged exposure (>3hrs). These researchers used a forward genetic screen to identify the voltage gated Ca^{2+} channel *unc-2* as required for this adaptation to the behavioral effects of DA. This is intriguing given the role mammalian D2 receptors have been shown to play in regulating voltage-gated Ca^{2+}

channels (Olson et al., 2005), and might suggest a conserved role for DA in regulating such channels.

Shortly after the work by Schafer et al, Weinshenker and colleagues also observed inhibitory effects of DA on egg-laying, and observed similar effects on defecation. Additionally, in worms with a gain-of-function mutation in the potassium channel *egl-2*, D2 receptor antagonists induced both egg-laying and defecation, indicating that loss of *egl-2* brought online an inhibitory action of DA on these behaviors that were not present in wild-type worms. Interestingly, Vidal-Gadea et al. more recently reported that exposing swimming worms to DA induces land-associated behaviors including both egg-laying and defecation (Vidal-Gadea et al., 2012). This apparent stimulation of these behaviors by DA is puzzling, and indicates that DA control of egg-laying and defecation may be context dependent, and that DA dictates the selection of a specific set of behaviors that are appropriate for the current environment. The basis of this context-dependent control is unclear at this point, however.

Associative and Non-Associative Learning

DA signaling in the worm has been shown in a number of paradigms to be critical for associative learning. One such paradigm was employed by Voglis et al., who showed that if animals are starved in the presence of normally chemoattractive compounds such as isoamyl alcohol, the animals will show an aversion to this compound upon subsequent exposure (Voglis and Tavernarakis, 2008). The authors demonstrated that DA was required for this associative learning, as *cat-2* mutants and worms with genetically ablated DA neurons did not show this same aversion. Addition

of DA during conditioning in either of these cases, however, restored the aversion behavior, indicating that DA is both necessary and sufficient for this associative learning. They went on to show that the DEG/ENaC acid-sensing ion channel *asic-1* was expressed in DA neurons, and was required for the associative learning effects of DA in this paradigm, as *asic-1* mutants behaved like *cat-2* mutant animals, and the loss of associative learning in *asic-1* mutants could also be rescued by DA exposure. Additionally, using a fluorescence recovery after photobleaching (FRAP)-based monitoring of SV fusion, they showed that conditioning increased DA SV fusion, but this increase was blunted in *asic-1* mutant animals. The authors thus created a model in which ASIC-1 promotes DA release upon conditioning through a positive feedback loop of protons released by SVs activating ASIC-1 and leading to further depolarization of the DA neuron terminal and further SV release. Importantly, the FRAP technique for monitoring fusion of DA-containing SVs has been implemented by our lab to monitor the synaptic effects of DA modulatory genes, some of the results of which are presented later in this thesis.

An example of DA regulating non-associative learning comes from work by Kimura et al., who showed that pre-exposure of worms to repellant odors 1-octanol and 2-nonanone resulted in an enhanced aversion to these repellants upon subsequent exposure (Kimura et al., 2010). This enhanced response was not dependent on the presence or absence of food during conditioning (making the learning non-associative), and the authors showed that this behavior required the D2-like receptor *dop-3*. Importantly, the *dop-3* receptor was not required for the associative learning observed by Voglis et al., who instead found a requirement for the *dop-1* and *dop-2* receptors.

This suggests that the circuits involved in regulating non-associative and associative learning may be independent, though some interaction between these circuits is possible.

DA is also involved in the regulation of habituation to mechanical stimuli, specifically a tapping of the plate. This non-directional, generalized mechanical stimulus causes worms to move backwards, and this "tap withdrawal" response will decrease with subsequent stimuli. This behavior is known as tap habituation, and can be considered as a form of short-term learning. DA seems to antagonize this tap habituation response, as loss of *cat-2* or *dop-1* causes a more rapid habituation, specifically in the presence of food (Sanyal et al., 2004). The requirement for food indicates that normally, DA release is stimulated by exposure to food (see subsequent section on locomotion) and slows the habituation response, and loss of DA signaling via mutation in *cat-2* or *dop-1* blocks this slowing of the habituation. The authors show in a subsequent study that DA acts through *dop-1* receptors in the ALM anterior touch neurons to modulate touch responsiveness such that loss of this signal causes these neurons to adapt to mechanical stimuli more quickly (Kindt et al., 2007). Additionally, elevating DA via loss of *dat-1*, which normally clears DA and loss of which leads to hyperdopaminergia, causes a slowing of habituation compared to wild-type animals. This work reveals a role for DA in antagonizing a learning response, in this case the habituation to a mechanical stimulus. The varied roles for DA in learning, from facilitating both associative and nonassociative learning, to antagonizing habituation is interesting, and demonstrates that different contexts and circuits dictate what role DA plays in learning in this model.

Locomotion

A role for DA in regulating locomotion in *C. elegans* was revealed early on by studies performed by Schafer et al., who observed that exposure of worms to exogenous DA resulted in a robust slowing of movement, and paralysis at higher concentrations (Schafer and Kenyon, 1995). These results were interesting as they implicated DA signaling in the regulation of worm locomotion using exogenous DA exposure, but the role for endogenous DA signaling in this regulation remained undefined. Later work by Sawin et al. identified just such a role in looking at worm rates of locomotion while feeding. They reported that worms dramatically slow their movement when exposed to a lawn of bacteria, a behavior that they called the basal slowing response (BSR). Additionally, they found that starvation of worms prior to exposure to bacteria cause an even more dramatic slowing, which they called the enhanced slowing response (ESR). They also found that *cat-2* mutants did not exhibit a BSR, but still showed an ESR upon starvation indicating that DA is required for the former but not the latter. Interestingly, DA-deficient *bas-1* and *cat-4* mutants were defective in both behaviors, but mutation in these genes would also prevent 5-HT biosynthesis. This led to the model where DA is required for the BSR, and 5-HT for the ESR, and support for this model came from the observation that exogenous DA and 5-HT could rescue the BSR and ESR, respectively. Additionally, laser ablations of DA neurons individually and in combination revealed a redundant role for DA neurons in mediating BSR, though the strongest single effect was seen with CEP ablation. Indeed, recent work by Hardaway et al. used *in vivo* calcium imaging to show that entry of a

worm into a lawn of bacteria increases CEP neuron activity, supporting the model of Sawin and colleagues (Hardaway et al., 2015). Based on the anatomy of DA neurons, all having cilia that terminate in the worm subcuticle, Sawin et al. also reasoned that the BSR might be mediated via mechanosensation by DA neurons. To test this, they used glass beads instead of a lawn of bacteria, and observed the BSR phenotype in this context as well. Importantly, *cat-2* mutants and DA neuron laser-ablated animals again did not show BSR in response to these beads. This indicated that the mechanical stimulus of the bacterial lawn is the cue for DA neuron activation and subsequent worm slowing.

Further understanding for how endogenous DA acts to control worm locomotion came from work by Chase and colleagues (Chase et al., 2004a). They found that loss of the DA receptor *dop-3* caused a complete loss of the BSR. They similarly found a resistance of *dop-3* mutants to the paralytic effects of exogenous DA, though loss of both *dop-3* and the D1-like DA receptor *dop-1* resulted in WT levels of paralysis. In subsequent work, they used cell-specific rescue experiments to reveal that both *dop-3* and *dop-1* act in cholinergic motor neurons to mediate the effects of DA on locomotion, and expression of both of these receptors in these cells was verified by promoter fusion experiments (Allen et al., 2011). Based on homology, *dop-3* is thought to be a D2-like receptor, and DA stimulation of *dop-3*-expressing cells in culture resulted in an inhibition of forskolin stimulation of cAMP production, consistent with this receptor being an inhibitory $G\alpha_{i/o}$-coupled GPCR. Therefore, activation of these receptors likely silences the activity of the *dop-3*-expressing motor neurons, which leads to slowing of locomotion. Indeed, the researchers used sensitivity to the acetylcholinesterase

aldicarb to show that *dop-3* and *dop-1* reduce and enhance cholinergic signaling, respectively. This indicates that these two receptors act in cholinergic motor neurons to antagonistically regulate acetylcholine release. This is reminiscent of antagonistic control of DA signaling on medium spiny neurons in the mammalian brain by D1 and D2 receptors, though in mammals these receptors are generally expressed by distinct populations of medium spiny neurons (Beaulieu and Gainetdinov, 2011). This group went on to perform a forward genetic screen using exogenous DA sensitivity to reveal components of the $G\alpha_o$ (*goa-1, dgk-1*) and $G\alpha_q$ (*eat-16, gpb-2*) signaling pathways that again act antagonistically to modulate this phenotype.

Another action of DA in controlling locomotion is through the modulation of area restricted search (ARS). ARS is a behavior that occurs shortly after an animal encounters a food source such as a lawn of bacteria (Hills et al., 2004). When away from this food source, such as when the experimenter moves the animal to a food-free plate, the animal will increase the angle of its turns to restrict its search area to try to find the food source again. This behavior will persist for a short time, and gradually disappear after 30 min as the animal begins to move in a more linear pattern, presumably to look for a new food source. Interestingly, ablation of DA neurons using the cell death-inducing human caspase interleukin-1β-converting enzyme (ICE) expressed in DA neurons (*pdat-1::ICE*) caused a loss of this ARS behavior. Similarly, *cat-2* mutant animals were also defective for ARS, and exposure of either *cat-2* mutants or *pdat-1::ICE* expressing worms to exogenous DA rescued this loss of ARS. Additionally, the D2-like receptor antagonist raclopride completely blocked ARS, suggesting that DA acts through a D2-like receptor, presumably *dop-2* or *dop-3*, to

regulate the ARS behavior. Whether regulation of ARS by DA utilizes the same circuits as the regulation of BSR is unclear at this point, however.

Swimming-Induced Paralysis

The work by Chase et al. (Chase et al., 2004a) was instrumental in revealing many of the important molecular components of DA signaling, particularly at the postsynaptic site of DA action. The forward genetic screen they used was critical in these efforts, but unfortunately the design of this screen did not allow for identification of presynaptic or upstream regulators of DA signaling. The exogenous DA sensitivity assay isolates postsynaptic sites of DA actions, and BSR is not particularly sensitive with revealing alterations in DA levels beyond complete or near complete loss of DA (ie. *cat-2* mutants). Excitingly, an observation made by McDonald et al. revealed a novel DA-dependent phenotype that is sensitive to increased levels of endogenously-released DA (McDonald et al., 2007). This phenotype was observed in *dat-1* loss-of-function mutants that are unable to clear DA, and therefore exhibit a hyperdopaminergic state. This state was revealed upon placing these worms in water, where they exhibited robust paralysis that was not observed in wild-type animals (Fig. 6). Importantly, this paralysis could be prevented by treatment with the VMAT/CAT-1 antagonist reserpine, which, by analogy to mammalian VMAT, is suspected to prevent DA loading into SVs. Additionally, loss of either *cat-2* or *dop-3* completely reversed this paralysis, verifying the DA-dependence of this phenotype. Having a phenotype that reveals states of increased DA signaling, our lab performed a forward genetic screen using EMS mutagenesis to produce mutant lines that exhibited reserpine-sensitive Swip (Fig. 7)

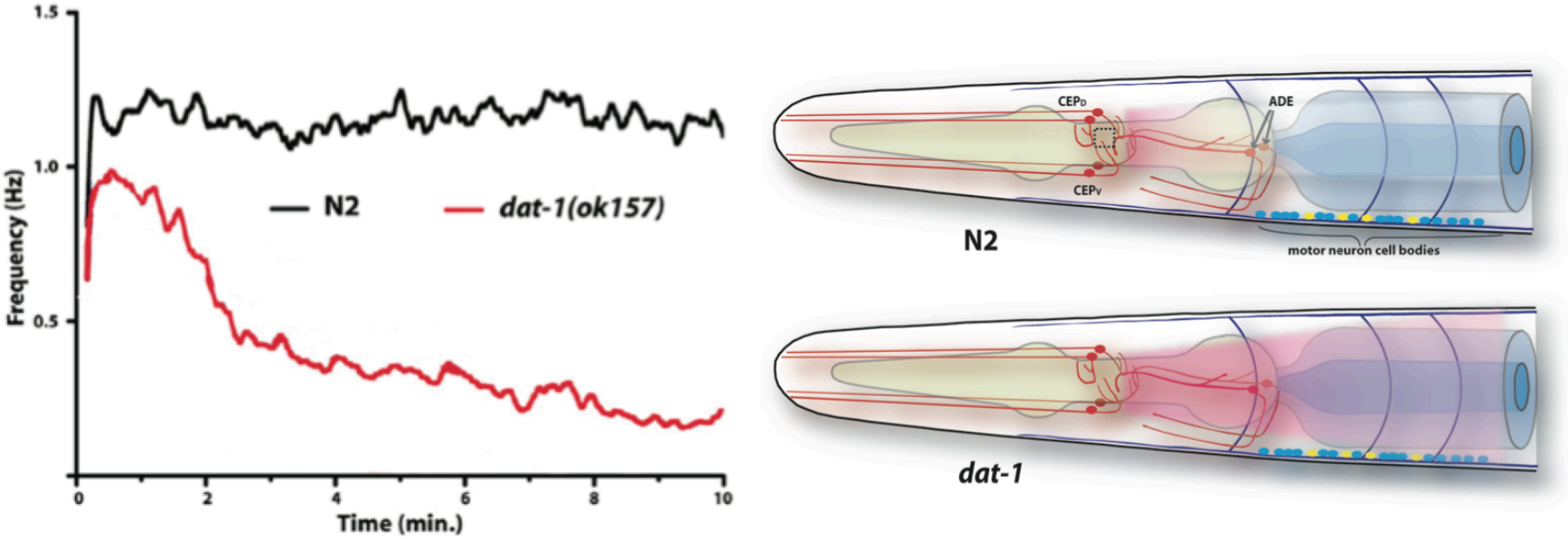

Figure 6 – *dat-1* mutants exhibit robust Swip. (A) Plot showing the average frequency of swimming of a population of N2 and *dat-1(ok157)* animals. N2 animals swim robustly for 10+ minutes, whereas *dat-1(ok157)* animals paralyze rapidly. (B) Model for how Swip phenotype is generated. DA neurons are shown in red, and DA is shown in pink gradient. Loss of *dat-1* causes excessive spillover of DA, which acts on motor neurons (blue, yellow) to inhibit motor neuron activity and cause paralysis.

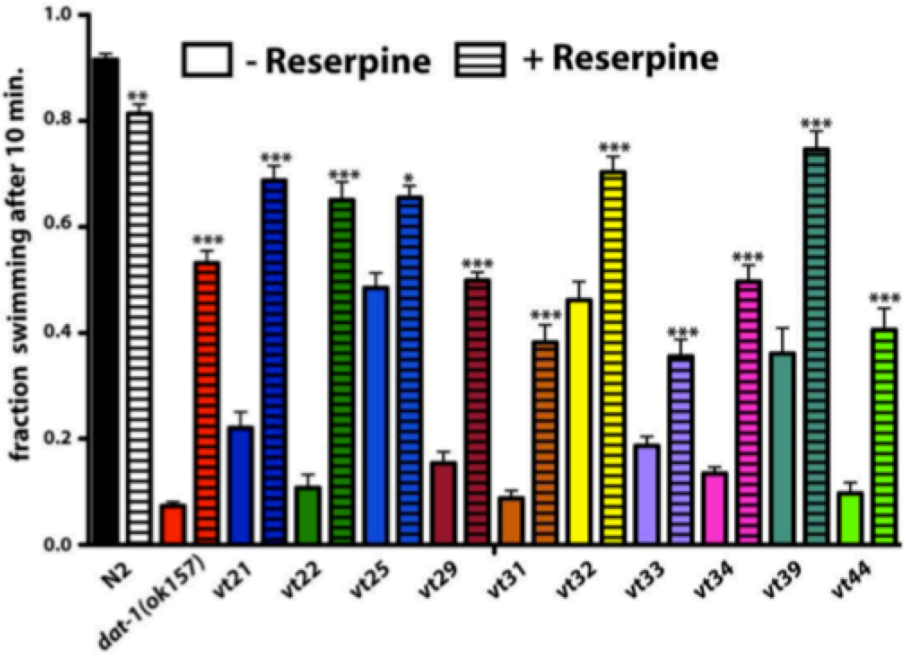

Figure 7 – Lines generated by Swip mutagenesis screen. Lines that demonstrated robust Swip and rescue by reserpine pretreatment. *vt21* and *vt22* harbored mutations in *dat-1*.

(Hardaway et al., 2012). Importantly, this screen generated two loss-of-function *dat-1* alleles, validating the design of the screen. Two other lines, *vt29* and *vt33*, were found to have mutations in the same gene, F53B1.6, which was named *swip-10* (Hardaway et al., 2015). Characterization of *swip-10* indicated that this gene acts in glial cells, and rescue experiments using glutamate receptor mutants indicated a role for glutamate in the hyperdopaminergic state in these animals likely through increased excitation of DA neurons. In support of this idea, calcium imaging and FRAP analysis of vesicle release supported an increase in DA neuron activity in *swip-10* mutants. The identification of a gene that impacts DA neuron activity through control of glutamate was exciting and unexpected, and validates the potential for this screen to reveal novel, interesting regulators of DA signaling.

The work presented in this thesis involves the identification and characterization of another gene harboring a mutation generated by the Swip screen, *vt32.* These efforts revealed the actions of the novel gene *swip-13* that, unlike *swip-10*, acts cell-autonomously (within the DA neurons themselves) to produce a hyperdopaminergic state. My studies will show that this state arises from loss of DAT-1 activity due to an apparent role of *swip-13* in regulating DAT-1.

CHAPTER III

IDENTIFICATION OF *SWIP-13*, A NOVEL GENETIC REGULATOR OF DOPAMINE SIGNALING IN *C. ELEGANS*

INTRODUCTION

As previously discussed, DA is utilized by the *C. elegans* nervous system to regulate multiple behaviors. Chief amongst these is the modulation of movement to adapt to different environmental contexts (Chase et al., 2004a; Sawin et al., 2000). The BSR and the paralytic effects of endogenous DA have been used to identify and characterize genes that are required for normal DA signaling in the worm, but these behaviors are not ideal for revealing states of hyperdopaminergia that might result from genetic manipulations. For this purpose, our lab has pioneered the use of the DA-dependent Swip phenotype to reveal such states and to identify novel regulators of DA signaling (Hardaway et al., 2012; McDonald et al., 2007). A forward genetic screen based on this behavior generated novel loss-of-function mutations in *dat-1*, as well as two mutations in a previously uncharacterized gene F53B1.6, later named *swip-10*. Interestingly, characterization of these *swip-10* mutants seemed to indicate that the hyperdopaminergic state seen in these animals was the result of enhanced glutamatergic signaling on DA neurons, with genetic evidence pointing towards dysfunction of glial control of glutamate levels (Hardaway et al., 2015). The potential role of this gene in regulating glial biology and impacting DA levels through glutamate is quite different from the mechanism of hyperdopaminergia seen in *dat-1* loss-of-function

mutants after which the Swip screen was designed, and demonstrates the power of this screen in identifying novel pathways that regulate DA signaling in *C. elegans*.

Another mutant generated by this screen that demonstrated reserpine-sensitive Swip was given the allele designation *vt32*. Here I describe the identification of the gene harboring this mutation as the gene C05D10.2, also uncharacterized in the worm. Mutation in this gene produces Swip that can be reversed by loss of DA synthesis and response genes, and cell-specific rescue experiments demonstrate that this gene is required in DA neurons to exert its control over DA signaling. Additionally, promoter and translational GFP fusions show that this gene is expressed in DA neurons and the protein it encodes is present at synapses, supporting a role for this gene in regulating DA signaling in DA neurons, potentially at the presynaptic terminal.

MATERIAL AND METHODS

C. elegans strains and husbandry

Strains were grown on bacterial lawns of OP50 and maintained at 12°C to 20°C as previously described (Brenner, 1974). N2 Bristol served as our wild-type strain. The strain VC2695 contains the allele *gk1234,* which possesses a large deletion of the gene C05D10.2, and was obtained from the Caenorhabditis Genetics Center (CGC, University of Minnesota, Minneapolis, Mn). The strain LX703 that contains a deletion in *dop-3 (dop-3(vs106*)) was also obtained from the CGC, and the *cat-2(tm2261)* strain was obtained from Shohei Mitani at the National Bioresource Project at the Tokyo Women's Medical University.

Swip Assay

For both manual and automated assays, staged L4 animals were generated by hypochlorite treatment of gravid adults and plating of synchronized L1 animals and growth for various days at 12-20°C. For manual assays, experimenters were blinded to genotype, and ~10 animals were picked into 100uL of water and analyzed for number of paralyzed animals after 10 min. For each genotype/treatment, ~80 animals were assayed per experiment, with at least 3 experiments performed by 1-2 experimenters. For reserpine experiments, synchronized L1s were plated on OP50 plates containing 0.6mM reserpine or DMSO vehicle and were grown for two days at 20°C to reach the L4 stage before Swip testing. For transgenic rescue experiments, 50-80 transgenic animals and non-transgenic animals were picked based on co-injections markers and at least 2 experiments were performed per line, with three independent lines per transgene. For automated analyses, animals were picked one at a time into 10uL of water and 10 minute movies of these individual worms' swimming behavior were captured and analyzed as previously described (Hardaway et al., 2014). Briefly, videos were first analyzed using the in house tracking software Worm Tracker, which fits a spine to the worm and calculates the frequency of body bends over time. This frequency information is then processed by another in house program called SwimR, which uses this information to calculate various parameters and to output visual representations of the data.

C. elegans mutagenesis screen

Standard methods for a nonclonal, F2 screen were performed as originally described (Brenner, 1974) and were used on wild-type hermaphrodite worms carrying a DAT-1 promoter-driven green fluorescent protein (GFP) transgene (BY200) (Nass et al., 2002). A semisynchronous population of healthy, well-fed late L4 animals was exposed to either 47 mM ethylmethanesulfonate (EMS) or 0.5 mM N-ethyl-N-nitrosourea at room temperature for 4 hr in a chemical fume hood. After 24 hr of recovery, 30 gravid adult worms were placed on each of eight 10-cm OP50 plates and allowed to lay ~50 eggs each (the F1s) before being discarded. After reaching adulthood and laying 20 to 30 eggs each for a total of 1000 to 1500 developing F2 animals per plate, the F1 animals were discarded. When F2 animals reached the L4 stage, they were batch screened for the Swip phenotype by rinsing off the plate and analyzing 50 to 100 animals per well as described previously. We tracked the source plate of each F2 so that only one stable mutant line was kept for each plate of the mutant F1s. After 10 min, animals that exhibited Swip were replated and allowed to recover. Swip-positive animals that recovered normal movement on solid media were cloned and retested in Swip assays to establish phenotype stability. Only lines in which at least 50% of the animals displayed Swip on retest were saved for a test of reserpine reversal of Swip, as described previously. In later rounds of screening, this convention was increased to 80% to improve recovery of stable lines. Stable lines that demonstrated a significant rescue of Swip after reserpine treatment were kept for further analysis. All recovered lines that had significant rescue of Swip after growth on 0.6mM reserpine were outcrossed to the N2 strain a minimum of three times before further analysis. After each outcross, lines

were rehomozygosed and retested for stable Swip on separate days with multiple parental founders before proceeding to the next cross. All lines recovered from the screen were sequenced with sense and antisense primers that span all DAT-1 exons and includes 1 kb upstream of the transcription start site as well as 50 bp downstream of the translational stop codon) using Big Dye Terminator Cycle Sequencing Mix (ABI, Foster City, CA). PCR products were sequenced on an ABI 3730xl DNA Analyzer (DNA Sequencing Core Facility, Vanderbilt Division of Medicine).

SNP mapping

Mapping of mutant loci was performed as described previously (Davis et al., 2005). In summary, stable outcrossed Swip strains were crossed to the CB4856 strain. For bulk segregant analysis, lysates from both Swip-positive and Swip-negative F2 populations were generated and used as the input for genome-wide, 96-well PCR. N2 animals were not used as a control in these efforts because we found nonspecific N2 Bristol islands in both the Swip-positive and Swip-negative F2s on the left arm of LGI. The bulk segregant protocol was used to identify linkage groups that can serve for fine mapping with experiments replicated at least twice with separate populations to demonstrate consistent linkage. For fine-interval mapping, individual Swip-positive F2s were cloned, and their F3 progeny were tested for a stable Swip phenotype. Mutations were considered homozygous if the F3 population demonstrated Swip comparable to the original strain. Populations were manually scored in at least four to five assays using 40 to 50 worms. DNA from individual clones was then used as the input for PCR of individual intervals to ascertain a specific Bristol island on the mapped linkage group.

Whole genome sequencing and sequence analysis

Genomic DNA was isolated as described previously (Sarin et al., 2008). Briefly, BY200 (parental strain) and *vt32* worms were harvested from a 10 cM 8p/NA22 plate by rinsing with M9. After a brief preclearing wash with M9, worms were rocked in M9 for 2–3 h to clear ingested bacteria and then washed with M9 and pelleted for DNA extraction. Before extraction, the worm pellet was incubated at −80°C for 1 h to overnight. Genomic DNA was extracted from the worm pellet using a Qiagen Gentra Puregene kit as described by the manufacturer and a post hoc phenol/chloroform extraction, RNase A digestion, and additional phenol/chloroform extraction. Quality of the gDNA was confirmed on a 2% agarose gel before submitting the samples for Illumina sequencing (Vanderbilt Genome Technology Core). Sequencing libraries were generated from gDNA as described previously (Sarin et al., 2008). Each sample was assigned a unique barcode so that samples could be pooled onto several flow cells of an Illumina Genome Analyzer Iix for sequencing as single-end 76mers. Sequence reads were filtered for quality and offloaded in Fastq format for subsequent analysis. Sequence data were analyzed in MaqGene (Bigelow et al., 2009) and a text file containing mutations against the reference sequence (WS180) was extracted. We then compared these mutant strain lists against the parental strain (BY200) to identify mutagen-induced single nucleotide polymorphisms (SNPs) and compared these with the mapped interval on LGIII to identify potential genes containing the *vt32* mutation.

Genetic crosses and genotyping

Crosses were performed using integrated fluorescent markers *in trans.* In order to verify presence of mutations, single worm PCR was used using a three primer multiplex strategy. N2 and mutant control reactions were run in parallel, along with a synthetic heterozygote reaction containing both N2 and mutant DNA. Platinum PCR Supermix was used for all genotyping PCR reactions and reactions were analyzed via agarose gel electrophoresis. The following oligonucleotide primers were used for genotyping mutations used in this study:

swip-13(gk1234):

5' sense – GGAATGTGTTACACCGGTGAG

3' antisense - GTTTATCCACCACTTCCGGA

inner sense – CTGCGATTGATATGGTTCAGAG

dop-3(vs106):

5' sense – TCAAGAAGTGGGAGACGGAACGAA

3' antisense - gacctggcaatgtctgggtagaaa

inner antisense – GTGGTGTTGTCCAGCCAACATTCT

cat-2(tm2261):

5' sense – ctccaacaactgaacgacgaagg

3' antisense - atttctcgtagacagccttccacg

inner antisense – agcagctctgccgagtgaattaa

Creation of plasmids and transgenic animals

Plasmids: The plasmid *pdat-1::swip-13(g)* was generated by amplification of genomic *swip-13* with primers that introduced AscI and KpnI sites in the 5' and 3' ends, respectively. This AscI/KpnI digested fragment was then ligated to AscI/KpnI digested plasmid pRB1106 (containing the *dat-1* promoter and *unc-54 3'UTR*) using T4 DNA ligase. A similar strategy was used to generate *pdat-1::gfp::swip-13(g),* except an initial overlap PCR amplification reaction was first utilized to generate a *gfp::swip-13* fragment with AscI/KpnI sites. To generate the K42R kinase dead mutation in the *pdat-1::gfp::swip-13(g)* plasmid, Agilent QuikChange II Site-Directed Mutagenesis kit was used to engineer in a coding mutation to substitute an Arg for a Lys at position 42. For mammalian expression vectors, the plasmid pCR3.1 HA-ERK8 was generously gifted by Dr. Mark Abe (University of Chicago). The R59Q and K42R mutations were again engineered using a similar strategy as described above using Agilent's QuikChange II Site-Directed Mutagenesis kit.

Transgenics: Transgenic animals were generated via microinjection as previously reported (Brenner, 1974). Transgenic F1 progeny were selected based on presence of fluorescent co-injection markers, and lines with F2s having stable expression of the transgene were selected for analysis. The following injections mixes were used for lines generated in this study:

swip-13(vt32) Ex139-141 (C05D10.2 genomic fragment)

40ng/uL C05D10.2 genomic PCR fragment

30ng/uL *punc-122::GFP*

30ng/uL *pdat-1::mCherry*

swip-13(gk1234) Ex142-144 (pdat-1::swip-13)

40ng/uL *pdat-1::swip-13*

30ng/uL *punc-122::RFP*

20ng/uL *pelt-2::GFP*

10ng/uL *pdat-1::mCherry*

N2 *Ex191 (pswip-13::GFP)*

10ng/uL *pswip-13::GFP*

60ng/uL *punc-122::RFP*

30ng/uL *pdat-1::mCherry*

N2 *Ex192 (pdat-1::GFP::swip-13)*

40ng/uL *pdat-1::GFP::swip-13*

30ng/uL *punc-122::RFP*

30ng/uL *pdat-1::mCherry::rab-3*

swip-13(gk1234) Ex193-195 (pdat-1::GFP::swip-13)

40ng/uL *pdat-1::GFP::swip-13*

30ng/uL *punc-122::RFP*

30ng/uL *pdat-1::mCherry*

swip-13(gk1234) Ex239-241 (pdat-1::GFP::swip-13(K42R))

40ng/uL *pdat-1::GFP::swip-13(K42R)*

30ng/uL *punc-122::RFP*

30ng/uL *pdat-1::mCherry*

Confocal imaging

Confocal images were acquired on a Zeiss LSM 510 inverted confocal microscope. Worms for imaging were prepared by placing young adult transgenic animals onto 2% agarose pads and worms were immobilized using 0.05% levamisole in M9. Slides were covered with 1mm coverslips and sealed with paraffin wax prior to imaging. Captured images were analyzed using ImageJ software. Magnification power for captured images is noted in figure legends.

Mammalian cell culture and transfections

HEK-293T cells were maintained in Dulbecco's Modified Eagle Medium (DMEM) media supplemented with 10% fetal bovine serum, 100 I.U./mL penicillin, and 100 μg/mL streptomycin. For *in vitro* kinase assays, cells were plated in 6-well dishes at a density of 2 x 10^5 cells per well. One day after plating, cells were transfected with Mirus TransIT LT1 transfection reagent according to manufacturer's specifications at a ratio of 1:3 DNA/transfection reagent. Two days post-transfection, cells were lysed and used for *in vitro* kinase assay.

***In vitro* kinase assay**

Lysates from transfected HEK 293T cells were incubated with Anti-HA Affinity Matrix (Roche, Indianapolis, IN) at 4°C for 1 hr with constant agitation. Beads were then pelleted and washed 5 times with lysis buffer for 5 minutes each, again with constant agitation. Beads were then washed once in kinase assay buffer (50 mM Tris, 0.1mM EGTA, 10 mM $MgAc_2$, 0.1% (v/v) BME, 1 mM Sodium othrovanadate) for 5

minutes, and then beads were pelleted and again resuspended in kinase assay buffer plus 1nmol MBP and 50 uM ATP (2500 cpm/pmol). Reaction was placed at 30°C for 15 min and was stopped and proteins eluted by the addition of SDS sample buffer. Proteins were resolved by SDS-PAGE and the gels were stained with Coomassie-blue. SDS-PAGE gels were dried and incorporation of ^{32}P was assed by autoradiography.

Graphical and Statistical Methods

Data were analyzed and graphed using either SwimR software (described above), or using Prism 6.0 (GraphPad, Inc., La Jolla, CA). All statistical analyses and curve fits were performed in Prism 6.0. Descriptions of all statistical tests are noted in the figure legends, and $P<.05$ was taken as statistically significant in all tests.

RESULTS

In previous work, the mutant line *vt32* was identified as demonstrating reserpine-sensitive Swip behavior (Fig. 8), consistent with a hyperdopaminergic state (Hardaway et al., 2012). SNP mapping indicated that this mutation was located on LGIII, which also harbors the *dat-1* gene. Sequencing of the *dat-1* locus, however, revealed no coding changes in this gene, and whole genome sequencing was performed to identify unique coding changes in the putative *vt32*-containing region. One of the candidates, C05D10.2, had an amino acid substitution of an Arg to a Gln. We used the online tool Wormviz to examine transcript levels of this gene in various cell types across development. Wormviz is a tool that uses data generated by multiple research groups as part of the modENCODE project to perform transcriptional profiling of various *C.*

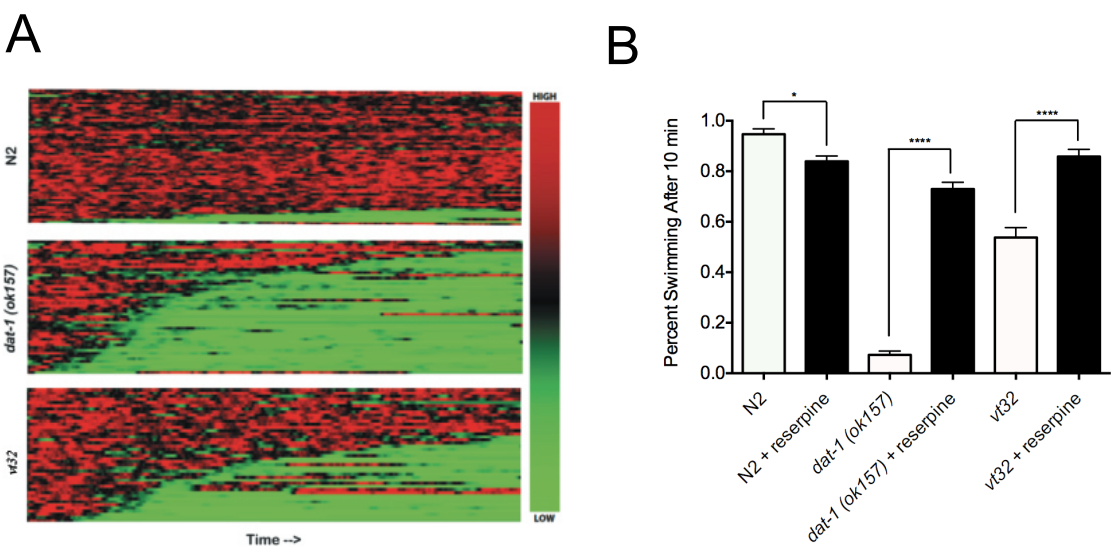

Figure 8 - *vt32* mutants display reserpine-sensitive Swip. (A) Heat maps showing the swimming behavior of N2, *dat-1(ok157),* and *vt32* animals. Each horizontal line represents the frequency of swimming over time for a single worm, going from 0 to 10 min from left to right, with red representing high frequency values and green representing low frequency values. N2 animals show very little paralysis, as demonstrated by the minimal green colored lines, and *dat-1(ok157)* animals show robust paralysis as demonstrated by the high prevalence of green lines. *vt32* animals have more intermediate paralysis. (B) Reserpine pretreatment rescues Swip behavior in both dat-1(ok157) animals and vt32 animals. Significance was calculated using a one-way ANOVA with Bonferonni posttests comparing each genotype without reserpine to the same genotype with reserpine. Significance was set at P<.05. *P<.01 ****P<.0001

elegans cell types across development (Gerstein et al., 2010; Spencer et al., 2011). Using this tool, we observed a dramatic peak in C05D10.2 mRNA levels in late embryonic and L3/L4 DA neurons, compared to other cell types. Importantly, transgenic expression of the wild-type C05D10.2 gene in a *vt32* mutant background led to a significant suppression of the Swip phenotype (Fig 9). Having identified the gene that harbors the *vt32* mutation, C05D10.2 was thus named *swip-13*. C05D10.2/*swip-13* is a gene located on LGIII at -1.42cM and consists of 10 exons (Fig 10A). *swip-13* is a highly conserved ortholog of the mammalian atypical MAP kinase ERK7/8, and sequence alignments show a high level of conservation in the kinase domain between *C. elegans* and mouse/human, including conservation of the arginine residue that was mutated in the *swip-13(vt32)* line (Fig. 10B). In support of C05D10.2 as the locus for the *swip-13* mutation, a deletion allele of *swip-13, swip-13(gk1234)* (Fig. 11A), demonstrated a similar Swip phenotype to that of *swip-13(vt32)*. Additionally, complementation testing showed that *gk1234*/+; *vt32*/+ double heterozygotes showed significant Swip comparable to the Swip of single *gk1234* or *vt32* mutants (Fig. 11B). The Swip phenotype of *swip-13(gk1234)* was also rescued by pretreatment with reserpine, supporting the DA dependence of this paralysis (Fig. 12A). To further test the DA dependence of the paralysis seen in *swip-13(gk1234),* these animals were crossed to *dop-3(vs106)* and *cat-2(tm2261),* both of which were previously shown to reverse the Swip phenotype of *dat-1* mutants. Loss of either of these genes resulted in a significant suppression of Swip in *swip-13(gk1234)* animals, effects observed with both manual assays, as well as with automated SwimR analyses (Fig. 12B,C).

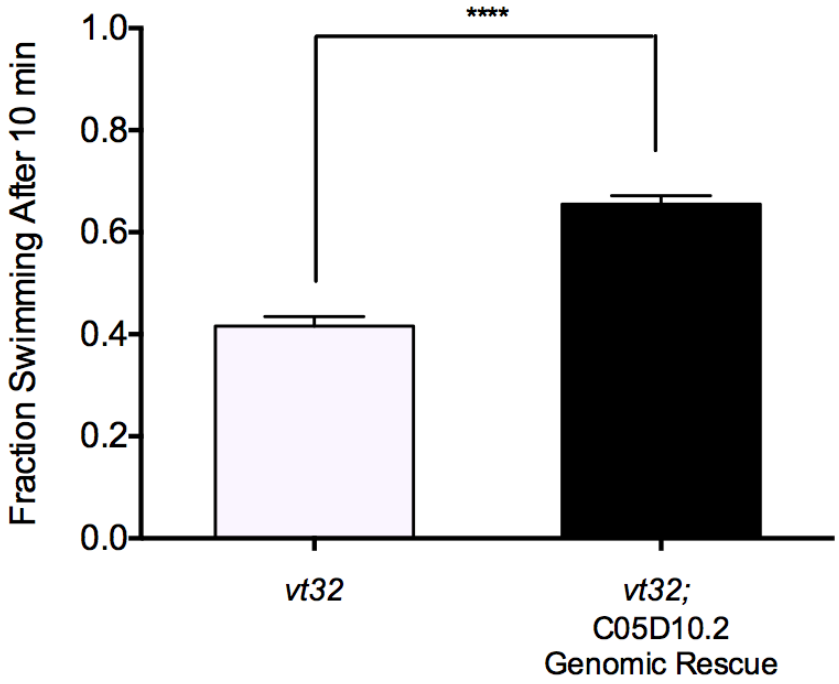

Figure 9 - Genomic C05D10.2 rescues *vt32* Swip behavior. A genomic PCR fragment containing the C05D10.2 genomic locus, including 1kb upstream and downstream to include putative promoter and 3'UTR sequences, was trasngenically expressed in *vt32* mutant animals. Comparison of transgenic and non-transgenic animals revealed a significant suppression of Swip with expression of wild-type C05D10.2. Bars represent the average of three transgenic lines with at least 100 animals per line. Significance was calculated using a two-tailed Student's t-test with significance set at P<.05. ****P<.0001

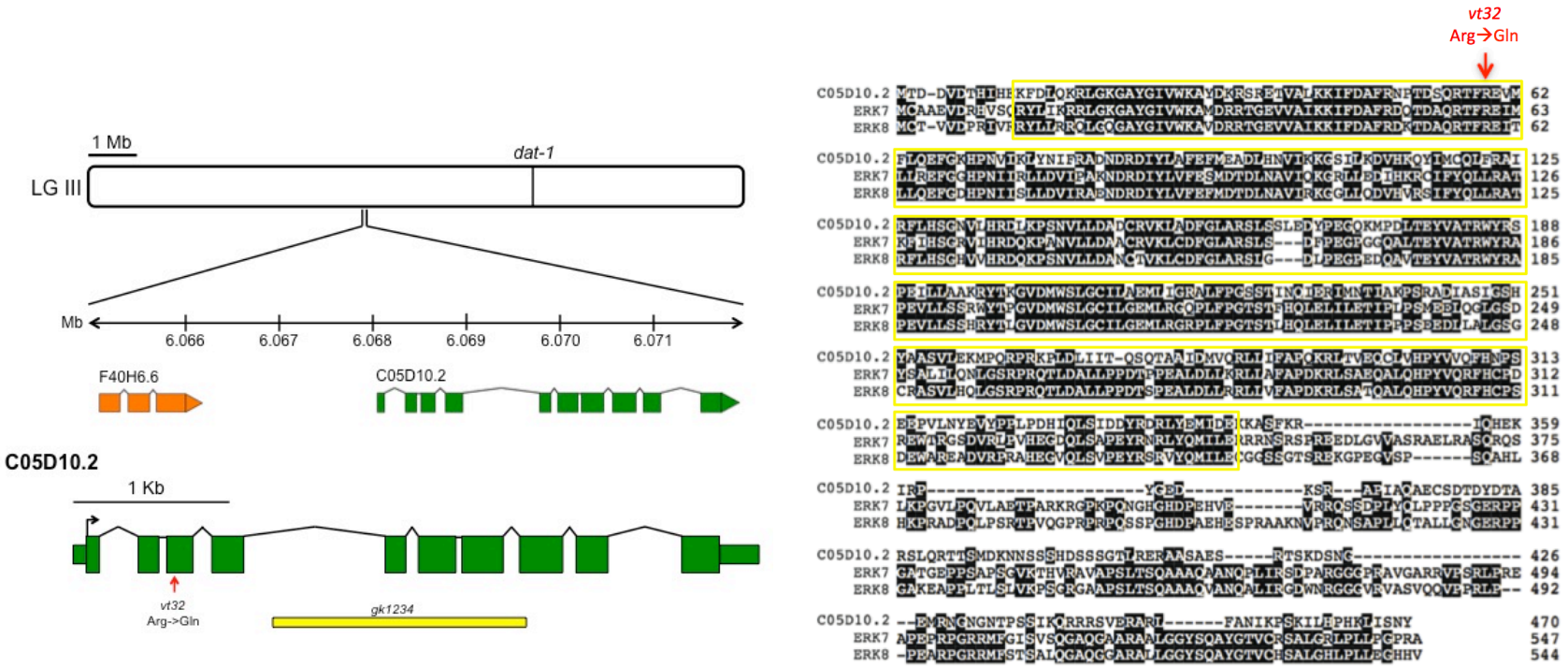

Figure 10 - C05D10.2 encodes a gene on LGIII orthologous to mammalian ERK7/8. (A) C05D10.2 is located on chromosome III at -1.42 cM. The *vt32* mutation was located in exon 3, and results in an Arg to Gln substitution. *gk1234* is a large deletion allele of C05D10.2 that deletes all of exons 5-7, and part of exon 8. (B) Sequence alignment of C05D10.2 with mouse ERK7 and human ERK8 shows a high level of sequence identity, including the site of the vt32 mutation (red arrow). Conservation between these proteins is highest in the putative kinase domain (yellow box), and the majority of divergence appears to be in the long C-terminal tail region.

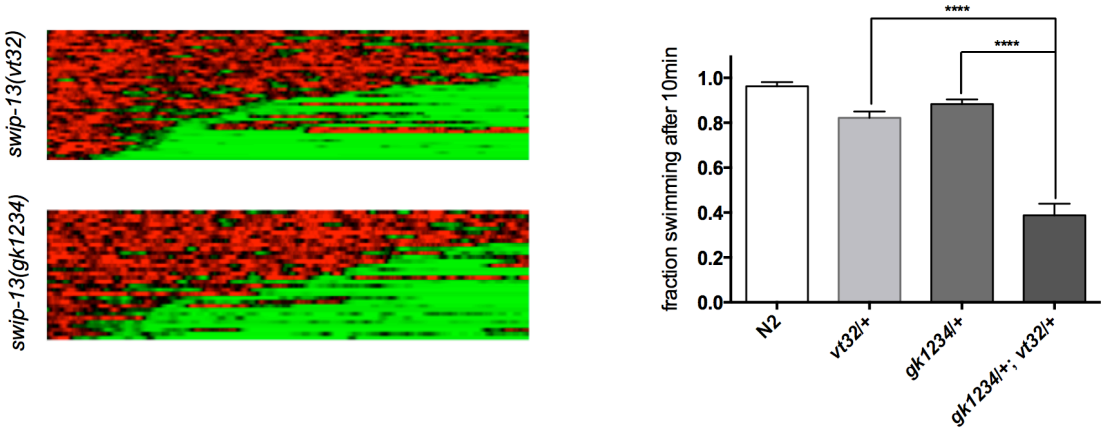

Figure 11 – *gk1234* and *vt32* fail to complement. (A) Comparison of Swip behavior using heat map analysis between *swip-13(gk1234)* and *swip-13(vt32)* shows a high degree of similarity in Swip behavior between these two lines. (B) *vt32* and *gk1234* fail to complement. Heterozygous *vt32*/+ and *gk1234*/+ animals swim normally, but double heterozygous *gk1234/vt32* animals demonstrate significant paralysis. Data was analyzed using a one-way ANOVA with Bonferonni posttests comparing *gk1234/vt32* double heterozygotes to both *vt32*/+ and *gk1234*/+ single heterozygotes. Significance was set at P<.05. ****P<.0001 Data acquired with the assistance of Osama Refai.

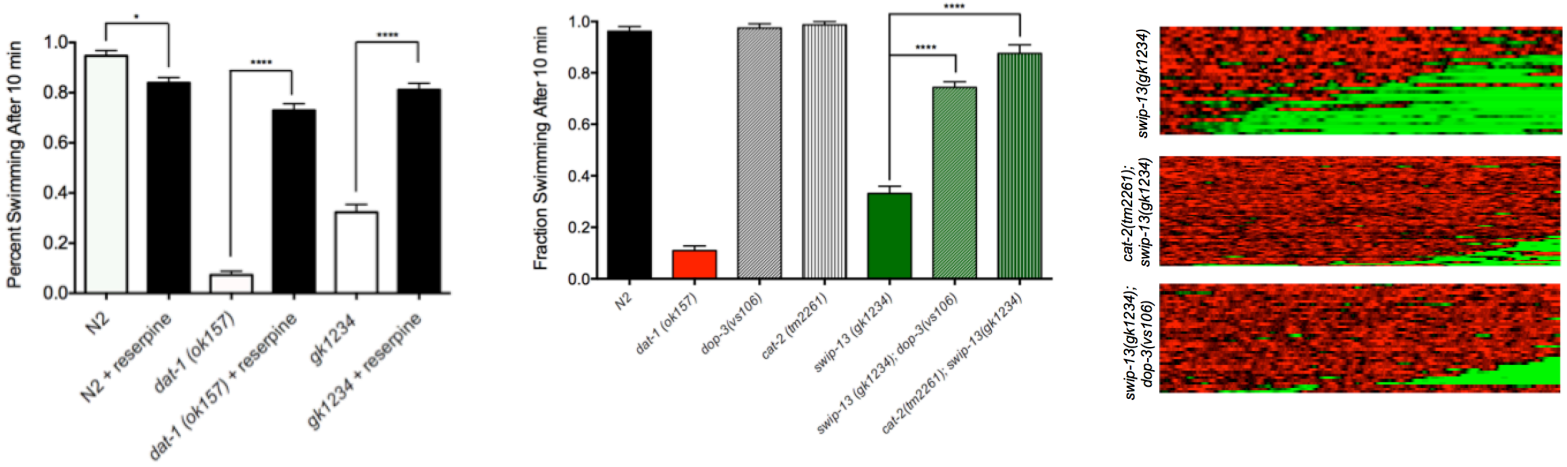

Figure 12 – *swip-13(gk1234)* animals display DA-dependent Swip. (A) Like *swip-13(vt32)* animals, *swip-13(gk1234)* Swip behavior is also rescued by reserpine pretreatment. Data was analyzed using a one-way ANOVA with Bonferonni posttests comparing each genotype without reserpine to the same genotype with reserpine. Significance was set at P<.05. *P<.01 ****P<.0001. (B) Both *dop-3(vs106)* and *cat-2(tm2261*) mutations signicantly suppress Swip in *swip-13(gk1234)* animals. Data was again analyzed using a one-way ANOVA with Bonferonni posttests comparing *swip-13(gk1234)* to both *swip-13(gk1234);dop-3(vs106)* and *cat-2(tm2261);swip-13(gk1234).* Significance was set at P<.05. ****P<.0001 (C) Heat map analysis again shows a near complete rescue of Swip in *swip-13(gk1234);dop-3(vs106)* and *cat-2(tm2261);swip-13(gk1234)* animals.

Together, these results confirm that mutation in *swip-13* causes a DA dependent paralysis, consistent with the reversal of Swip by reserpine of the original *vt32* line.

In order to localize the expression and function of *swip-13*, a construct was made driving GFP by the putative *swip-13* promoter, encompassing the 1kb of sequence upstream of the ATG start codon (*pswip-13::GFP*). Confocal images of worms expressing this transgene show GFP expression in a number of head neurons, a pair of neurons resembling PDE, and a handful of tail neurons (Fig. 13). To demonstrate that among these neurons were the CEP, ADE, and PDE DA neurons, a marker labeling these neurons with mCherry (*pdat-1::mCherry*) was co-injected, and consistent co-labeling with GFP was observed in all DA neurons. After establishing that *swip-13* is endogenously expressed in DA neurons, we next sought to establish that this was its relevant site of expression for regulating DA signaling. Establishing expression in DA neurons is important, as expression in other cell types may impact DA signaling at sites either presynaptic or postsynaptic to the DA neurons. We therefore generated a construct driving the *swip-13* genomic sequence by the *dat-1* promoter to restrict expression of *swip-13* to DA neurons (*pdat-1::swip-13*). This transgene was injected into *swip-13(gk1234)* animals, and we observed a robust, significant rescue of the Swip phenotype in these transgenic animals (Fig. 14). Together, these results establish that *swip-13* is expressed in DA neurons, and that this expression is necessary for regulating DA signaling.

To begin to understand the potential function of *swip-13* in regulating DA signaling, we wished to establish the subcellular localization of SWIP-13 expression within the DA neurons. By understanding which compartments contain the SWIP-13

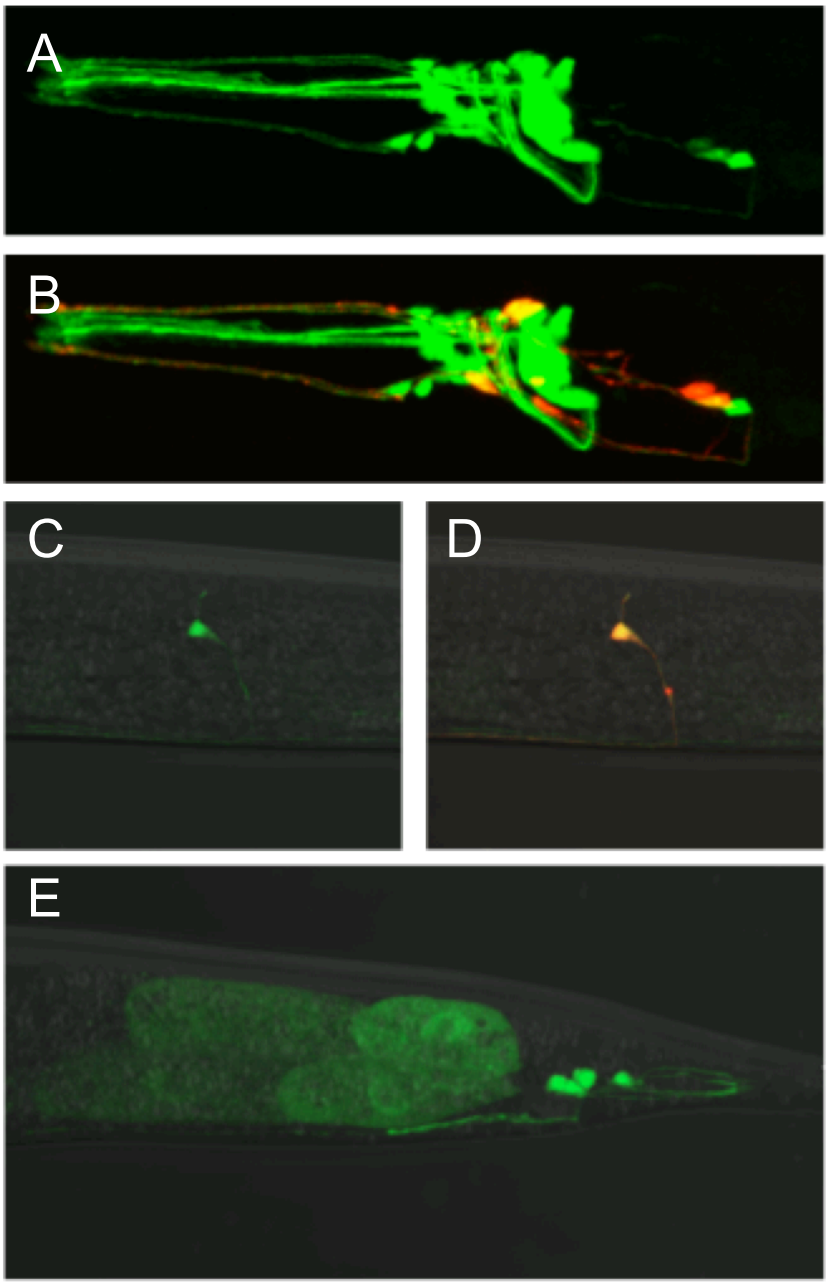

Figure 13 - Analysis of *swip-13* expression pattern. A fusion construct using 1kb upstream upstream of the *swip-13* ATG start site fused to GFP drives GFP expression in *swip-13* expressing cells. GFP (green) is observed in a number of neurons in the (A) head, (C) body, and (E) tail of the animal. Co-expression of *pdat-1::mCherry* (red) to label DA neurons shows complete colocalization of *swip-13*-driven GFP and DA neurons. This is shown by yellow overlap in the CEP and ADE neurons in the head (B) and in the PDE neurons in the body (D). All images were acquired with a 63X objective and represent compressed z-stacks.

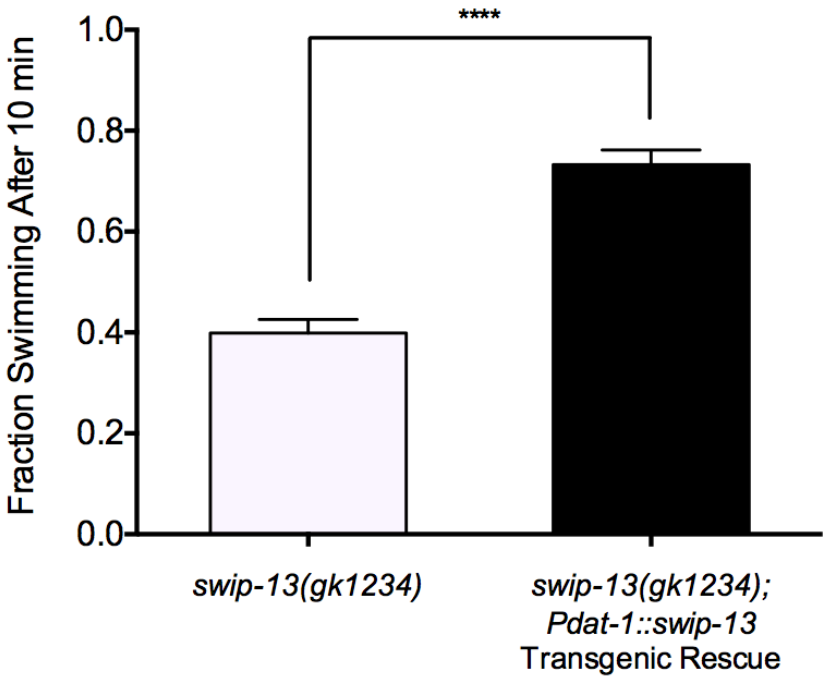

Figure 14 – *swip-13* acts in DA neurons to regulate Swip. A transgene driving genomic *swip-13* by the *dat-1* promoter *(pdat-1::swip-13*) was made to restrict *swip-13* expression to DA neurons. *swip-13(gk1234)* animals expressing this transgene showed a significant suppression of Swip compared to non-transgenic *swip-13(gk1234)* animals. Bars represent the average of three transgenic lines with at least 100 animals per line. Significance was calculated using a two-tailed Student's t-test with significance set at P<.05. ****P<.0001

protein, we might begin to hypothesize its potential functions in regulating DA signaling. To achieve this goal, we generated a fusion protein with GFP cloned in frame to the N-terminus of *swip-13*. This translational fusion gene was driven by the *dat-1* promoter to restrict its expression to the DA neurons (*pdat-1::GFP::swip-13*). Confocal images of animals expressing this transgene showed a distribution of the fusion protein throughout the cell, including the cell bodies and processes (Fig. 15). A marker of synapses (*pdat-1::mCherry::rab-3*) showed robust colocalization with *GFP::swip-13* in CEP, ADE, and CEP, suggesting that a fraction of *swip-13* is localized to synapses in these cells. Additional sites of expression include the cell body and the ciliated endings in all three types of DA neurons. Importantly, this transgene also rescued the Swip phenotype in *swip-13(gk1234)* mutant animals, indicating that it is a functional protein that is expressed at its relevant site of action for regulating DA signaling (Fig. 16). The cilia localization of SWIP-13 is interesting and might suggest a role for SWIP-13 in the regulation or perhaps development/maintenance of cilia. This is supported by the finding that *swip-13(gk1234)* animals show a mild dye-filling (Dyf) defect in the phasmid neurons (Fig. 17). The potential implications of this apparent cilia defect for the roles of *swip-13* in regulating DA signaling are unknown, however. We also observed that a mutation in *swip-13* based on analogous residues in related mammalian MAP kinases that should render the kinase inactive (K42R) resulted in an inability to rescue the Swip phenotype (Fig. 16). This indicates that *swip-13* is likely a functional kinase, and that its kinase activity is required for its regulatory actions on DA signaling. Due to this kinase-dependence of Swip rescue, we wondered whether the *vt32* mutation disrupts *swip-13*

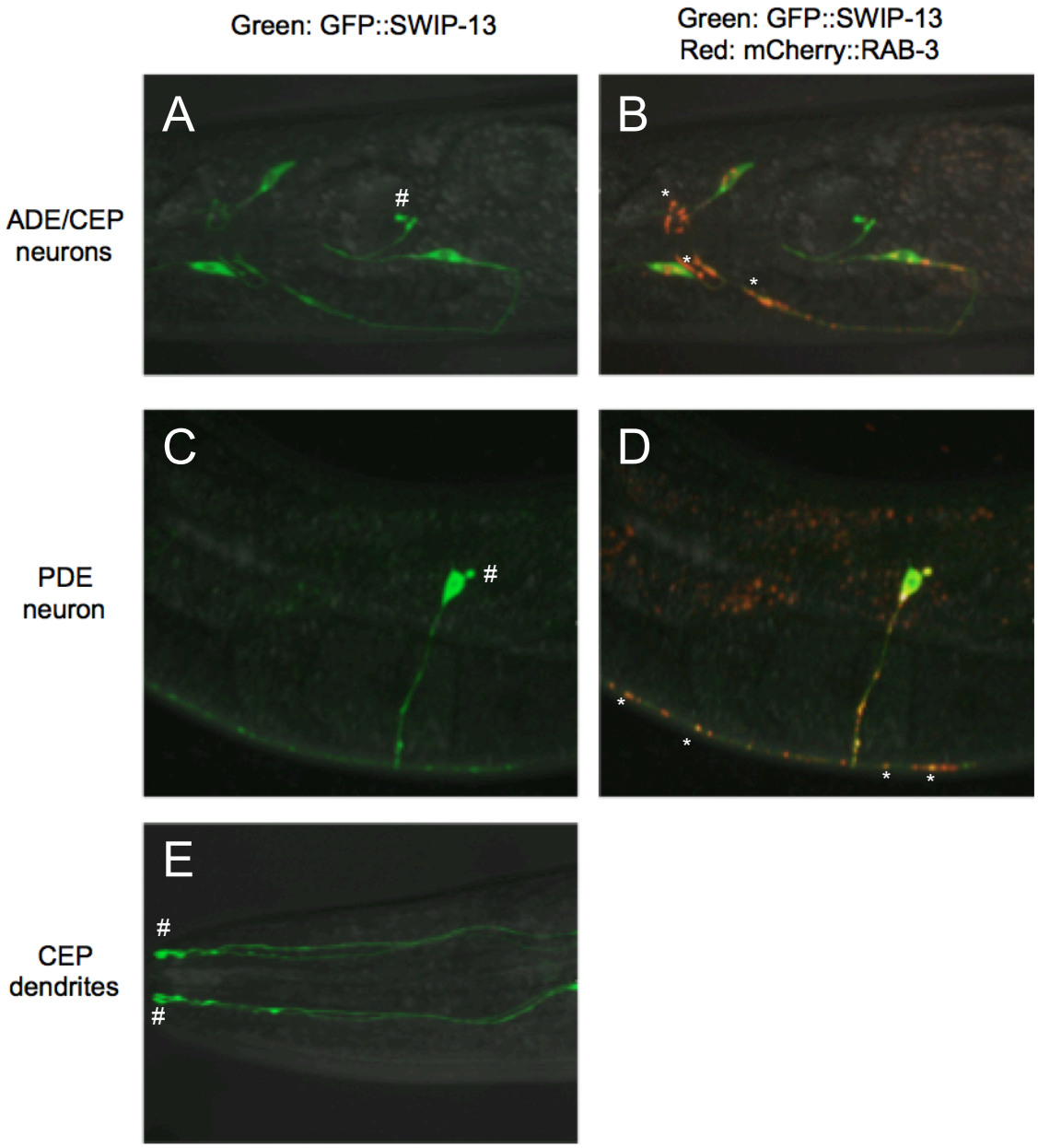

Figure 15 – SWIP-13 subcellular expression in DA neurons. (A) GFP::SWIP-13 fusion protein is seen in CEP and ADE cell bodies and processes, as well as ADE cilia (#). (C) In PDE, GFP::SWIP-13 is again seen in the cell body and processes, including the cilia (#) (B,D) Colabelling with synaptic marker mCherry::RAB-3 shows colocalization with GFP::SWIP-13 at putative synapses (*) in CEP, ADE (B) and PDE (D). (E) In CEP dendrites, GFP::SWIP-13 is seen along the process, and enriches at the ciliated endings (#). All images were acquired with a 63X objective and represent compressed z-stacks.

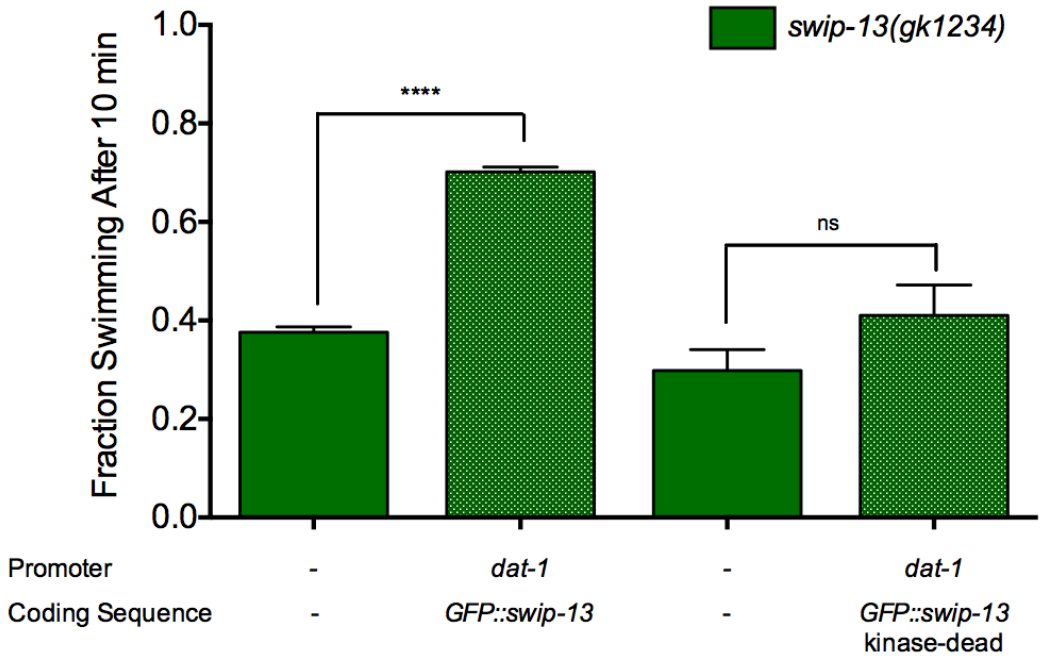

Figure 16 – GFP-tagged *swip-13* rescue of Swip. GFP-tagged *swip-13* used in figure 12 for subcellular *swip-13* localization is a functional transgene. DA neuron-specific expression of GFP::*swip-13* in *swip-13(gk1234)* mutants results in significant Swip suppression. A kinase-dead GFP::*swip-13* fusion, made by introduction a K42R mutation, does not significantly suppress *swip-13(gk1234)* Swip. Bars represent the average of three transgenic lines with at least 100 animals per line. Significance was calculated using a two-tailed Student's t-test for each transgene (transgenic vs. non-transgenic) with significance set at P<.05. ****P<.0001

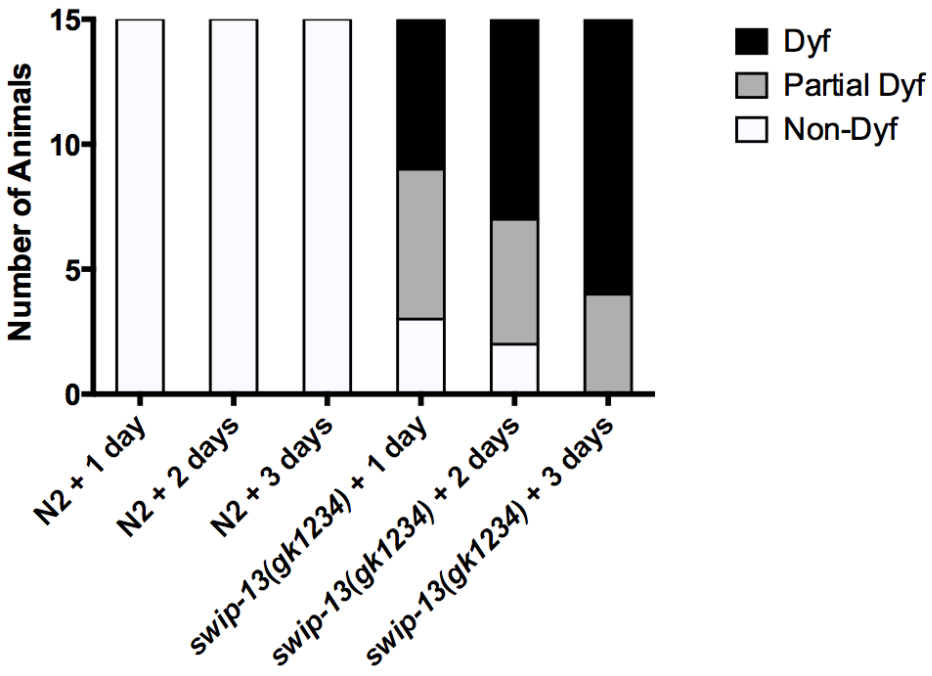

Figure 17 – *swip-13(gk234)* animals display a dye-filling defect in phasmid neurons. Animals were treated with the lipophilic dye DiI, and dye-filling was assess by the presence of red fluorescence in the phasmid neurons. Animals were staged as L4 animals and assayed after 1, 2, and 3 days at 20C. *swip-13(gk1234)* animals show dye-filling defects (Dyf) that worsen with age. For each condition, 15 animals were tested per day on 3 different days.

activity through loss of kinase activity. To observe the effects of mutation of this conserved arginine residue to glutamine, we used human ERK8 due to the ability to assess kinase activity of this protein using the artificial substrate myelin basic protein (MBP). We engineered in the *vt32*-analogous mutation (R59Q), as well as the kinase-dead mutation K42R into ERK8, and compared the ability of these mutants and wild-type ERK8 to phosphorylate MBP using an isotopic *in vitro* kinase assay. As has previously been reported, ERK8 efficiently phosphorylates MBP, and the kinase-dead ERK8(K42R) is incapable of increasing MBP phosphorylation above background levels (Fig. 18). Interestingly, ERK8(R59Q) appears to phosphorylate MBP to a small degree, but significantly less than wild-type ERK8. Additionally, ERK8 was shown to autophosphorylate, as has previously been reported, and again ERK8(K42R) showed no autophosphorylation, and ERK8(R59Q) had reduced levels of autophosphorylation. Altogether, these results indicate that mutation of Arg59 reduces its kinase activity on the artificial substrate MBP. Whether this is due to loss of intrinsic kinase activity, or loss of substrate recognition is unclear at this point, however.

DISCUSSION

The Swip phenotype is a powerful tool for observing states of elevated DA signaling in *C. elegans*. Here we have reported the identification of novel regulator of DA signaling revealed by a forward genetic screen based on the Swip phenotype. The *vt32* mutant generated via EMS mutagenesis demonstrates an intermediate Swip phenotype that is strongly rescued by reserpine pretreatment, consistent with a DA-dependent mode of paralysis. Importantly, despite the fact that *vt32* mapped to a region

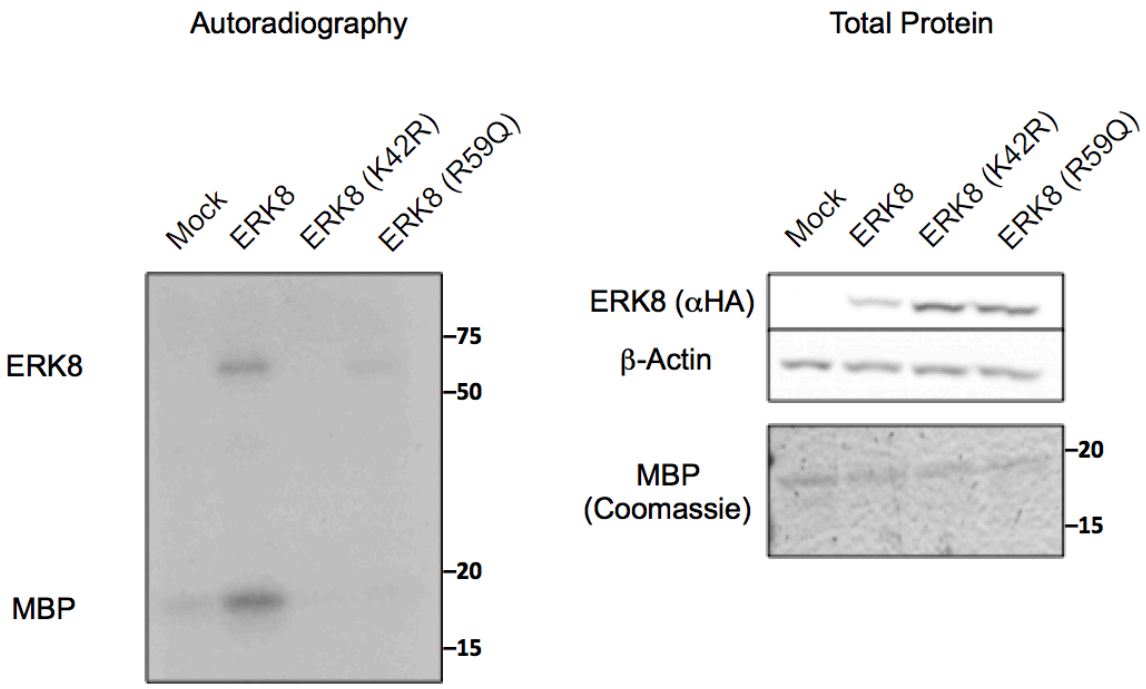

Figure 18 – *In vitro* kinase assay. ERK8 phosphorylates MBP above background levels. Kinase-dead ERK8(K42R) does not phosphorylate MBP above background levels, and ERK8(R59Q) has significantly reduced MBP phosphorylation compared to ERK8. WT ERK8 is also able to autophosphorylate, and ERK8(K42R) shows no autophosphorylation. ERK8(R59Q) has reduced autophosphorylation compared to WT ERK8. *In vitro* kinase assays were performed by Christian Marks from Roger Colbran's lab.

of LGIII that contained *dat-1*, sequencing of the *dat-1* genomic locus revealed no coding changes in *vt32* mutants. Whole-genome sequencing demonstrated the presence of a number of coding variants in genes located in the *vt32*-mapped region, and one of these genes, C05D10.2, encoded an uncharacterized mitogen-activated (MAP) kinase orthologous to the human gene ERK8. This candidate was exciting given the known roles of other MAP kinases in regulating DA signaling and specifically DAT function. The related MAP kinases ERK1/2 play many known roles in regulating DA neuron function, including regulation of DA release, DA synthesis, and DAT activity and trafficking (Bolan et al., 2007; Kivell et al., 2014; Moron et al., 2003; Subramanian and Morozov, 2011; Yu et al., 2011). The effects on DAT were particularly interesting with regards to potential roles of C05D10.2 given the fact that ERK1/2 are thought to positively regulate DAT function and trafficking, and if C05D10.2 plays a similar role, then loss of this gene would be expected to demonstrate a phenotype similar to a *dat-1* loss-of-function mutant. Importantly, analysis of the transcriptional profile of C05D10.2 using the online tool Wormviz, which shows relative expression of genes in various *C. elegans* cell-types across development (Gerstein et al., 2010; Spencer et al., 2011), revealed an enrichment of C05D10.2 in both late embryonic and L3/L4 DA neurons.

As the strongest candidate for the gene harboring the Swip-causing *vt32* mutation, we attempted transgenic rescue of *vt32* Swip using the wild-type C05D10.2 genomic locus, including 1kb upstream and downstream of the coding region to include putative regulatory regions. This transgene significantly rescued the Swip phenotype of *vt32* mutants, though this rescue was incomplete. We believe that this incomplete rescue is reflective of the nature of transgenic rescue experiments using transgenes expressed

as extrachomosomal arrays. This method of transgene expression results in mosaic and variable expression of the transgene, and selection of transgenics was based on a fluorescent co-injection marker (*punc-122::RFP*) that does not guarantee expression of C05D10.2 in its relevant cell type in every animal tested. Further support of the identity of the *vt32*-harboring gene came from analysis of the C05D10.2 deletion allele *gk1234.* This mutant demonstrated Swip at comparable levels to *vt32*, and was also significantly rescued by reserpine pretreatment. These lines of evidence all provide compelling evidence for the identity of the gene harboring the *vt32* mutation as C05D10.2, and we thus named this gene *swip-13*.

Crossing *swip-13(gk1234)* mutants with *dop-3(vs106)* and *cat-2(tm2261)* mutants further supported the DA-dependent nature of *swip-13(gk1234)* paralysis, as both of these mutations significantly rescued *swip-13(gk1234)* Swip. Interestingly, the rescue was not quite complete, particularly in the *swip-13(gk1234);dop-3(vs106)* double mutant, which might suggest that some aspect of *swip-13(gk1234)* paralysis could be DA-independent, but these genetic experiments suggest that at least the majority of the paralysis phenotype is DA-dependent. Importantly, *swip-13* promoter fusion with GFP revealed that *swip-13* is expressed in all DA neurons in the hermaphrodite, in addition to a number of additional unidentified head and tail neurons. Because of the expression in these other neurons, it was possible that *swip-13* acts in one of these other cell types to regulate DA signaling, possibly via actions of one of these neurons on DA neuron activity. A similar such mechanism appears to underlie the DA regulatory role of the previously characterized *swip-10* gene, which controls DA neuron activity through glial regulation of glutamate signaling on DA neurons (Hardaway et al., 2015). To rule out a

similar non-cell-autonomous role of *swip-13* and to localize the function of *swip-13* in its regulation of DA signaling, we generated a transgene driving genomic *swip-13* by the *dat-1* promoter (*pdat-1::swip-13*) to restrict expression to DA neurons. This transgene was expressed in a *swip-13(gk1234)* background, and we again observed a significant rescue of the Swip phenotype. This result demonstrates that DA neuron expression of *swip-13* is sufficient for normal DA signaling as revealed by normal swimming behavior in worms only expressing *swip-13* in these cells. This cell-autonomous role of *swip-13* in regulating DA signaling is exciting as it suggests that *swip-13* is a novel regulator of DA signaling that plays some role in the DA neuron itself, and could potentially regulate some aspect of DA neuron activity, DA release, or DAT-1 activity. Importantly, analysis of subcellular expression of the SWIP-13 protein using a GFP-tagged *swip-13* transgene revealed expression at presynaptic terminals. This synaptic site of expression makes *swip-13* well-poised to play some role at the presynaptic terminal where it could potentially regulate DA release or DAT activity. We cannot rule out actions at other sites, however, as expression was also observed in DA neuron cell bodies and cilia. Indeed, the mammalian orthologs of *swip-13,* ERK7/8, have been shown to play roles in regulating nuclear hormone receptors and cell division, as well as in regulating protein secretion from the endoplasmic reticulum, supporting potential roles of *swip-13* in biological processes localized to the cell body. Additionally, *Xenopus* Erk7 was recently shown to regulate ciliogenesis, making the cilia localization of *swip-13* unsurprising, though whether this potential action of *swip-13* impacts DA signaling is unknown at this point. Arguing against this idea, mutation of *che-3*, which is required for cilia establishment and maintenance, does not induce a Swip phenotype on its own, making

potential cilia defects in *swip-13* mutants unlikely to be the cause of Swip in these animals. In fact, preliminary qualitative analysis of *che-3;dat-1(ok157)* double mutant animals seemed to indicate perhaps a mild suppression of Swip, which could potentially explain the incomplete penetrance of the Swip phenotype in *swip-13* mutants due to a mild suppression of hyperdopaminergia due to cilia defects (personal communication, Andrew Hardaway). The validity of the *che-3* suppression of *dat-1* Swip requires more analysis, however, and any role potential ciliary defects in *swip-13* mutants might play in altering DA signaling has not been investigated.

Another important finding was the kinase-dependence of Swip rescue by the *GFP::swip-13* transgene. Because the kinase-dead version of this transgene was unable to rescue Swip in *swip-13* mutants, it seems likely that the SWIP-13 protein is a functional kinase, and the role it plays in regulating DA signaling requires this kinase activity. Due to the apparent kinase-dependence of swip-13 in regulating DA signaling, we wondered whether the vt32 mutation generated Swip due to loss of *swip-13* kinase activity. To monitor kinase activity, we utilized mammalian ERK8, which contains the Arg residue that was mutated to Gln in the *vt32* mutant line, and which we could use to monitor phosphorylation of the artificial substrate MBP. Previous work showed efficient phosphorylation of this protein by ERK8 *in vitro*, and the kinase-dead mutation K42R used in our Swip rescue experiments was shown to abolish MBP phosphorylation (Abe et al., 2002). We replicated these findings here, and also showed that the *vt32*-analogous R59Q mutation reduced phosphorylation of MBP. We also observed a reduction in autophosphorylation in this mutant. These results suggest a reduction in kinase activity resulting from mutation of Arg59 to Gln in ERK8, and likely in SWIP-13

as well. This is unsurprising given the high level of conservation of this Arg residue, which was reported by one group to have the highest level of evolutionary constraint amongst all residues in the CMGC family of kinases to which MAP kinases belong (Kannan and Neuwald, 2004). Based on modeling studies, this Arg residue is near the substrate phosphorylation site, and is thought play an important role in substrate recognition and kinase activation, suggesting that mutation of this residue would likely have drastic effects on the activity of SWIP-13 and ERK8. The fact that ERK8 seems to retain some kinase activity might suggest that this mutation does not completely eliminate activity of the protein, though the stoichiometric ratio between ERK8 and MBP in this assay might be significantly greater than that of ERK8/SWIP-13 and their relevant substrate for regulating DA signaling *in vivo*. Therefore, it remains possible that the R59Q mutation could be an effective null with regards to this regulation. What the substrate of SWIP-13 might be in its regulation of DA signaling *in vivo* remains to be determined, however, and is the subject of current investigation.

CHAPTER IV

SWIP-13/ERK8 EXERTS CONTROL OVER DA SIGNALING VIA REGULATION OF DA TRANSPORT BY DAT-1/DAT

INTRODUCTION

In the previous section, *swip-13* was established as a gene that acts in *C. elegans* DA neurons to regulate DA signaling and prevent the hyperdopaminergic Swip phenotype. *swip-13* encodes an ortholog of mammalian ERK7/8, the most recently discovered of the mammalian ERK family of MAP kinases. ERK7 was first cloned from rat brain using degenerate primers designed against conserved MAP kinase domains (Abe et al., 1999). This MAP kinase contained the signature ERK TEY activation motif, but was not activated by upstream activators that activate other MAP kinase proteins. Instead, ERK7 was found to be autoactivated by an intramolecular reaction involving its C-terminal domain, which was a unique 195 amino acid extension not found in other MAP kinases such as ERK1/2 (Abe et al., 2001). Shortly after the discovery of ERK7, human ERK8 was discovered using rat ERK7 cDNA to screen a human cDNA library (Abe et al., 2002). Surprisingly, ERK8 only showed 69% sequence identity with ERK7, and most of the divergence appeared to occur in the C-terminal tail region, where the proteins were only 53% identical compared to 82% in the kinase domain. This surprising amount of divergence suggested perhaps functional differences between these proteins, and indeed it was observed that, unlike ERK7, ERK8 had low constitutive activity and could be activated by serum and co-transfection of Src. Additionally, ERK8 was unable to phosphorylate the ERK7 substrate c-Fos, suggesting

possible differences in substrates between these two kinases. Despite these differences, however, ERK7 and ERK8 likely play a number of conserved roles. ERK7 and ERK8 have been shown to play roles in regulating nuclear hormone receptor signaling (Henrich et al., 2003; Rossi et al., 2011; Saelzler et al., 2006), autophagy (Colecchia et al., 2015; Colecchia et al., 2012), ciliogenesis (Miyatake et al., 2015), and cell proliferation (Iavarone et al., 2006; Rossi et al., 2016; Yang et al., 2013), among others. A role for ERK7/8 in the nervous system or in regulating DA signaling has not been reported as of yet, however.

Due to *swip*-13's site of action in DA neurons, it seemed reasonable that this gene might regulate DA neurons activity, DA release, or reuptake such that loss of this gene might perturb one or more of these mechanisms of DA signaling control and thus lead to a hyperdopaminergic state. As loss of *dat-1* function was the basis for the Swip screen that generated the *swip-13(vt32)* allele, a possible function of the SWIP-13 protein is regulation of DAT-1 function. If SWIP-13 positively regulates DAT-1 in some fashion, then loss of *swip-13* might be expected to result in reduced DAT-1 activity and a resulting Swip phenotype. Such a role has indeed been shown for mammalian ERK1/2, which are closely related to ERK7/8. ERK1/2 have been shown to regulate the trafficking of mammalian DAT, and act downstream of receptors such as D2 and KOR to mediate this regulation (Bolan et al., 2007; Kivell et al., 2014; Moron et al., 2003). It is therefore a possibility that SWIP-13/ERK8 perform a related role in regulating DAT-1/DAT function.

Aside from DAT-1 regulation, there are other potential roles for *swip-13* in the regulation of DA signaling. *swip-13* may act in a pathway that impacts the activity state

of DA neurons, which is controlled by the actions of receptors and ion channels whose dysfunction could potentially generate a hyperdopaminergic phenotype through increased DA neuron firing. One such mechanism appears to underlie the Swip phenotype of previously characterized *swip-10* mutant worms, though this gene appears to act in glia to regulate glutamate signaling on DA neurons. It is possible, however, that a gene such as *swip-13* might produce a hyperdopaminergic phenotype in a similar manner, though through direct actions on activity-controlling ion channels and receptors in the DA neurons themselves. There are a few candidate channels, such as the stretch receptor *trp-4* and the amine-gated chloride channel *lgc-55* that are expressed in DA neurons and control their activity, and manipulation of which can impact Swip (Li et al., 2006b; Ringstad et al., 2009; Safratowich et al., 2014; Safratowich et al., 2013). SWIP-13 may also act to regulate DA release more locally at the presynaptic terminal, where actions on SNARE machinery and associated regulatory signaling pathways could potentially impact DA vesicle fusion. Again, work from the related ERK1/2 have revealed roles for these proteins in regulating exocytosis, with evidence suggesting roles in both enhancing and inhibiting exocytosis (Jovanovic et al., 2000; Kushner et al., 2005; Subramanian and Morozov, 2011; Vara et al., 2009). If *swip-13*/ERK8 similarly acts to inhibit exocytosis, then that might explain the hyperdopaminergia of *swip-13* mutants, which could result from a loss of a *swip-13*-mediated exocytotic braking mechanism.

In this section, we attempt to identify the role that *swip-13* and ERK8 play in regulating DA signaling. We show here, using a combination of genetics, and biochemical and *in vivo* assays that SWIP-13 and ERK8 regulate DAT-1/DAT activity.

We also identify a potential ERK8/RhoA/DAT pathway through which this regulation might occur.

MATERIALS AND METHODS

C. elegans strains and husbandry

Strains were grown on bacterial lawns of OP50 and maintained at 12°C to 20°C as previously described (Brenner, 1974). N2 Bristol served as our wild-type strain. The strain VC2695 contained the allele *gk1234,* which was a large deletion of the gene C05D10.2, and was obtained from the Caenorhabditis Genetics Center (CGC, University of Minnesota, Minneapolis, Mn). The strain LX703 containing a deletion in *dop-3 (dop-3(vs106*)) was also obtained from the CGC, and the *cat-2(tm2261)* strain was obtained from Shohei Mitani at the National Bioresource Project at the Tokyo Women's Medical University. The strain IR724 (N2; *uvEX724 [pasic-1:SNB-1::SEpHluorin, pRF4*]) that was used for FRAP experiments was obtained from Nektarios Tavernarakis (Greece).

Swip assays

For both manual and automated assays, staged L4 animals were generated by hypochlorite treatment of gravid adults and plating of synchronized L1 animals and growth for various days at 12-20°C. For manual assays, ~10 animals were picked into 100uL of water and analyzed for number of paralyzed animals after 10 min. For each genotype/treatment, ~80 animals were assayed per experiment, with at least 3

experiments performed by 1-2 experimenters. For automated analyses, animals were picked one at a time into 10uL of water and 10 minute movies of these individual worms' swimming behavior were captured and analyzed as previously described (Hardaway et al., 2014). Briefly, videos were first analyzed using the in-house tracking software Worm Tracker, which fits a spine to the worm and calculates the frequency of body bends over time. This frequency information is then processed by another in-house program called SwimR, which uses this information to calculate various parameters and to output visual representations of the data. For osmosuppression experiments, MilliQ water was supplemented with sucrose to achieve an osmolarity of 150 mOsm.

Genetic crosses and genotyping

Crosses were performed using integrated fluorescent markers *in trans.* In order to verify presence of mutations, single worm PCR was used using a three primer multiplex strategy. N2 and mutant control reactions were performed in parallel, along with a synthetic heterozygote reaction containing both N2 and mutant DNA. For generation of the *swip-13(gk1234);dat-1(ok157)* double mutant, recombination was required due to the location of both genes on LGIII. After selfing of the double heterozygote, lines that appeared to be homozygous for either *dat-1(ok157) or swip-13(gk1234),* and heterozygous for the other mutation were selected. These lines were then selfed and a double homozygous knockout line was selected. Platinum PCR Supermix was used for all genotyping PCR reactions and reactions were analyzed via agarose gel electrophoresis. The following oligonucleotide primers were used for genotyping mutations used in this study:

swip-13(gk1234):

5’ sense – GGAATGTGTTACACCGGTGAG

3’ antisense - GTTTATCCACCACTTCCGGA

inner sense – CTGCGATTGATATGGTTCAGAG

dat-1(ok157):

5’ sense – cttgcctgggggcttcattattt

3’ antisense - cgcattgacgaatttgtagattcctacc

inner antisense – tcttcagcagctgaaatcttttcagc

6-OHDA degeneration assay

Assays were performed as previously described (Nass et al., 2002), with minor modifications. BY250 animals were used due to the presence of GFP in DA neurons, allowing for visualization of DA neuron morphology. Synchronized L1 worms were plated on 10 cm 8P plates seeded with NA22 bacteria (8P/NA22) for 1 day at 20°C until they reached the L2-L3 stage. These animals were then washed in M9 three times, and pelleted worms were then treated with 25, 35, or 50 mM 6-OHDA supplemented with ascorbic acid (5, 7, or 10mM, respectively). Worms were covered and gently agitated for 1 hr at room temperature, and then the entire volume of worm solution was plated on 8P/NA22 plates. These plates were placed at 20°C for 3 days, allowing these worms to grow to adults, and these animals were scored for degeneration. Scoring consisted of selecting a concentration of 6-OHDA that caused robust, yet incomplete DA neuron degeneration in wild-type, and then mounting worms on 2% agarose pads with 2.5mM levamisole used as a paralytic. CEP neuron degeneration was scored by assigning a

number 0-4 for each animal, with 0 representing complete loss of CEP dendrites, and 4 representing intact dendrites for all 4 neurons. For each genotype, 50 worms were scored in triplicate with experimenter blinded to genotype and experiments were performed on three separate days.

C. elegans embryonic cell cultures

N2, *swip-13*, and *dat-1* worms were maintained at 20° C. Embryonic cell culture was performed as described previously (Carvelli et al., 2004). Briefly, animals full of embryos were collected into 15 mL tubes and washed at least 3 times by centrifugation at 1350 rpm for 3 minutes in water until any visible bacterial residue was removed. After the last wash, water was removed and the worm pellet was suspended in a solution containing 2 mL bleach and 0.5 mL 10N NaOH and then filling to 10 mL water. Animals were incubated in this solution on a shaking rocker at room temperature for 3-5 minutes or until 70-80% of animals had their cuticle broken and embryo released, as verified by placing a few microliters of solution on a coverslip and observing through a microscope. Reaction was stopped by filling the tube with egg buffer (NaCl 118 mM, KCl 48 mM, CaCl2 2 mM, MgCl2 2 mM, HEPES 25 mM, pH 7.3, 340 mOsm) and centrifuging. The pellet was then washed 3 more times with egg buffer and centrifugation. After last wash, egg buffer was removed and 5 mL 60% sucrose was added then tube was filled to 10 mL with water for a final concentration of 30% sucrose. Tubes were then centrifuged for 6 minutes at 1200 rpm. Following centrifugation embryos float at the solution meniscus, embryos were collected into a new tube. Embryos were then washed with water 2 times with centrifugation at 1,350 rpm for 3 minutes. After last wash, water was removed and

embryos were moved to 1.5-2 mL tubes with 1 mL chitinase solution (1 U per ml). Embryos were then incubated in chitinase solution at room temperature on tube rotator. Incubation was carried out for approximately 1 hour or until 80% of embryos have their egg shell digested. Tubes were then centrifuged at 3,800 rpm for 3 min. Solution was then aspirated off and 1 mL of L-15 media (Leibovitz's L-15 media with 10% fetal bovine serum, 10 U ml-1 penicillin and 50 µg ml-1 streptomycin adjusted to 340 ± 5 mOsm) was used to resuspend the pellet. In order to dissociate the cells, samples were pipetted up and down several times with intermediate centrifugations and resuspension with L-15 buffer. When the majority of embryos were dissociated the tubes were again centrifuged, solution aspirated, and 1 mL of L-15 was added. The solution was than filtered to remove hatched larvae, clumped cells, or undissociated embryos using 5 µm filters applied to 3-5 mL syringe. Solution was filtered (what kind of filter) and washed twice with 2 mL of L-15. Samples were centrifuged at 3,800 rpm for 3 minutes. Following centrifugation solution was aspirated down until 5 mL of solution remained and pellet was resuspended. Cells were counted by using a Countess Automated Cell Counter (Invitrogen) and 2 million cells were plated on peanut lectin-treated glass coverslips. The next morning after cells settled an additional 1 mL of L-15 media was added to cells. Peanut lectin-treated coverslips were obtained by incubating sterilized glass coverslip with 0.5 mg ml-1 peanut lectin for 30 minutes under a sterile hood. Peanut lectin was then aspirated off and plates were left under UV light overnight.

[3H] DA uptake in *C. elegans* cultures

Uptake assays were carried out 4 days after primary cell preparation. Cells were washed with 1 mL bath solution (145 mM NaCl, 5mM KCl, 1 mM CaCl2, 5 mM MgCl2, 10 mM HEPES, 20 mM D-Glucose, pH 7.2, 350 mOsm) 3 times, followed by an incubation with 5nM [3H] DA in bath solution containing TAP (100 µM ascorbic acid, µM tropolone, and µM pargyline) for 5 minutes with or without 10µM Imipramine present. Cells were then washed 4 times with 1 mL ice cold bath TAP solution. Lastly 500 mL 1% TRITON-X was added and samples were incubated for 10 minutes on a shaking rocker to lyse the cells. Samples were collected and 8 mL scintillation cocktail (Research Products International Corp., Econo-Safe Biodegradable Counting Cocktail) was added before counting in scintillation counter (Beckman Coulter LS 6500).

Fluorescence recovery after photobleaching (FRAP) assay

Young adult animals were staged by picking L4 animals and growing at 20°C overnight. The day of the experiment, animals were mounted on 2% agarose pads and immobilized using 0.05% levamisole. Fluorescence recovery after photobleaching (FRAP) experiments were performed using a Zeiss LSM 510 inverted confocal microscope. PDE synapses were chosen for these analyses due to the more 2D layout and lack of overlap of the PDE processes compared with the CEP and ADE projections. Synapses were identified by Synaptobrevin::SEpHluorin fluorescence in the PDE processes and were bleached with a laser at 488 nm, 15 mW for 5–10 s to an intensity 20–30% that of the original fluorescence value. Fluorescence was then monitored every 10 s for 2 min and analyzed using Zeiss LSM 510 software. Percentage recovery was

then calculated as the fluorescence at each time point divided by the initial fluorescence value after bleaching. We analyzed 20–25 PDE synapses per genotype, with an average of 3–5 synapses per animal. Recovery plots were fit by nonlinear regression methods to a one-phase exponential model in Prism 5.0 (GraphPad).

In vitro expression of ERK8/DAT and regulators

Human SH-SY5Y cells were obtained from ATCC and were grown in 1:1 F12/DMEM solution supplemented with 10% fetal bovine serum and penicillin/streptomycin. Cells were plated in either 24-well (single point DA uptakes), 96-well (DA uptake saturation curves) or 10cm plates (biochemical experiments) at a density of 9×10^4 cells per cm^2. HEK-293T cells were grown in DMEM supplemented with 10% fetal bovine serum with penicillin/streptomycin and were plated at 2×10^5 cells per well in 6-well dishes for Rho activation assays. For DA uptake and biotinylation experiments, plates were first coated with poly-D-lysine to enhance cell adherence. In all experiments, cells were grown at 37°C for one day before transfection with Mirus TransIT LT1 transfection reagent in OptiMEM media at a ratio of 1:3 DNA/Reagent, with the amount of DNA scaled to the size of the plate according to the manufacturer's instructions. The following ratios of DNA were used for each experiment:

DA uptakes and biotinylations: 1:4 DAT/pcDNA3.1, 1:4 DAT/HA-ERK8

GFP control experiments: 1:4 GFP/pcDNA3.1, 1:4 GFP/HA-ERK8

Rho Activation Assays: 100% pcDNA3.1 or HA-ERK8

GFP-C3 DA uptakes: 1:4 DAT/pcDNA3.1, 1:1:3 DAT/pcDNA3.1/HA-ERK8, 1:1:3 DAT/GFP-C3/pcDNA3.1, 1:1:3 DAT/GFP-C3/HA-ERK8

Cells were then grown for an additional two days before DA uptake or biochemical experiments.

DA uptake assays in SH-SY5Y cells

DA uptake assays were performed in triplicate or quadruplicate as previously described (Apparsundaram et al., 1998). Briefly, cells were washed with KRH buffer three times before incubation in KRH containing 10μM desipramine (to block background endogenous norepinephrine transport activity), 100μM pargyline, 100μM tropolone, and 100μM ascorbic acid with or without 10μM cocaine at 37°C for 15 min. A 5X concentrated solution of 5% [^{3}H]DA/ 95% unlabeled DA was then added to each well for to achieve a 1X concentration of DA, and cells were again incubated at 37°C for 15 min. For DA uptake saturation curves, final total concentrations of DA used were 500nM, 1uM, 2uM, 3uM, and 6uM. Need to note what was used to define nonspecific counts. For single point DA uptake assays, 6uM DA was used. After incubation in DA solution, cells were then washed with ice cold KRH three times and then Microscint 20 scintillation fluid was added to the cells. Cells were incubated in this solution for at least an hour before being analyzed by TopCount Microplate Scintillation Counter. Cells plated and transfected in parallel were used to determine protein concentrations in each condition to normalize uptake to total protein.

Cell surface biotinylation assays

Transfected cells in 10cm dishes were washed twice in ice-cold PBS supplemented with 0.1 mM $CaCl_2$ and 1 mM $MgSO_4$. Cells were then incubated in

Sulfo-NHS-Biotin at 1 mg/mLfor 30 min at 4°C with very gentle agitation. Excess biotin was quenched with 0.1 M glycine in PBS and then cells were lysed in ice cold hypotonic lysis buffer (10 mM Tris-HCl pH7.5) containing Sigma protease inhibitor cocktail. The membrane pellet was then solubilized in ice-cold lysis buffer (20 mM Tris-HCl pH 8, 137mM NaCl, 2mM EDTA, 1% TritonX-100), and cell lysates were analyzed by BCA assay to determine protein concentration. Equal amounts of protein were either placed in Laemmli sample buffer for total protein anaylsis, or were placed on prewashed Steptavadin-conjugated beads and incubated at room temperature for 1 hour. Beads were then washed three times with ice-cold lysis buffer, and samples were eluted in Laemmli sample buffer before analysis via SDS-PAGE electrophoresis and Western blotting. Equal amounts of total cell lysates were analyzed in parallel to determine total protein levels. A rat anti-hDAT antibody (Millipore; MAB 369; 1:1000) was used to visualize DAT and mouse anti-TfR (ThermoFisher; H68.4, 13-6890; 1:1000) antibody was used to detect transferrin receptor as a loading control. HRP-conjugated goat anti-rat and goat anti-mouse secondary antibodies (1:10,000) were used. Total DAT was normalized to total TfR, and surface DAT was normalized to surface TfR.

Rho Activation Assay

For Rho activation assays, a RhoA pull-down activation assay kit (Cytoskeleton, Inc.) was used. Transfected HEK-293T cells were washed in ice-cold TBS and lysed in supplied lysis buffer with protease inhibitors. Lysates were clarified by centrifugation and immediately snap frozen in liquid nitrogen and stored at -80 to prevent loss of active Rho due to Rho-GAP activity. Protein concentrations were determined using Bio-Rad

protein assay, and frozen lysates were rapidly thawed and 800ug of protein was added to 30uL of GST-RBD beads and incubated with mixing at 4 for 1 hour. Beads were then washed once with supplied wash buffer and 2X Laemmli buffer was added to elute protein from the beads. Eluates, along with pure RhoA protein and 30ug of total lysates from each sample were run on a 12% SDS-PAGE gel and transferred to Bio-Rad Immun-Blot PVDF with 1.5 micron pore size for better retention of small proteins. After transfer, membrane was dried for 30 minutes, and then rewet with methanol followed by TBST. Membrane was blocked in 5% dry milk in TBST for one hour, and then incubated in 1:500 anti-RhoA antibody in TBST overnight at 4. Membrane was then washed once in TBST, and incubated in 1:10000 HRP-conjugated goat anti-mouse antibody for one hour at room temperature followed by five 10 minute washes in TBST. Membrane was imaged using Bio-Rad Clarity ECL reagent. The membrane was then stripped and reprobed with monoclonal mouse anti-HA antibody (12CA5, 1:1000, goat anti-mouse 1:10,000), followed by HRP-conjugated anti-β-actin antibody (1:20,000). Total RhoA was normalized to β-actin, and active RhoA was normalized to this value.

Graphical and Statistical Methods

Data were analyzed and graphed using either SwimR software (described above), or using Prism 6.0 (GraphPad, Inc., La Jolla, CA). All statistical analyses and curve fits were performed in Prism 6.0. Descriptions of all statistical tests are noted in the figure legends. A $P<.05$ was taken as statistically significant.

RESULTS

After establishing the DA dependence of *swip-13* mutants and localizing its function to DA neurons, we wished to investigate potential mechanisms underlying the hyperdopaminergic state in these animals. As loss of *dat-1* was the basis for the screen that generated the *swip-13(vt32)* mutant, one potential mechanism for Swip in *swip-13* mutants would be reduced *dat-1* activity. We observed that overexpression of *dat-1*, using an integrated GFP-tagged *dat-1* transgene that we have previously shown to be functional, rescued *swip-13* paralysis to near wild-type levels (Fig. 19). This demonstrates that increasing the amount of *dat-1* can compensate for the defect in DA signaling in *swip-13(gk1234)* animals, but does not necessarily indicate that loss of *dat-1* activity underlies the hyperdopaminergic state of *swip-13* mutants.

To begin to address this possibility, we utilized a previously characterized assay for probing DAT-1 activity *in vivo* in the worm. This assay employs the use of the DAT-1 substrate 6-hydroxydopamine (6-OHDA) that, when DAT-1 is functioning properly, will enter the DA neurons and induce cell death (Nass et al., 2002). We can observe this cell death using a line with an integrated transgene expressing GFP in DA neurons (*vtIs7*), and loss of this fluorescence is indicative of cell death. N2 animals show dramatic cell death when treated with 6-OHDA, whereas *dat-1(ok157)* animals are highly resistant. Both *swip-13(vt32)* and *swip-13(gk1234)* animals displayed an intermediate sensitivity to 6-OHDA, with a significant reduction in cell death compared to N2 animals, but not as much protection as seen with *dat-1(ok157)* animals (Fig. 20).

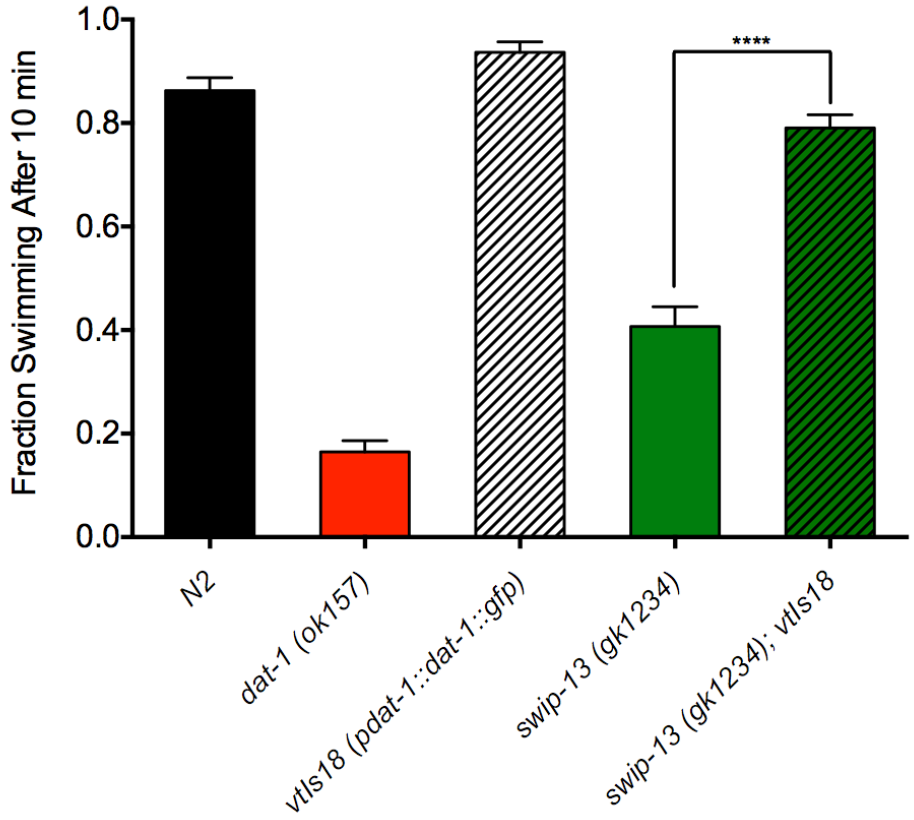

Figure 19 – GFP-tagged DAT-1 overexpression rescues *swip-13(gk1234)* Swip. A functional DAT-1::GFP expressing transgene *vtIs18* (*pdat-1::dat-1::gfp*) rescues the paralysis of *swip-13(gk1234)* mutant animals. This is demonstrated by the significant difference between *swip-13(gk1234)* and *swip-13(gk1234); vtIs18* animals. Data was analyzed using a one-way ANOVA with Bonferonni posttests comparing *swip-13(gk1234)* to *swip-13(gk1234); vtIs18.* Significance was set at P<.05. ****P<.0001

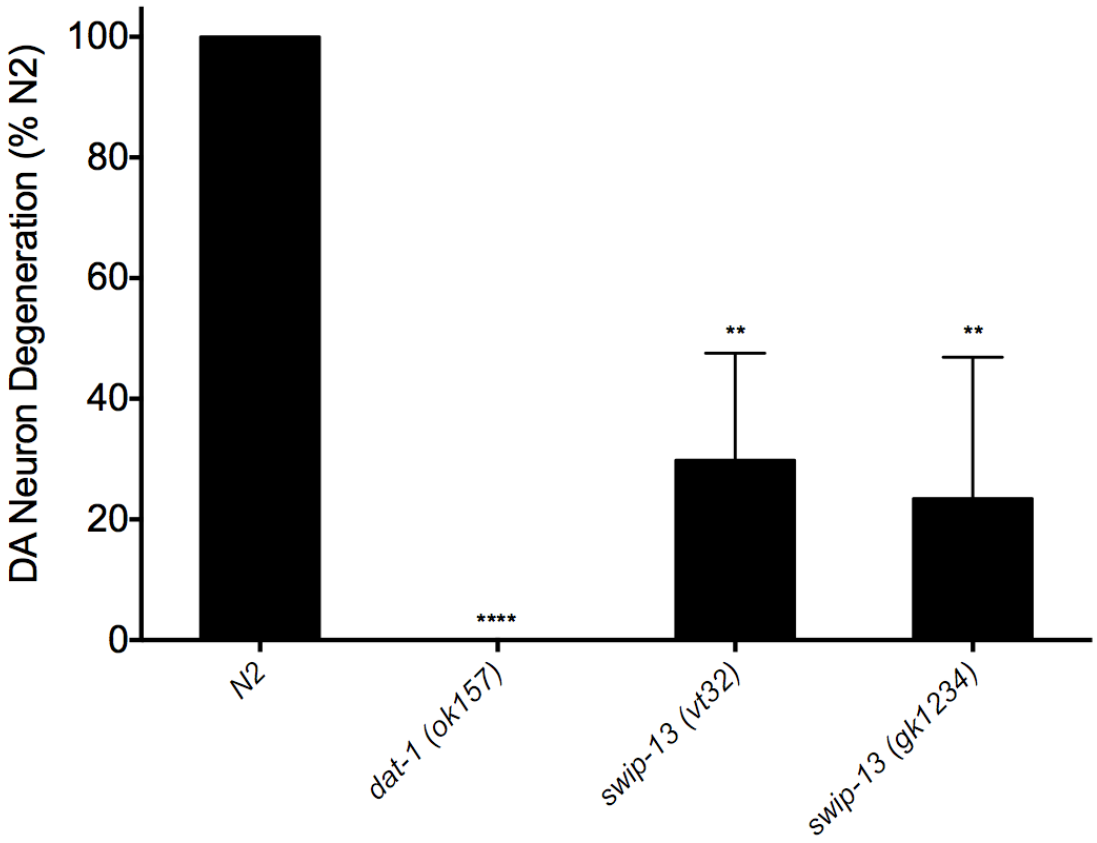

Figure 20 – *swip-13* mutants have reduced sensitivity to 6-OHDA. Treatment of N2 animals with GFP-labeled DA neurons with the DA-neuron selective, DAT-1-dependent neurotoxin 6-OHDA leads to robust degeneration of DA neurons, as measured by loss of GFP-labeled CEP dendrites. *dat-1(ok157)* mutants are insensitive to this neurotoxin, shown as an absence of DA neuron degeneration. Both *swip-13(vt32) and swip-13(gk1234)* have reduced sensitivity to 6-OHDA compared to N2 animals. Data was analyzed using a one-way ANOVA with Bonferonni posttests comparing all genotypes to N2. Significance was set at P<.05. **P<.01 ****P<.0001

This finding is consistent with the model of loss of *swip-13* leading to reduced, and not complete loss of, DAT-1 activity. To test this model using a genetic approach, *swip-13(gk1234)* was crossed to *dat-1(ok157)* to create *swip-13(gk1234);dat-1(ok157*) double mutants, and the Swip phenotype of these animals was compared to that of the single mutants. In water, there was no significant enhancement of Swip in *swip-13(gk1234);dat-1(ok157)* animals compared to *dat-1(ok157)* animals, suggesting these genes act in the same pathway (Fig. 21A). A concern about this experiment was the potential ceiling effects seen with *dat-1(ok157)* animals, which paralyze at near completion in water. To get around this issue, we used osmosuppression in sucrose solution to increase the dynamic range in which we might see additivity between these two mutations. Our lab has previously reported that *dat-1(ok157)* paralysis can be suppressed by increasing the osmolarity of the solution in which the worms are swimming, and this osmosuppression was utilized by our lab to demonstrate that *dat-1* and another Swip mutant *swip-10* act in different genetic pathways to regulate DA signaling based on additivity of their Swip phenotypes (Hardaway et al., 2015). Using this same strategy, we again observed no additive effects of combined *swip-13(gk1234)* and *dat-1(ok157)* mutations in 150 mOsm solution (Fig. 21B). This was reflected in more detail in a comparison of heat maps between genotypes in both water and 150mOsm conditions, where both qualitatively and quantitatively the paralysis of *swip-13(gk1234);dat-1(ok157)* and *dat-1(ok157)* were comparable (Fig. 21C,D). Finally, to more directly test a potential influence of *swip-13* mutation on *dat-1* activity, our collaborator Lucia Carvelli (University of North Dakota) performed [3H]DA uptake in

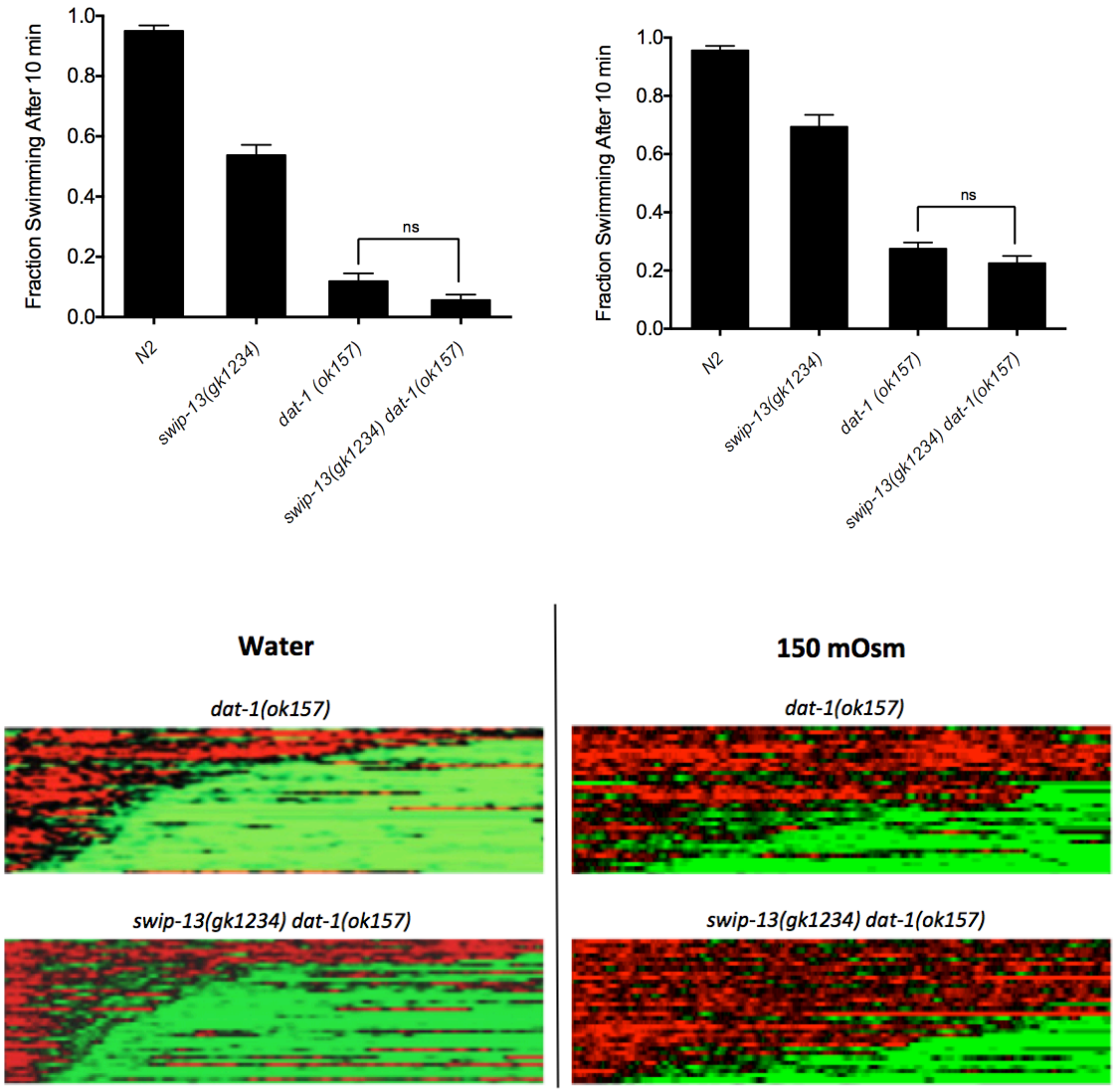

Figure 21 – *swip-13* and *dat-1* act in the same genetic pathway to generate Swip. (A) In water, *dat-1(ok157) and swip-13(gk1234) dat-1(ok157)* mutants display similar Swip behavior, with no significant difference between genotypes. (B) To increase the range in which we might see additivity between *swip-13(gk1234)* and *dat-1(ok157*), we performed Swip assays in 150mOsm sucrose-supplemented water to suppress Swip. In this context, there is still no significant difference between *dat-1(ok157)* and *swip-13(gk1234) dat-1(ok157)* animals. Data was analyzed using a one-way ANOVA with Bonferroni posttests comparing dat-1(ok157) to swip-13(gk1234) dat-1(ok157) in both (A) and (B). (C,D) Heat map analysis shows no enhancement of Swip in *swip-13(gk1234) dat-1(ok157)* animals compared to *dat-1(ok157)* mutants in either water (C) or 150 mOsm solution (D). Data acquired with the assistance of Osama Refai.

primary neuron cultures from dissociated worms. As expected, *dat-1(ok157)* mutants had almost no specific DA uptake, as assessed by subtracting out uptake in the presence of the DAT-1 antagonist imipramine (Fig. 22). Excitingly, *swip-13(gk1234)* animals had an approximately 50% reduction in DA uptake compared to N2 animals. This level of uptake is consistent with the intermediate Swip phenotype observed in *swip-13(gk1234)* animals, and is also in line with the intermediate 6-OHDA sensitivity observed in these animals.

The above experiments strongly support a model where *swip-13* and *dat-1* act in the same genetic pathway to produce Swip. To test an alternative hypothesis that *swip-13* may influence vesicle fusion and DA release, we employed a fluorescence recovery after photobleaching (FRAP) assay using a pH-sensitive SNB-1::SepHluorin transgene expressed in DA neurons (Voglis and Tavernarakis, 2008). This technique takes advantage of the fact that this fluorophore is localized to the vesicle lumen, where the pH is low and the fluorophore is quenched. When the vesicle is fused to the plasma membrane, however, the fluorescence increases, and by photobleaching a synapse, the rate of recovery of fluorescence can be used as a proxy for the rate of vesicle fusion. Using this technique, we observed no difference in fluorescence recovery rates between N2 *and swip-13(gk1234)* animals (Fig. 23), suggesting that the rate of DA vesicle fusion is not different between these two genetic backgrounds

Due to the high level of similarity between *swip-13* and its human ortholog ERK8, we wished to test whether the apparent interaction between *swip-13* and *dat-1* might be paralleled by an interaction between human ERK8 and DAT. To test this idea, we co-expressed these two proteins in the human neuroblastoma cell line SH-SY5Y. We

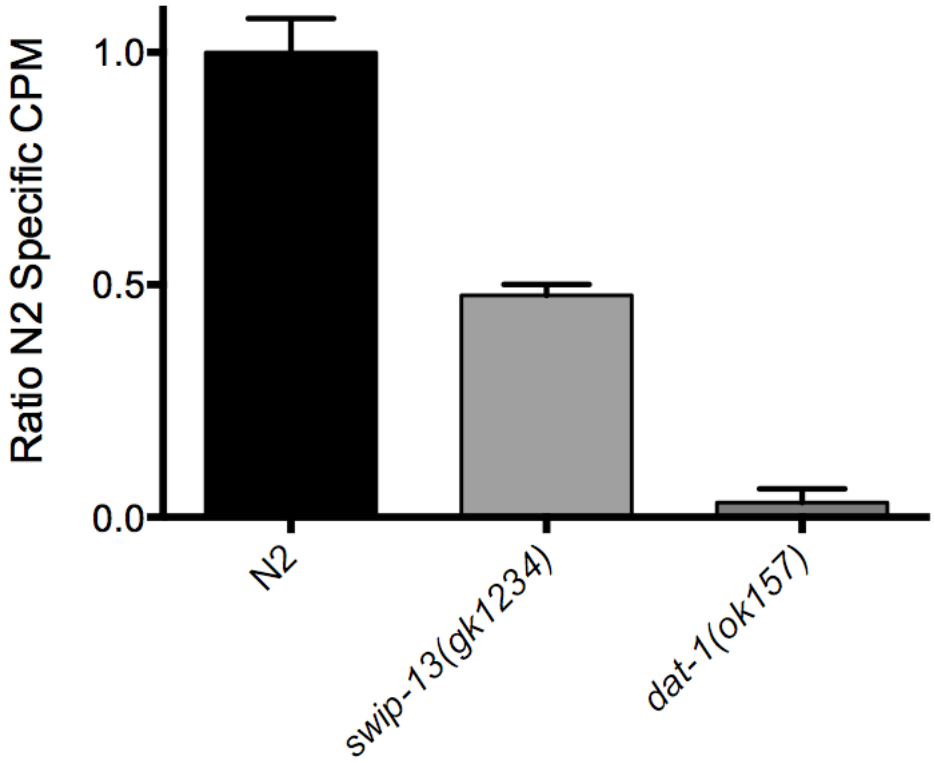

Figure 22 – [3H]DA uptake in *C. elegans* primary cultures. Primary embryonic cultures were treated with [3H]DA, and specific uptake was calculated by subtracting uptake in the presence of the DAT-1 inhibitor imipramine. Preliminary results show a decrease in [3H]DA uptake in cultures from *swip-13(gk1234)* animals compared to those from N2 animals. Uptakes were performed by the lab of Lucia Carvelli at the University of North Dakota.

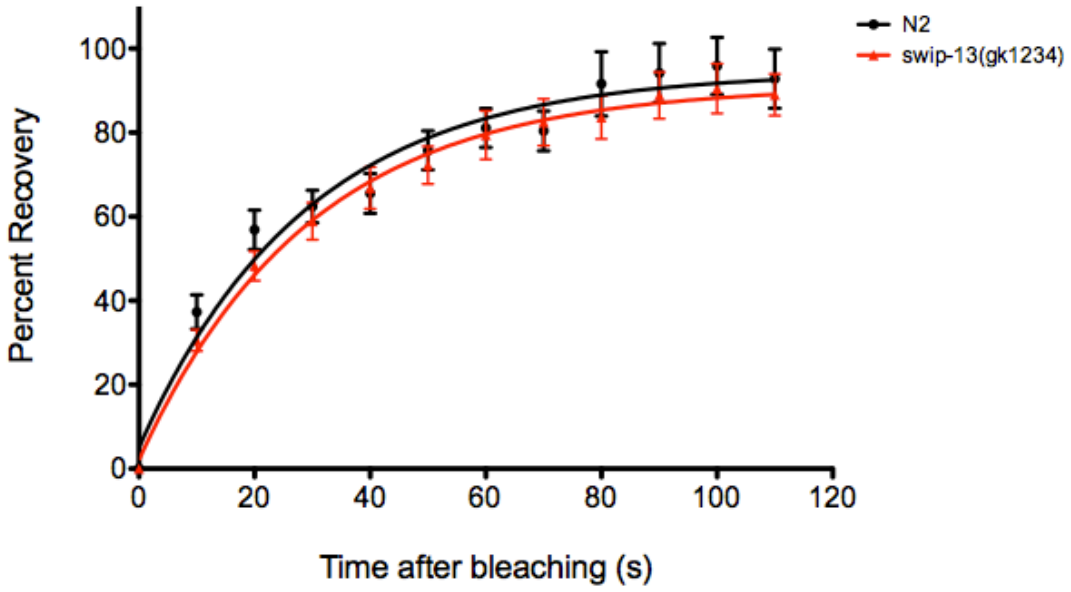

Figure 23 – Fluorescence recovery after photobleaching (FRAP) measurement of vesicle fusion. A transgene driving expression of a SNB-1::SEpHluorin fusion protein in DA neurons (*pasic-1::SNB-1::SEpHluorin*) was used to measure SV fusion rate. This fluorophore is quenched by the low pH of the SV lumen, and fluoresces upon vesicle fusion due to the higher pH of the extracellular space. Bleaching of this fluorescence and analysis of the recovery of the fluorescent signal allows for a measurement of the rate of SV fusion. Comparison of this recovery between N2 and *swip-13(gk1234)* animals expressing this transgene revealed no significant difference between genotypes. Recovery plots were fit by nonlinear regression methods to a one-phase exponential model, and data was analyzed using a repeated measures ANOVA, with significance value set at $P<.05$

chose this cell line due to the fact that these cells have neuronal characteristics and catecholaminergic phenotypes such as TH and NET expression, which might represent an environment somewhat similar to the environment in which ERK8 and DAT might interact *in vivo*. We found that cells expressing both ERK8 and DAT had a 97% of DAT trafficking by the small GTPase RhoA. The Amara lab recently demonstrated that RhoA regulates DAT endocytosis in response to AMPH treatment (Wheeler et al., 2015), and we thought that this pathway was worth investigating with respect to the regulation of DAT by ERK8. First, we wished to determine whether ERK8 might increase in the V_{max} of DA uptake compared to cells expressing DAT alone (Fig. 24). This increase suggests that the amount of available transporter may be increased in ERK8 transfected cells, and this was tested using a cell surface biotinylation assay. Indeed, cells transfected with ERK8 had a greater than 2 fold increase in surface labeled DAT protein compared to cells transfected with DAT alone (Fig. 25). Interestingly, total DAT protein levels were increased to a similar degree, suggesting perhaps a post-transcriptional regulation of DAT protein levels. Transcriptional regulation is unlikely as the DAT expressed by this construct is driven by the CMV promoter, and we found that ERK8 had no effect on the levels of GFP driven by this same promoter (Fig. 26). To test whether ERK8 regulation of DAT is kinase-dependent, and whether mutation of the residue analogous the initial *vt32* mutation would disrupt ERK8 regulation of DAT, we looked at DA uptake in cells expressing these mutations. Neither the kinase-dead (K42R) or *vt32*-imitating (R59Q) ERK8 mutants increased DA uptake in a single point DA uptake assay (Fig. 27). As ERK8 regulation of DAT is sensitive to the same perturbations that seem to influence *swip-13* regulation of DA signaling, it is likely that

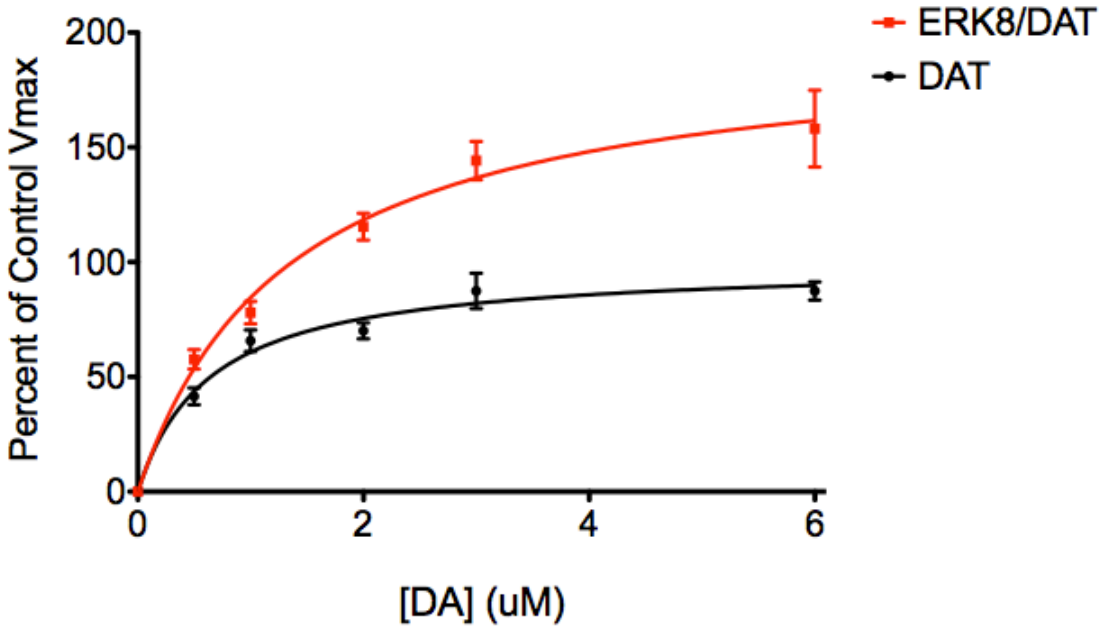

Figure 24 – ERK8 overexpression increases DAT activity in human SH-SY5Y cells. Transfection of human DAT into SH-SY5Y (black line) cells results in saturable, cocaine-sensitive [3H]DA uptake. Co-transfection of ERK8 with DAT (red line) leads to an increase in this 3H]DA uptake, as shown by a ~98% increase in the Vmax of DA uptake. Data is the average of 4 experiments, and specific DA uptake was calculated by subtracting DA uptake in the presence of cocaine. In each experiment, DA uptake was normalized to protein levels for each transfection condition, and then each data point was normalized to the Vmax of the DAT transfection alone control from that day, calculated using the Michaelis-Menton equation. Curves were generated using a Michaelis-Menton non-linear fit.

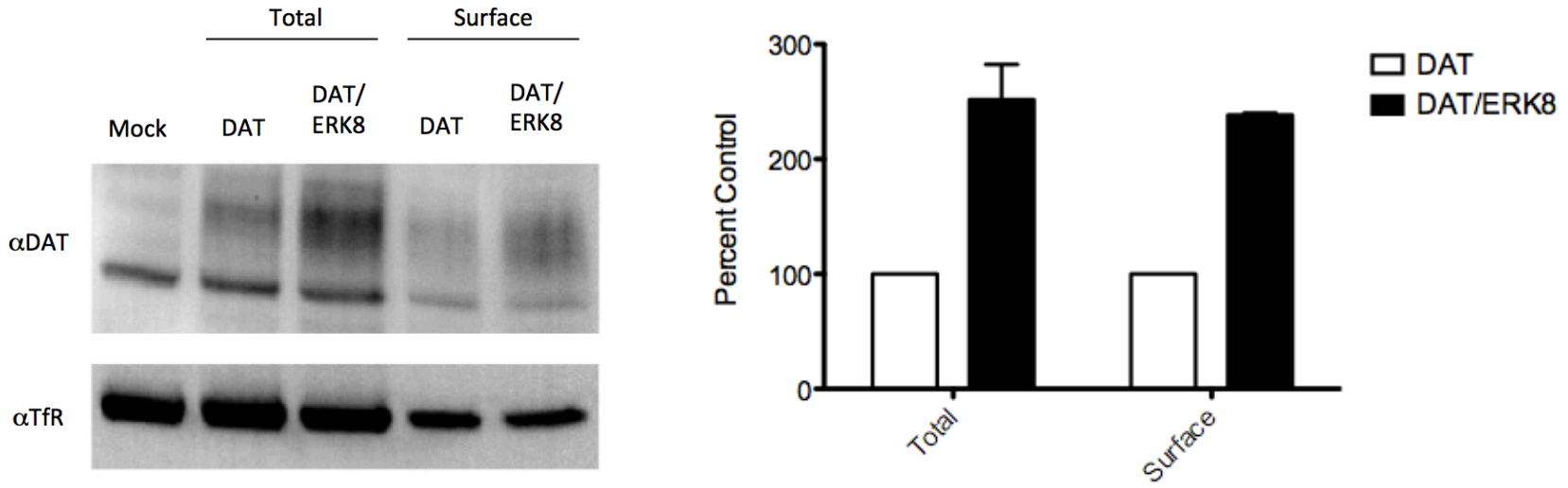

Figure 25 – ERK8 overexpression increases total and surface DAT protein. (A) Lysates from SH-SY5Y cells treated with the surface biotinylating agent Sulfo-NHS-biotin were subjected to pull-down using Streptavadin-conjugated beads and eluates from these beads are labeled as "Surface". Total protein before pulldown was run in parallel ("Total"). Mock transfected cells show no anti-DAT staining at the expected molecular weight of DAT of ~80kDa, and DAT/ERK8 transfected cells show a robust increase in labeling compared to DAT transfection alone. A similar increase is seen in surface DAT. Anti-TfR was used as a loading control. (B) Quantification of (B), total DAT was normalized to TfR and these values were normalized to control DAT transfection alone to generate a percent control value. For surface levels, surface DAT was normalized to surface TfR, and again values were normalized to control surface levels to generate a percent control value. Data are the average of three experiments and were analyzed using two-tailed Student's t-tests for each group of data (Total and Surface), and a significance threshold was set at $P<.05$. ****$P<.0001$.

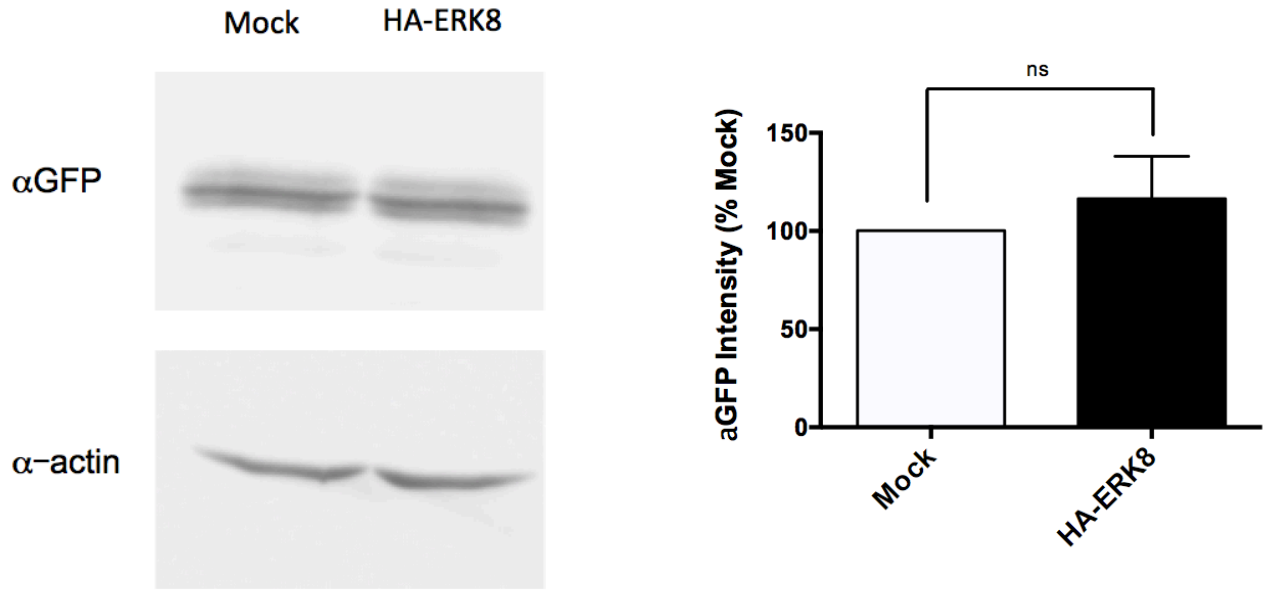

Figure 26 – ERK8 does not increase GFP driven by CMV promoter. (A) Transfection of ERK8 into SH-SY5Y cells has no effect on amount of GFP expressed. (B) Quantification of three experiments, no significant difference in αGFP intensity was observed between mock transfected and HA-ERK8 transfected cells. Data were analyzed using a two-tailed Student's t-test comparing mock transfected to HA-ERK8 transfected conditions, and a significance threshold was set at $P<.05$.

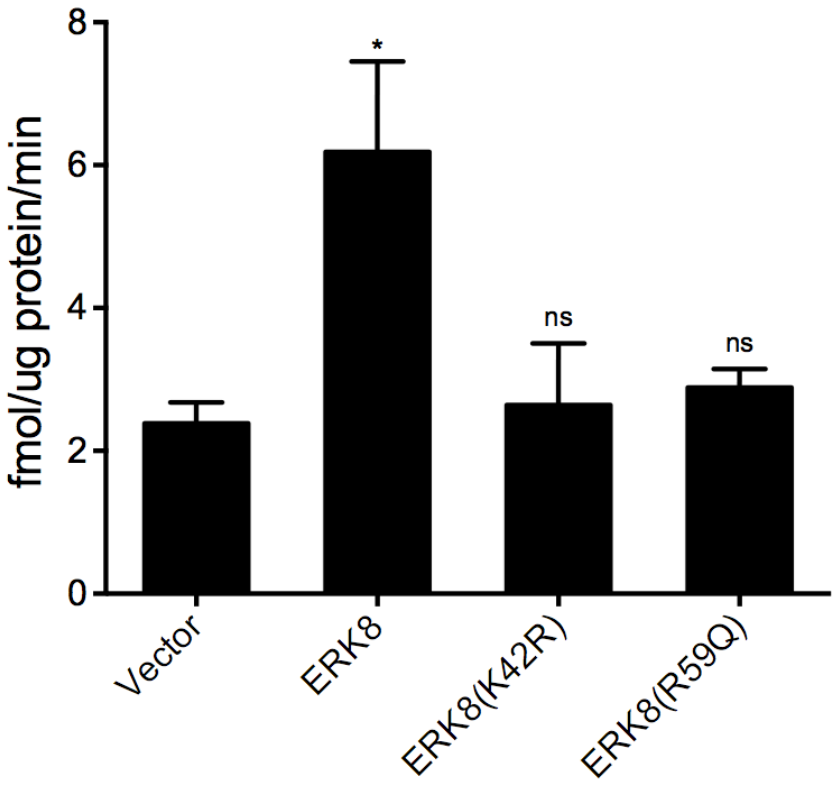

Figure 27 – ERK8 mutants do not increase DAT activity. Transfection of kinase-dead ERK8(K42R) and *vt32*-analogous ERK8(R59Q) mutants do not increase DA uptake in SH-SY5Y cells co-transfected with DAT. As previously shown, wild-type ERK8 significantly increases DAT activity. Data were analyzed using a one-way ANOVA with Bonferroni posttests comparing each condition to vector control. Significance was set at P<.05. *P<.01

the ERK8/DAT interaction represents a conserved interaction analogous to the SWIP-13/DAT-1 interaction described above.

We next wished to discover the mechanism through which SWIP-13/ERK8 may regulate DAT-1/DAT. One potential pathway in which ERK8 might act is the regulation influence the activity state of RhoA. To do this, we performed a pull-down with GST beads conjugated to a Rho-binding domain (RBD) that only binds active Rho. We then blotted for RhoA pulled down by these beads from mock- and ERK8-transfected HEK-293T cells. We found that ERK8 transfection significantly increased active RhoA, supporting the hypothesis that ERK8 is a positive regulator of RhoA activity (Fig. 28). To determine whether this potential interaction was required for ERK8 regulation of DAT, we transfected SH-SY5Y cells with the GFP-tagged exotoxin C3 (GFP-C3), which is an inhibitor of Rho proteins, to determine whether this treatment would block the increase in DAT activity seen with ERK8 transfection. Indeed, we found that GFP-C3 blocked the effect of ERK8 on DAT activity, with no increase in DA uptake seen in cells transfected with both GFP-C3 and ERK8 (Fig. 29). Importantly we found no effect of GFP-C3 transfection alone, suggesting that Rho activity does not influence basal DAT activity in this context, and only upon apparent Rho activation by ERK8 is a requirement of Rho revealed. This finding supports a model in which ERK8 acts through Rho to regulate DAT activity.

DISCUSSION

In the previous chapter, we established that *swip-13* is an uncharacterized gene that acts in DA neurons to play a role in DA signaling regulation. Knowing that loss of

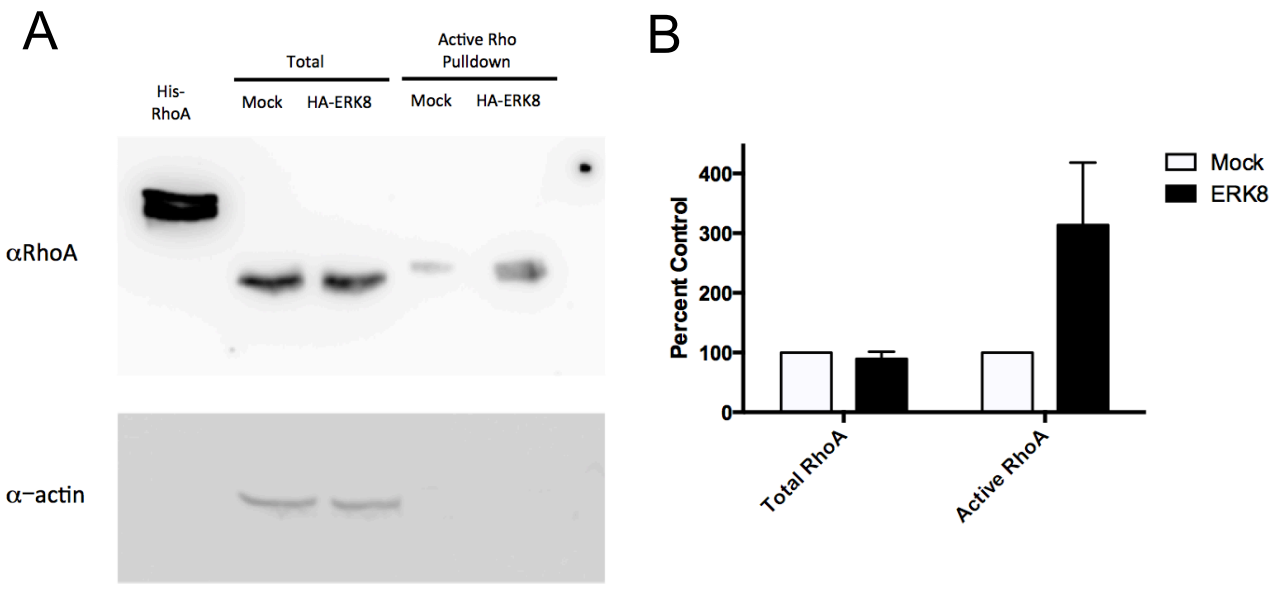

Figure 28 – ERK8 overexpression increases RhoA activation in HEK-293T cells. (A) Cells transfected with HA-ERK8 plasmid show an increase in active RhoA protein compared to mock transfected cells. Active RhoA was measured by pulldown using GST-RBD beads that bind active Rho. (B) Quantification of three experiments. Active RhoA was increased in HA-ERK8 transfected cells, with no significant change in total RhoA protein levels.

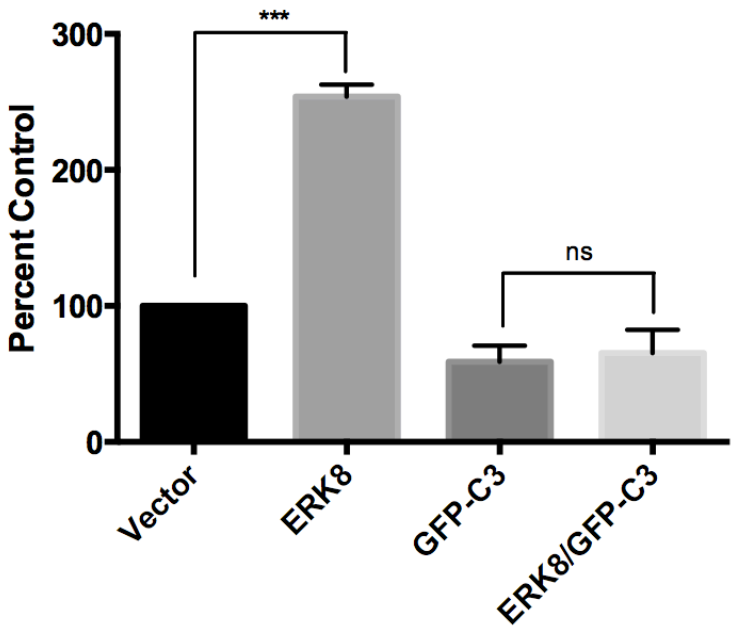

Figure 29 – Rho inactivation via GFP-C3 blocks ERK8 enhancement of DAT activity. As shown previously, ERK8 overexpression significantly increases DAT activity compared to vector-transfected cells. Transfection of GFP-C3 prevents any increase in DAT activity with ERK8 overexpression (ERK8/GFP-C3 vs. GFP-C3). Data were analyzed using a one-way ANOVA with Bonferroni posttests comparing ERK8 to Vector, and ERK8/GFP-C3 to GFP-C3. Significance was set at P<.05. ***P<.001

swip-13 led to a hyperdopaminergic state via some change in the DA neurons, potential mechanisms for how this state could arise were explored here. Because the Swip phenotype was first observed in animals lacking the DA transporter DAT-1, one obvious potential mechanism for the hyperdopaminergic state seen in *swip-13* mutants was a reduction in DAT-1 activity. We observed that overexpression of functional GFP-tagged DAT-1 resulted in a suppression of *swip-13(gk1234)* Swip, consistent with a reduction in DAT-1 activity in this mutant background. A similar rescue with DAT-1 overexpression, however, was previously shown to occur in *swip-10* mutants as well, which display a non-cell autonomous mechanism for Swip that involves glial regulation of DA neuron activity, indicating that this DAT-1 rescue is not specific for states of reduced DAT-1 activity (Hardaway et al., 2015). Importantly, several observations support a role for reduced DAT-1 function in the mechanism for *swip-13* mutant Swip. First, *swip-13* mutants have a reduced sensitivity to the neurotoxin 6-OHDA, which would be consistent with reduced actions of the requisite transporter DAT-1 that the neurotoxin uses to enter and kill the cell. However, reduced sensitivity to this neurotoxin could reflect changes in other aspects of the DA neuron function that might render the neuron resistant even in the case of equal 6-OHDA transport. In mammals, 6-OHDA-induced DA neuron cell death appears to involve multiple cell death pathways, including the canonical apoptosis cell death program (Marti et al., 1997; Walkinshaw and Waters, 1994). In *C. elegans*, mutations in the apoptosis genes *ced-3* and *ced-4* do not prevent 6-OHDA-induced cell death (Nass et al., 2002), but other genetic pathways leading to cell death may still be critical for this cell death. It is possible that instead of reduced

DAT-1 activity in *swip-13* mutants, there may be reduced activity of these cell death pathways, or upregulation of protective genetic pathways that could result in reduced sensitivity to 6-OHDA and related toxins. Because of the general non-specificity of this assay, other lines of evidence were necessary to support a role for *swip-13* in regulation of DAT-1.

Another observation that supports the regulation of DAT-1 by *swip-13* is the reduced [3H]DA uptake seen in neuron cultures from *swip-13* mutants compared to N2 neurons. This more directly shows that DAT-1 activity seems to be reduced in *swip-13* mutants, consistent with *swip-13*'s role as a positive regulator of DAT-1. There still remained the possibility that *swip-13* may impact DA signaling through other mechansims outside of DAT-1, for instance through the regulation of DA neuron activity and DA release. Two lines of evidence suggest that this is not the case, however. First, genetic interaction studies of *swip-13* and *dat-1* suggest that these genes act in the same genetic pathway to produce Swip. This conclusion is based on the observation that *swip-13(gk1234) dat-1(ok157)* double mutants have the same percentage of Swip as *dat-1(ok157)* mutants. This was seen both in water and in osmosuppressed conditions, the latter of which was used to get around potential ceiling effects with the near complete Swip seen in *dat-1(ok157)* mutants in water. A similar strategy was employed in a previous study by Hardaway et al., who showed that additivity between *swip-10* and *dat-1* mutations were revealed in osmosuppressed conditions where ceiling effects are not an issue (Hardaway et al., 2015). The observation here that no additivity is observed even in osmosuppressed conditions suggests that *swip-13* and *dat-1* mutations produce Swip through the same mechanism.

Combined with the rescue of *swip-13* with DAT-1 overexpression, this supports the model of *dat-1* acting downstream of *swip-13* to control DA signaling impacting swimming behavior.

The second observation that argues against the alternative hypothesis that *swip-13* may regulate DA release are the resulta from the FRAP experiments. This method was generated by Voglis et al., who showed that it could be used to reveal a state of reduced DA release in *asic-1* mutants, which also display behavioral evidence for reduced DA signaling (Voglis and Tavernarakis, 2008). They proposed that *asic-1* acts as a positive regulator of DA signaling via its activation by protons released from SVs, causing a positive feedback loop promoting further SV fusion. This loss of a positive regulator of DA release would be expected to produce the opposite result in this FRAP assay from a negative regulator of DA release, which should have an increased rate of recovery after bleaching. Indeed, in published studies, I observed just this effect in *swip-10* mutants, which are thought to have hyperactive DA neurons due to loss of glial control of glutamate signaling (Hardaway et al., 2015). In the present work, however, I found no effect of *swip-13* mutation on FRAP recovery rates, suggesting no difference in DA release between N2 and *swip-13* mutants. A caveat to this interpretation, however, is that these animals are paralyzed and pinned to an agar pad, and it is possible that this context may not elicit an enhanced rate of release that might be observed in other contexts, such as swimming in water. However, this result combined with genetic evidence and assays of DAT-1 activity all support the hypothesis that *swip-13* acts through *dat-1* to regulate DA signaling, and is consistent with this being the

exclusive pathway through which loss of *swip-13* generates the DA-dependent Swip phenotype.

To determine if the apparent role of *swip-13* in regulating DA transport might be conserved in human ERK8, I co-transfected ERK8 and DAT into human neuroblastoma-derived SH-SY5Y cells to look at the effects of ERK8 on DAT activity. SH-SY5Y cells were selected based on their catecholaminergic phenotypes such as TH activity and expression of NET (O'Neill et al., 1994; Perez-Polo et al., 1982), making this perhaps a good system to investigate signaling pathways that might impact DA signaling and DAT activity. Indeed, I found that cells co-transfected with both ERK8 and DAT had about a doubling of maximal uptake capacity for DA compared to cells transfected with DAT alone. The increase in the V_{max} of DA uptake pointed towards an increase in surface DAT protein levels, and to investigate this, I used a surface biotinylating agent to pulldown and blot for surface DAT protein. Indeed, surface DAT levels were increased to a similar degree as DA uptake capacity, though total DAT protein levels were increased by the same amount. Importantly, DAT expression in these experiments is driven by the CMV promoter, and ERK8 was found not to increase GFP driven by the same promoter, suggesting this is not an artifact of the promoter used in these experiments. Additionally, we observed that the kinase-dead K42R and *vt32*-analogous R59Q mutations both blocked ERK8's actions on DAT, just as they appear to impact SWIP-13's actions on DA signaling regulation in *C. elegans*. Future studies using co-expression of SWIP-13 and DAT-1 in SH-SY5Y cells to parallel the ERK8/DAT experiments will further validate this idea.

The above results suggest that ERK8 regulates DAT through a post-transcriptional mechanism, possibly through mRNA stablilization, increased translation, or decreased DAT degradation. Importantly, multiple signaling pathways have been shown to stabilize DAT surface levels and prevent targeting of this protein for degradation. Degradation of DAT can be inhibited by the MAP kinase phosphatase MKP3 as well as by palmitoylation of the transporter (Foster and Vaughan, 2011; Mortensen et al., 2008), and is promoted by PKC signaling (Hong and Amara, 2013; Miranda et al., 2005). Multiple lines of evidence support the model that DAT is routed to different compartments upon endocytosis, and this targeting can control whether the transporter is degraded or recycled (Gabriel et al., 2013; Hong and Amara, 2013; Sorkina et al., 2006; Vuorenpaa et al., 2016). If ERK8 impacts this targeting of DAT, or just generally inhibits endocytosis or promotes DAT trafficking to the surface, it is possible that DAT is thus stabilized and protected from degradation after ERK8 overexpression. The nature of transfecting in ERK8 and waiting a few days to assay DA transport makes it difficult to separate acute from chronic effects of enhanced ERK8 signaling on DAT. Unfortunately, specific inhibitors of ERK8 have not yet been developed, and current drugs that are known to inhibit ERK8 also act on other kinases that are known to impact DAT regulation, including PKC. Future development of more specific ERK8 inhibitors or activators will make it easier to investigate what the acute effects of ERK8 activity are on DAT regulation.

Due to the relative lack of study on the newly discovered ERK7/8, it is difficult to use leads from the literature to investigate a mechanism for how ERK8/SWIP-13 might regulate DAT/DAT-1. One recent discovery of interest regarding the actions of ERK7/8

was the finding that Xenopus ERK7 regulates ciliogenesis (Miyatake et al., 2015). Because we had evidence that loss of *swip-13* might impact cilia integrity based on the mild dye-filling defect seen in *swip-13* mutants, we reasoned that this role of Erk7 might be conserved in *C. elegans*. It was also found that ERK7 binds to another regulator of ciliogenesis Dishevelled. There have been multiple studies on Dishevelled regulation of ciliogenesis, and loss of signaling by this protein causes cilia defects including defective basal body migration and formation of a subcortical actin network necessary for normal ciliogenesis (Park et al., 2008). Interestingly, loss of ERK7 caused these same defects, suggesting that these proteins might act together to regulate ciliogenesis. Another protein that binds to Dishevelled and regulates ciliogenesis is the small GTPase RhoA, and loss of this protein also causes defective basal body migration and formation of a subcortical actin network (Pan et al., 2007). Therefore, it seems possible that ERK7, through binding to Dishevelled, might activate Rho to regulate ciliogenesis, and this activation might have relevance outside of ciliogenesis, for instance in DAT regulation. We've shown here that overexpression of human ERK8 in HEK-293T cells results in an increase in active RhoA, supporting the idea that ERK8 is an activator of RhoA. This is exciting with respect to DAT regulation as RhoA has recently been show to regulate DAT trafficking in response to AMPH (Wheeler et al., 2015). AMPH has long been known to induce a rapid endocytosis of DAT, and inhibition of Rho blocks this effect.

Having established ERK8 as a potential activator or Rho, I wished to test whether ERK8 requires Rho activation to regulate DAT. To do this, I inhibited Rho using the genetically-encoded Rho-inhibiting exotoxin C3 and observed that ERK8 lost its ability to enhance DAT activity if Rho is inhibited, suggesting that Rho is required for ERK8's

actions on DAT. Because Rho appears to promote endocytosis of DAT, and ERK8 appears to increase DAT activity, it seems counterintuitive that ERK8 would act through this pathway to increase DAT activity. However, AMPH-triggered DAT internalization, which acts through Rho, appears to route DAT to recycling pathways, as opposed to other signaling pathways such as those activated by PKC that can target DAT for degradation (Hong and Amara, 2013). If ERK8 is promoting targeting of DAT to the AMPH/Rho endocytosis pathway, then one might expect DAT protein to accumulate due to targeting away from degradative pathways. Future work will attempt to investigate the differences in DAT targeting with and without ERK8 overexpression to see if this might indeed be the case.

How ERK8 might influence Rho activation is of particular interest. To date, we have only shown that overexpression of ERK8 increases Rho activity, but have yet to identify the mechanism of this activation. Recent work has identified the RhoGEF Vav2 as a regulator of DAT downstream of the RTK Ret (Zhu et al., 2015). Interestingly, Ret has also been identified as an activator of ERK8, acting through the TK c-Abl (Iavarone et al., 2006). It is possible that Ret/c-Abl signal through ERK8 onto Vav2 to activate Rho and impact DAT trafficking. We also know that PKA signaling opposes the actions of Rho on DAT trafficking induced by AMPH treatment via inactivation of Rho (Wheeler et al., 2015). ERK8 may inactivate PKA signaling to relieve this brake on Rho and allow for it to exert its effects on DAT. ERK8 may also directly phosphorylate Rho to impact its activation. Phosphorylation of RhoA has been reported to impact its binding to RhoGDI (Rho GDP-dissociation inhibitor), which can regulate the spatial distribution and activation of Rho via shuttling to membrane microdomains (Tkachenko et al., 2011). If

ERK8 impacts the binding between RhoA and RhoGDI, it may have functional consequences on RhoA actions, potentially including regulation of DAT trafficking. Other studies have also showed EGF stimulation of COS7 cells results in an increase in RhoA activity that is mediated by phosphorylation by ERK1/2 (Tong et al., 2016). Additionally, purified ERK1 was able to phosphorylate RhoA *in vitro*. Future work will hopefully determine whether ERK8 activates RhoA through direct phosphorylation, perhaps via one of the above mechanisms, or indirectly through control of GTP/GDP cycling via actions on RhoGEFs or RhoGAPs. Additionally, the requirement for Dishevelled, to which both ERK8 and RhoA bind to regulate ciliogensis, is unknown with regards to RhoA activation of ERK8. Perhaps Dishevelled acts as a scaffold to bring ERK8 and RhoA together to allow for functional interactions between these two proteins. It is intriguing to think that a Dishevelled/ERK8/Rho pathway may act at the synapse to regulate DAT function. Whether this is the case is another open question to hopefully be answered in the near future.

CHAPTER V

SUMMARY AND FUTURE DIRECTIONS

We have demonstrated here the power of *C. elegans* as a genetic model to study DA signaling. This model is useful due to its short lifespan, ease of genetic manipulation, its transparent cuticle allowing for visualization of the nervous system, and tools that allow for *in vivo* study of nervous system function, such as the 6-OHDA and FRAP assays used in these studies. Using this model to perform a forward genetic screen to identify novel regulators of DA signaling has produced exciting results, some of which have previously been published, and others of which have been presented here. This work has identified the conserved MAP kinase SWIP-13/ERK8 as a regulator of DA signaling through actions on the presynaptic DA transporter DAT-1/DAT. These actions were shown to occur *in vivo* in *C. elegans*, as well as *in vitro* in human cells using human ERK8 and DAT. This conservation of the role of this conserved MAP kinase in regulating the DA transporter is exciting and novel, and validates the use of the *C. elegans* model for discovery of novel genes that work across phylogeny to regulate neurotransmission, including DA neurotransmission.

Particularly exciting about the regulation of DAT by ERK8 is the potential role for Rho in mediating this regulation. RhoA, as well as the related Rho family GTPase Cdc42, have recently been shown to play roles in regulating DAT trafficking (Wheeler et al., 2015; Wu et al., 2015a), and the demonstration that ERK8 may act upstream of RhoA in this regulation is an intriguing possibility. We have shown that ERK8 overexpression increases RhoA activation, and that inhibition of Rho proteins blocks

ERK8's effects on DAT, providing strong evidence for interactions between ERK8 and RhoA in the regulation of DAT. More work will be necessary to verify this interaction, however. As SWIP-13 plays similar roles in regulating DAT-1, it will be vital to show that the *C. elegans* RhoA ortholog RHO-1 acts in this regulation as well. There are a few ways to go about testing this. One would be to overexpress *rho-1* in DA neurons in a *swip-13* mutant background and see if this rescues the Swip phenotype. As *rho-1* is expected to act downstream of *swip-13* in the regulation of *dat-1,* we might expect this increase in *rho-1* would overcome the loss of *rho-1* activation caused by *swip-13* deletion. It is possible that even with more r*ho-1*, there might be insufficient activation in the absence of *swip-13*. To get around this, overexpressing a constitutively-active *rho-1* might compensate for reduced activation and restore actions of RHO-1 on DAT-1. Additionally, we can look for genetic interaction between *rho-1* and *swip-13*. Unfortunately, *rho-1* mutants are not viable, and global loss of *rho-1* would likely impact locomotion in many nonspecific ways. One strategy to overcome this would be to knockdown *rho-1* in DA neurons specifically using cell-specific RNAi. We could do this in a wild-type background to look for a Swip phenotype, and then on a *swip-13* mutant background to see if there is additivity between these Swip phenotypes. If there is no additivity, then we can conclude that these genes act in the same pathway. Additionally, if we get a positive result in the *rho-1* rescue of *swip-13* experiments, then we could conclude that *rho-1* acts downstream of *swip-13* in this pathway to regulate DA signaling. Finally, we might want to test 6-OHDA sensitivity in *rho-1*-overexpressing *swip-13* mutants to see if DAT-1 function is restored to conclude that the *swip-13/rho-1* pathway in fact acts on *dat-1* to regulate DA neuron function. These results, combined

with the human cell culture results, would provide compelling evidence for a conserved pathway involving SWIP-13/ERK8 activation of RHO-1/RhoA to regulate DAT-1/DAT function.

Ultimately, we hope to establish that this potential ERK8/Rho pathway acts in the mammalian CNS to regulate DA neurotransmission. Should the above experiments provide compelling evidence for this pathway acting in *C. elegans* DA neurons to regulate DAT-1, the next logical step would be to investigate this pathway in a mammalian model such as mice. There are a number of approaches we could take to investigate this pathway in mice, including DA neurons specific knockout of ERK8 using a Cre-Lox system, or viral-mediated shRNA knockdown of ERK8 in DA neurons to first investigate the impact of loss of this gene in DA neurons. We might expect that loss of this gene, like in *C. elegans*, would reduce DAT activity, which we could test using *in vivo* electrochemical techniques or *ex vivo* synaptosomal DA uptake assays. Additionally, we may observe behavioral effects such as increased spontaneous locomotor activity, similar to what is observed in DAT knockout mice. We could also use these knockout/knockdown strategies to investigate regulation of DAT trafficking in the context of a loss of or reduction of ERK8 in DA neurons. Should the ERK8/Rho pathway acting on DAT remain intact in mouse DA neurons, then loss of ERK8 might lead to a loss of AMPH-induced DAT internalization, similar to what was seen by Wheeler et al. with Rho inactivation. Additionally, we might observe basal trafficking defects, such as reduced DAT recycling and increased DAT targeting to the lysosomal/degradation pathway based on evidence that AMPH, possibly acting through Rho, promotes recycling of DAT.

Finally, the relevance for this pathway to disease could also be investigated in mice. As of yet, there are no specific inhibitors of ERK8, but should one be developed, we might be able to use this drug to investigate the effects of ERK8 inhibition on behavior in models of DA-related diseases. As inhibition of DAT is the primary strategy for treatment of ADHD by drugs such as methylphenidate and AMPH, inhibition of ERK8 and subsequent loss of DAT activity might provide a similar therapeutic benefit. Our lab has recently generated a construct-valid model of ADHD based on a DAT variant (A559V) found in human ADHD patients, and it might be possible to use this model to investigate the potential therapeutic effects of ERK8 manipulation on ADHD-associated behaviors. Another disease that could potentially be treated by ERK8 manipulation is schizophrenia, which is clinically treated with D2 receptor antagonists, supporting a hyperdopaminergic state contributing to the symptomology of this disease. If we increase ERK8 activity in mouse DA neurons, either genetically through ERK8 overexpression or chemically with an ERK8 activator (of which none yet exist), then we might increase DAT activity like we observed in SH-SY5Y overexpressing ERK8. This increase in DAT activity should reduce DA neurotransmission, which, in a model of schizophrenia, might rescue some behavioral deficits seen in these models. Ultimately, the goal of these experiments is to find a translatable therapeutic strategy for treating these DA-related diseases, and hopefully new drugs for inhibiting and activating ERK8 will be generated to facilitate these avenues of research and potential therapy.

APPENDIX A

ACUTE BLOCKADE OF THE *C. ELEGANS* DOPAMINE TRANSPORTER DAT-1 BY THE MAMMALIAN NOREPINEPHRINE TRANSPORTER INHIBITOR NISOXETINE REVEALS THE INFLUENCE OF GENETIC MODIFICATIONS OF DOPAMINE SIGNALING *IN VIVO*

INTRODUCTION

The modulation of behavior by the neurotransmitter DA is evolutionarily conserved, evident in animals that range by orders of magnitude in complexity, from humans to the soil-dwelling nematode *Caenorhabditis elegans*. As in humans, DA signaling in *C. elegans* regulates multiple behaviors including locomotion (Chase et al., 2004a; Omura et al., 2012; Sawin et al., 2000) and associative learning (Voglis and Tavernarakis, 2008). The conservation of genes encoding proteins that support DA biosynthesis, vesicular packaging, release, and response, makes the worm a powerful tool to elucidate novel mechanisms that regulate DA signaling across phylogeny (McDonald et al., 2006a). Particularly useful is the amenability of this organism to rapid genetic manipulation and behavioral characterization. Additionally, pharmacological agents have been utilized successfully to elicit behavioral responses through pathways shared with more complex vertebrates (Choy and Thomas, 1999; Dwyer et al., 2014; Miller et al., 1996; Weinshenker et al., 1995). As in vertebrates, the latter agents offer the opportunity to manipulate chemical signaling at specific time points in development and, when activity is evident with acute exposure, lessen concern for the compensations that arise from constitutive genetic manipulations.

A powerful example of a rapidly acting drug that has been successfully used in the worm to manipulate a specific chemical signaling pathway is the acetylcholinesterase inhibitor, aldicarb, which has been used extensively to evaluate the capacity for cholinergic signaling (Bany et al., 2003; Iwasaki et al., 1997; Miller et al., 1996; Mullen et al., 2007). ACh is released at the neuromuscular junction in *C. elegans* to trigger muscle contraction. Aldicarb, by blocking the major determinant of extracellular ACh inactivation, acetylcholinesterase (AChE), induces rapid, hypercontracted, motor paralysis due to excessive activation of neuromuscular ACh receptors. Genetic and pharmacological modifiers of ACh signaling, such as proteins that regulate vesicular ACh release, can be studied via their ability to enhance or suppress aldicarb-induced paralysis (Jorgensen et al., 1995; Nonet et al., 1997). This enhancement or suppression can be used to determine how a particular genetic mutation or drug might be altering ACh signaling, even if there is no obvious phenotype in the absence of drug. Dozens of genes have been identified or studied based on the presence of a Ric or Hic (**R**esistance or **H**ypersensitivity to **I**nhibitors of A**C**hE) phenotype, and include genes that act both pre- and postsynaptically (For review, see (Rand, 2007)).

To date, examples of potent and selective agents that act like aldicarb at non-cholinergic synapses are limited, in part due to the high concentrations (typically mM) needed for many substances to afford penetration through the worm cuticle. Additionally, inactivation of small molecule neurotransmitters besides ACh is determined by transporter-mediated clearance, and many mammalian transporter antagonists lose potency as inhibitors of their *C. elegans* orthologs (Jayanthi et al., 1998; Ranganathan

et al., 2001). Thus, the *C. elegans* DA transporter (DAT-1) is one to two orders of magnitude less sensitive *in vitro* to the mammalian DAT inhibitors GBR12909 and nomifensine, respectively (Jayanthi et al., 1998). Interestingly, the mammalian NET-specific antagonist nisoxetine (NIS) exhibits low nanomolar potency for inhibition of DAT-1 mediated DA uptake (Jayanthi et al., 1998). Since the worm lacks a NET ortholog (worms do not make NE), we reasoned that NIS might prove a potent and selective antagonist of DAT-1 *in vivo*.

Here, we describe our efforts to demonstrate the utility of NIS as a potent pharmacological modulator of DA signaling-dependent behavior in the worm. The behavior monitored in our studies, Swimming-Induced Paralsis (Swip), was first described in worms bearing a *dat-1* deletion (McDonald et al., 2007). We demonstrated that loss of DAT-1 expression leads to premature paralysis when worms are placed in water, with paralysis emerging in a few minutes versus the stable (>10 min) swimming evident in wildtype (N2) worms. Swip produced by *dat-1* mutation can be rescued by mutation of DA biosynthetic and vesicular packaging genes (*cat-2* and *cat-1* respectively) as well as by loss of D2-like *dop-3* receptors (McDonald et al., 2007), supporting Swip as a behavioral readout of hyperdopaminergia. In this report, we demonstrate that Swip can be induced rapidly by incubation of worms with low concentrations of NIS, that Swip induction by NIS is DA-dependent, and that we can positively and negatively modify NIS-induced Swip by genetic manipulation of presynaptic regulators of DA release. By analogy to the utility of aldicarb for the study of cholinergic signaling, we discuss the potential for NIS to serve as a useful tool for the

identification and characterization of novel and potentially conserved regulators of DA signaling.

MATERIALS AND METHODS

C. elegans strains and husbandry

Strains were maintained at 15–20 °C using standard methods as described previously (Brenner, 1974). N2 (Bristol) served as our wild-type strain. Additional strains used in this work as follows: *dat-1(ok157); dop-2(vs105); asic-1(ok415); cat-2(e1112); dop-3(vs106); dat-1(ok157), dop-2(vs105); dat-1(ok157), dop-2(vs105) vtEx58 (Pdat-1::dop-2).*

dat-1(ok157), dop-2(vs105) vtEx58 (Pdat-1::dop-2) transgenic animals were generated by microinjection of *dat-1(ok157); dop-2(vs106)* worms with *pdat-1::dop-2* transgene and co-injection markers *punc-122::GFP* and *pdat-1::mCherry*. Stable transgenic line was selected based on presence and high transmission of *punc-122::GFP* fluorescence, and *pdat-1::mCherry* fluorescence was used to pick animals for behavioral experiments.

Plasmid Construction

The *pdat-1::dop-2* rescue construct was generated in the backbone pRB1106 which contains the *dat-1* promoter and unique restriction enzymes for subcloning of open reading frames (ORFs). *dop-2S* cDNA was amplified from *ceh-17::dop-2S* plasmid (provided by Satoshi Suo, University of Tokyo, Tokyo, Japan) with AscI and KpnI engineered into the 5’ and 3’ ends, respectively. This PCR fragment was digested

and subcloned into digested backbone. Successful cloning was verified by sequencing of the plasmid prior to microinjection.

Swip assays

Swip assays were performed as previously described (Hardaway et al., 2012; McDonald et al., 2007). Synchronous L4 worms were generated by hypochlorite treatment of adult animals, and plating of synchronized L1 animals. All manual assays were carried out by picking 10 L4 animals into a well of 100µL of water plus or minus nisoxetine hydrochloride (Sigma-Aldrich, St. Louis, MO) or methylphenidate (Sigma-Aldrich, St. Louis, MO) and scoring the number of animals paralyzed after 10 min. For osmosuppression studies, solutions of 100, 200, and 300 mOsm were generated with sucrose. Eight wells were scored per genotype/treatment, and were repeated on at least 3 separate days with 1-2 experimenters per day for an N=24-48 per condition. Experimenters were blind to genotype and/or drug. Automated analyses were performed using 10 min videos of individual worms captured from at least 25 worms per genotype/treatment using Tracker software and analyzed using SwimR software as previously described (Hardaway et al., 2015; Hardaway et al., 2014). Latency to paralysis was measured as the time until the thrashing frequency for each animal dropped below 20% of the maximum thrashing value for at least 20 seconds. Probability of reversion to swimming was measured as the percent of paralyzed animals that displayed bouts of thrashing above 20% of the maximum thrashing value after a bout of paralysis (defined as above).

For *dop-2* rescue experiments, worms expressing the *pdat-1::dop-2* transgene were selected based on the presence of the co-injection marker *pdat-1::mCherry* and

were picked as L2-L3 animals the day before video acquisition.

Graphical and Statistical Methods

Data was analyzed and graphed using either SwimR software (described above), or using Prism 6.0 (GraphPad, Inc., La Jolla, CA). All statistical analyses and curve fits were performed in Prism 6.0. Descriptions of all statistical tests are noted in the figure legends.

RESULTS

Wild-type worms placed in water with increasing concentrations of NIS demonstrated a dose-dependent increase in Swip, with diminished movement evident at 2 μM drug and that, by 20 μM, reached the paralysis levels observed in *dat-1* animals (Fig. 30A). Heat maps that plot the population behavior of NIS (5 μM)-treated animals revealed a pronounced induction of Swip with a probability of reversion to a swimming state following paralysis that is comparable to *dat-1(ok157)* mutants (N2 + 5 μM NIS: 33.3%; *dat-1(ok157):* 33.6%). To demonstrate DA-dependence of NIS-induced Swip, we examined NIS effects in the background of genetic mutations in *cat-2* (tyrosine hydroxylase) and *dop-3* (D2-like DA receptor) that prevent DA synthesis and DA response, respectively. Importantly, we have previously shown that mutations in these genes suppress *dat-1*-dependent Swip (McDonald et al., 2007). Indeed, at all doses of NIS tested, *cat-2(e1112)* and *dop-3(vs106)* animals swam at rates comparable to wild-

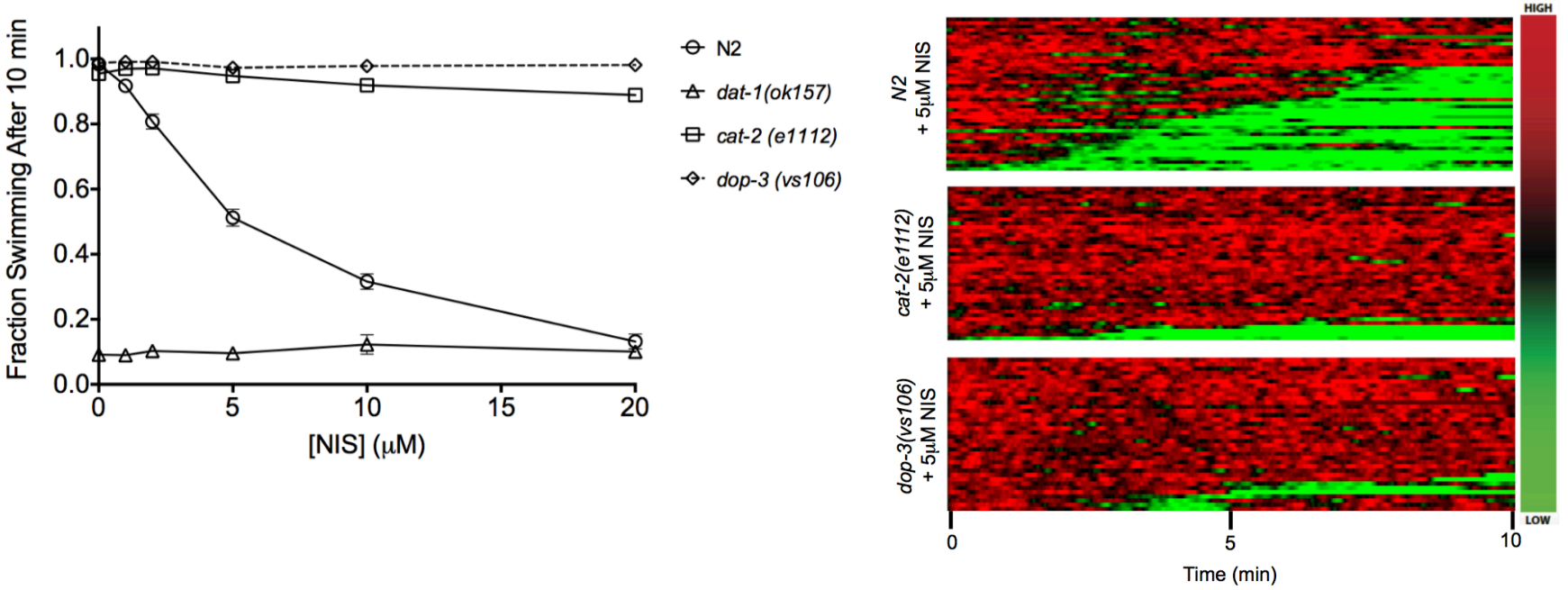

Figure 30 – NIS induces DA-dependent Swip. (a) NIS-treated N2 animals show dose-dependent Swip with a curve fit yielding an EC50 = 5.80 ± 0.12 mM. Neither *dop-3(vs106)* nor *cat-2(e1112)* animals demonstrate Swip at any NIS doses whereas *dat-1(ok157)* animals paralyze similarly at all doses of NIS. (b) Heat maps display thrashing frequencies of individual animals over time, with red designating high frequency values, and green designating low values. This analysis shows a high degree of Swip in N2 animals treated with 5 mM NIS, with very little paralysis observed in *cat-2(e1112)* and *dop-3(vs106)* animals treated with the same dose of NIS. n ≥ 40 for each condition.

type animals in the absence of drug (Fig. 30A). Heat map analysis demonstrated a dramatic reduction in penetrance of NIS-induced Swip in *cat-2(e1112)* and *dop-3(vs106)* mutants (Fig. 30B). *dat-1(ok157)* animals exhibited paralysis at all doses of NIS tested, with no increase in paralysis seen as the drug dose increased, supporting a lack of additivity between NIS-induced and *dat-1(ok157)* Swip. These results are consistent with NIS acting *in vivo* to antagonize DAT-1 mediated DA clearance and thereby generating hyperdopamergia that triggers extrasynaptic DA overflow and Swip.

To evaluate the specificity of NIS over other drugs, we compared the paralysis observed by NIS treatment with the paralysis previously reported with methylphenidate (MPH), a human DAT-specific antagonist (Izquierdo et al., 2013). We observed that whereas MPH produced dose-dependent Swip in N2 animals, these effects occurred at much higher concentrations than seen with NIS. Moreover, *cat-2(e1112)* animals displayed Swip after MPH treatment at levels comparable to N2 animals (Fig. 31), indicating that this drug induces paralysis through a DA-independent mechanism. Additionally, *dat-1(ok157)* animals displayed a trend towards increased paralysis in higher doses of MPH (Fig. 31). This finding supports the existence of other targets in the actions of MPH, though the effect did not reach significance, possibly due to floor effects.

Previously, we have reported that the Swip phenotype observed in *dat-1* mutants can be suppressed by increasing the osmolarity of the solution to which they are exposed (Hardaway et al., 2010). Similarly, the paralysis induced by 10 μM NIS treatment of N2 animals was suppressed by increasing assay solution osmolarity

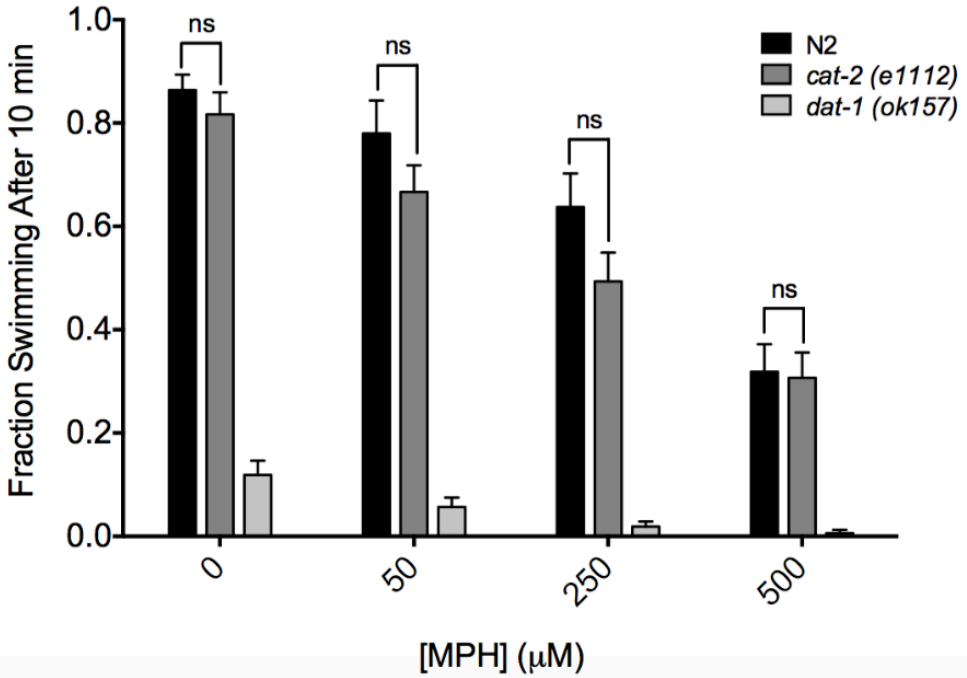

Figure 31 – MPH induces paralysis that is DA-independent. N2 animals treated with MPH show dose-dependent increases in paralysis, though *cat-2(e1112)* animals show paralysis comparable to N2 at all doses, with no significant difference (p>.05) between genotypes at any dose of MPH. *dat-1(ok157)* animals paralyzed in all doses of MPH. Significance was calculated using a two-way ANOVA with selected Bonferroni posttests comparing genotypes at each dose of MPH.

(achieved with sucrose supplementation), consistent with a mechanism that generates Swip like that imposed by loss of function mutations in *dat-1* (Fig. 32A). Importantly, under osmosuppressed conditions, where an intermediate level of paralysis is present and potential drug additivity less sensitive to floor effects, *dat-1(ok157)* mutant animals still demonstrated no increase in paralysis with NIS treatment relative to untreated *dat-1(ok157)* animals. In heat map analyses (Fig. 32B), *dat-1(ok157)* mutants treated with 5 μM NIS displayed nearly indistinguishable Swip onset and penetrance and no change in probability of reversion to swimming compared to untreated *dat-1(ok157)* animals. Along with the findings presented in Fig 1, these findings support the hypothesis that antagonism of DAT-1 is the basis of NIS actions to trigger Swip.

Having demonstrated that the actions of NIS likely derive from DAT-1 blockade and the resulting hyperdopaminergia, we wished to determine whether the drug could be useful as a tool to evaluate other elements of DA signaling. To explore this issue, we evaluated animals with a loss of function mutation in *asic-1*, which encodes an acid-sensing cation channel that can be activated by protons released by DA synaptic vesicles, thereby enhancing presynaptic depolarization and rates of DA release (Voglis and Tavernarakis, 2008). FRAP experiments have demonstrated that loss of *asic-1* diminishes DA release rates, paralleled by defects in associative learning (Voglis and Tavernarakis, 2008). However, as *asic-1* mutations have little to no effect on locomotion, effects on DA signaling are difficult to observe by assessment of worm movement assays, including Swip (Fig. 33A). However, NIS-induced Swip can be significantly suppressed in *asic-1(ok415)* animals, effects that are observed in both manual assays at 10 μM NIS (Fig. 33A) and in population heat maps generated with

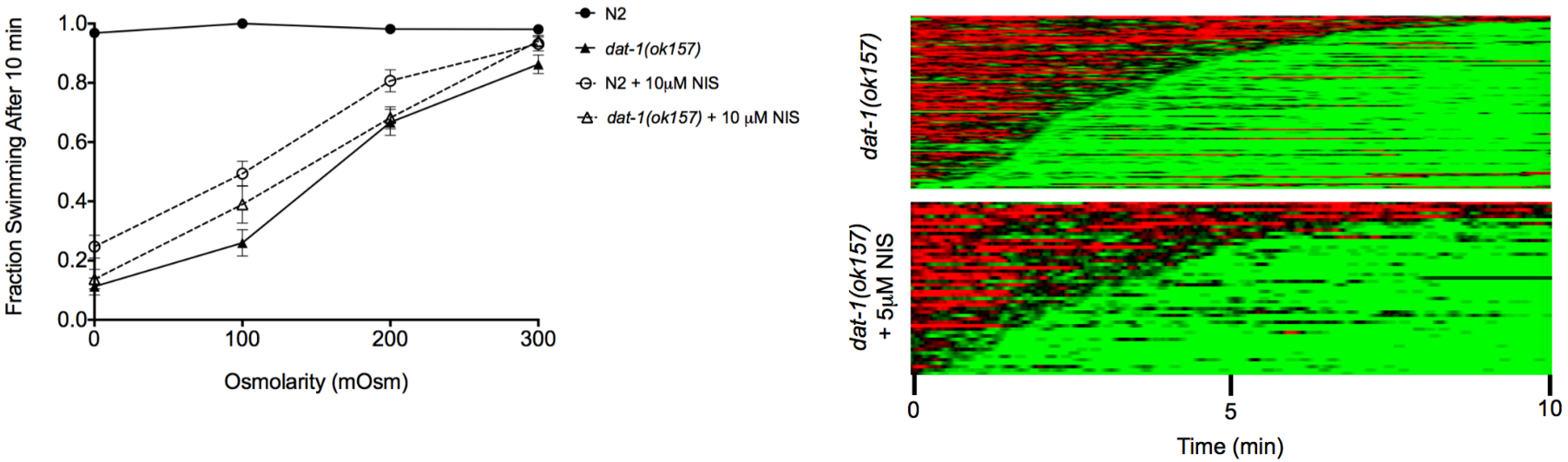

Figure 32 - NIS does not enhance Swip in *dat-1* mutants. (a) N2 animals treated with 10 μM NIS show robust Swip that is suppressed by increasing osmolarity. *dat-1(ok157)* animals display Swip suppression in higher osmolarity solutions, though *dat-1(ok157)* animals treated with 10 μM NIS exhibit no significant increase in Swip compared to untreated *dat-1(ok157)* animals at any osmolarity ($p>.05$). Data were analyzed using a two-way ANOVA with selected Bonferroni posttests comparing genotypes/treatments at each osmolarity. (B) Heat map analysis shows no significant difference between untreated *dat-1(ok157)* animals and those treated with 5 μM NIS. This similarity between treatments was reflected in percent paralysis (96.6% untreated vs. 90.2% treated), latency to paralyze (205 ± 11.5 sec untreated vs. 197 ± 16.8 sec treated, $P<.0001$ two-tailed Student's t-test), and percent reversions to swimming (33.6% untreated vs. 34.8% treated). $n \geq 50$ for each condition

5 μM NIS (Fig. 33B). Mutation of *asic-1* is also able to significantly suppress *dat-1(ok157)* paralysis, as demonstrated by comparison of thrashing frequency over time between *dat-1(ok157)* and *asic-1(ok157); dat-1(ok157)* animals (Fig. 34A). This suppression was less dramatic than the suppression we observe with 5 μM NIS treatment, however, where we see both significant genotype and time x genotype interaction effects when comparing *asic-1(ok157)* to N2 animals (Fig. 34B). We hypothesize that the constitutive nature of full loss of *dat-1* produces a level of hyperdopaminergia that results in robust Swip that loss of *asic-1* can only suppress to a small degree. The acute, titratable nature of DAT-1 blockade by NIS application may thus provide a more sensitive paradigm for evaluation of the contributions of genes like *asic-1* to the regulation of DA release.

As a second test of NIS utility for the study of DA release-modulatory genes, we sought to determine whether sensitivity to NIS treatments could reveal functional contributions to DA release exerted by negative modulators. For this evaluation, we examined drug sensitivity of animals lacking the D2-like dopamine receptor *dop-2,* which is expressed in a number of cells, including DA neurons (Suo et al., 2003). Although the function of *dop-2* has received little attention, in mammalian DA neurons, D2 receptors function as inhibitory autoreceptors, providing for feedback reductions in cell firing at the somatodendritic level and for diminished DA release at presynaptic terminals (De Mei et al., 2009; Ford, 2014; Mercuri et al., 1997). In keeping with these mechanisms, we observed that *dat-1(ok157);dop-2(vs105)* double mutants displayed a greater degree of Swip as compared to *dat-1(ok157)* mutants (Fig. 35A), consistent with a state of increased DA release due to reduced inhibitory feedback on firing and/or DA

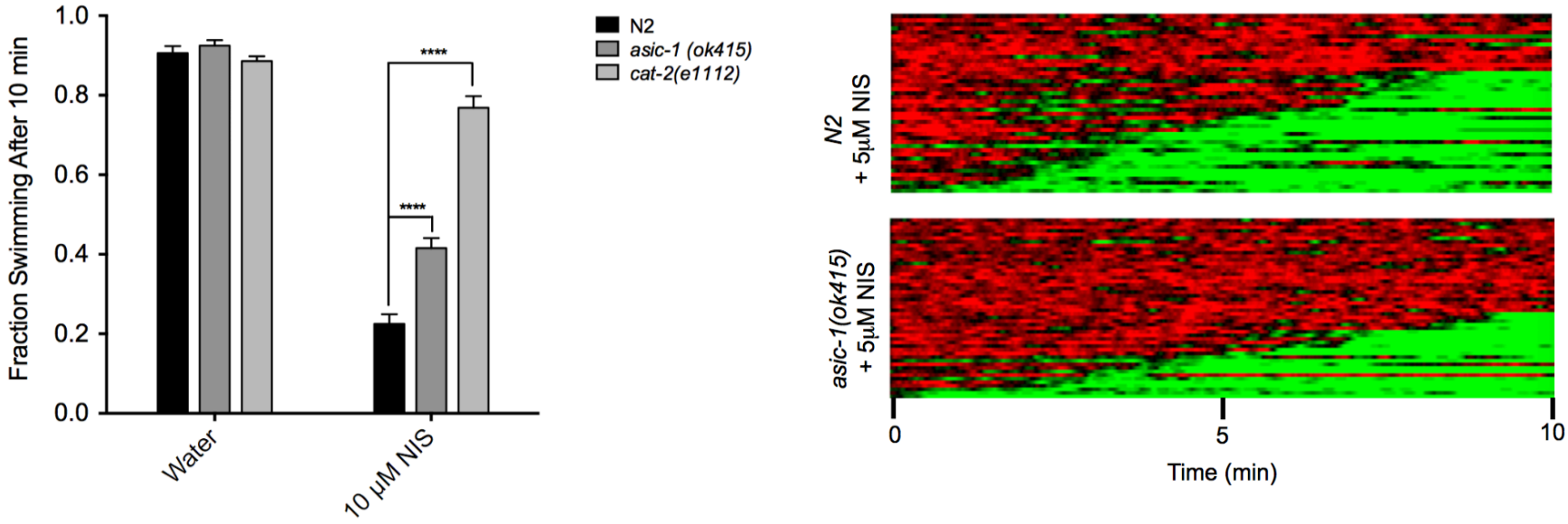

Figure 33 - NIS-induced Swip is suppressed by loss of *asic-1.* (a) *asic-1(ok415)* animals show no basal Swip in water, but display a significant reduction in Swip in 10 mM NIS compared to N2 animals. Data were analyzed using a two-way ANOVA with selected Bonferroni posttests comparing genotypes at each dose of NIS. **** P<.0001 (b) Heat map analysis shows *asic-1(ok157)* animals treated with 5 mM NIS have a suppression of Swip compared to N2 animals, with fewer *asic-1(ok157)* animals paralyzing (48.0% vs. 68.2% for N2).

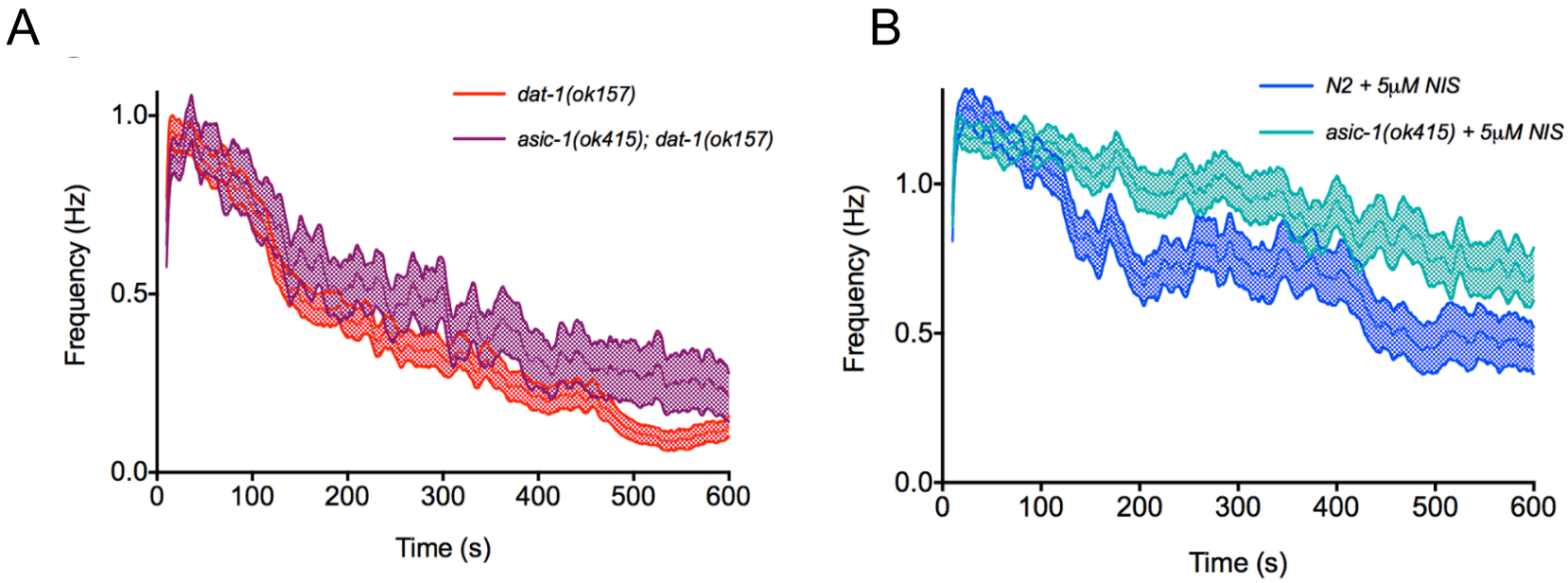

Figure 34 – *asic-1* mutation suppresses NIS Swip to a greater degree than *dat-1(ok157)* Swip. (a) Graphing of average thrashing behavior over time (mean ± SE) reveals a significant genotype difference in thrashing rates between *asic-1(ok415); dat-1(ok157)* double mutants and *dat-1(ok157)* animals (P<.0001). (b) Thrashing plots show *asic-1(ok415)* animals treated with 5 mM NIS have increased average thrashing rates compared to N2 animals treated with 5 mM NIS, with both significant genotype (P<.0001) and time x genotype interaction effects (P<.0001). n ≥ 34 for each condition

release. This hypothesis is supported by our finding of a reversal of the effects of *dop-2* mutation on Swip levels in the double mutant by DA neuron-specific expression of *dop-2,* evident in comparison of average thrashing rates over time (Fig. 35A) as well as the average latency to paralysis (Fig. 35B). Having provided evidence for a cell autonomous action of *dop-2* in suppressing DA signaling, we sought to determine whether loss of the receptor would enhance NIS-induced Swip as it does with genetic loss of *dat-1*. Indeed, we observed that *dop-2(vs105)* mutants treated with various doses of NIS displayed significantly increased Swip as compared to N2 animals (Fig. 36A). Heat map anaylses further demonstrate this enhancement, where we again observed a higher penetrance of Swip in *dop-2(vs105)* vs. N2 animals (Fig. 36B). Interestingly, we also found that the percent of animals reverting to swimming and the average number of reversion events were reduced in *dop-2(vs105)* animals (Fig. 36B). We hypothesize that this is another reflection of enhanced hyperdopaminergia that causes stronger paralysis that is more difficult to recover from. These findings of a hypersensitivity to NIS demonstrate that the drug can be used to interrogate mechanisms that afford inhibitory control of DA excitability of release and that the drug can reveal states of increased DA signaling that are too subtle to reliably observe via mutations alone.

DISCUSSION

The nematode *C. elegans* has long been a favorite model for geneticists interested in the molecular basis of neural development and function due to its ease of husbandry and genetic manipulation, and for the spectrum of simple behaviors that can

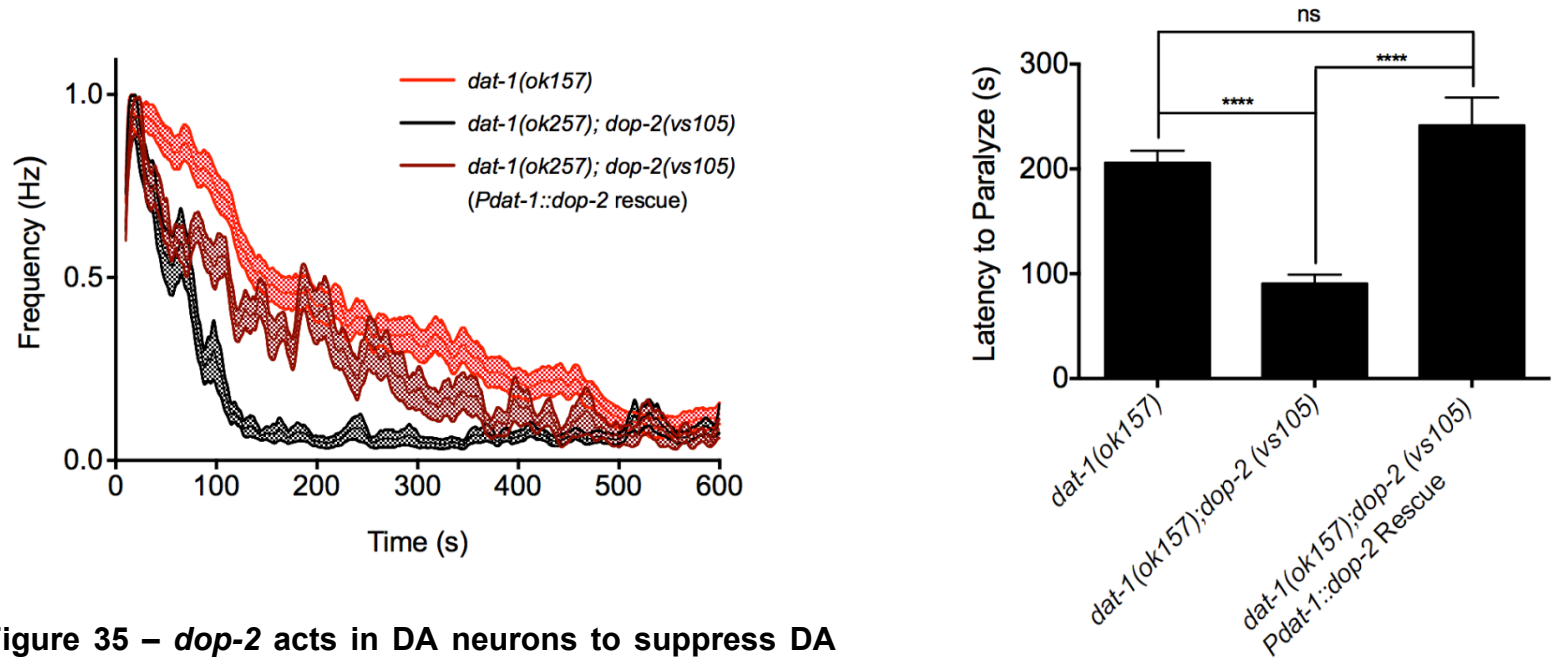

Figure 35 – *dop-2* acts in DA neurons to suppress DA signaling. (A) Average thrashing plots show enhanced paralysis in *dat-1(ok157); dop-2(vs105)* double mutants compared to *dat-1(ok157)* mutants. DA neuron expression of *dop-2* with the plasmid *Pdat-1::dop-2* suppressed this enhancement. (B) *dat-1(ok157); dop-2(vs105)* double mutants have a significantly decreased average latency to paralysis compared to *dat-1(ok157)* mutants, and DA neuron expression of *dop-2* rescues this effect up to *dat-1(ok157)* mutant levels. No significant difference was observed between *dat-1(ok157)* and *dat-1(ok157); dop-2(vs105) (pdat-1::dop-2)* transgenic animals. Data was analyzed using individual two-tailed Student's t-tests. ****P<.0001. n ≥ 25 for each condition.

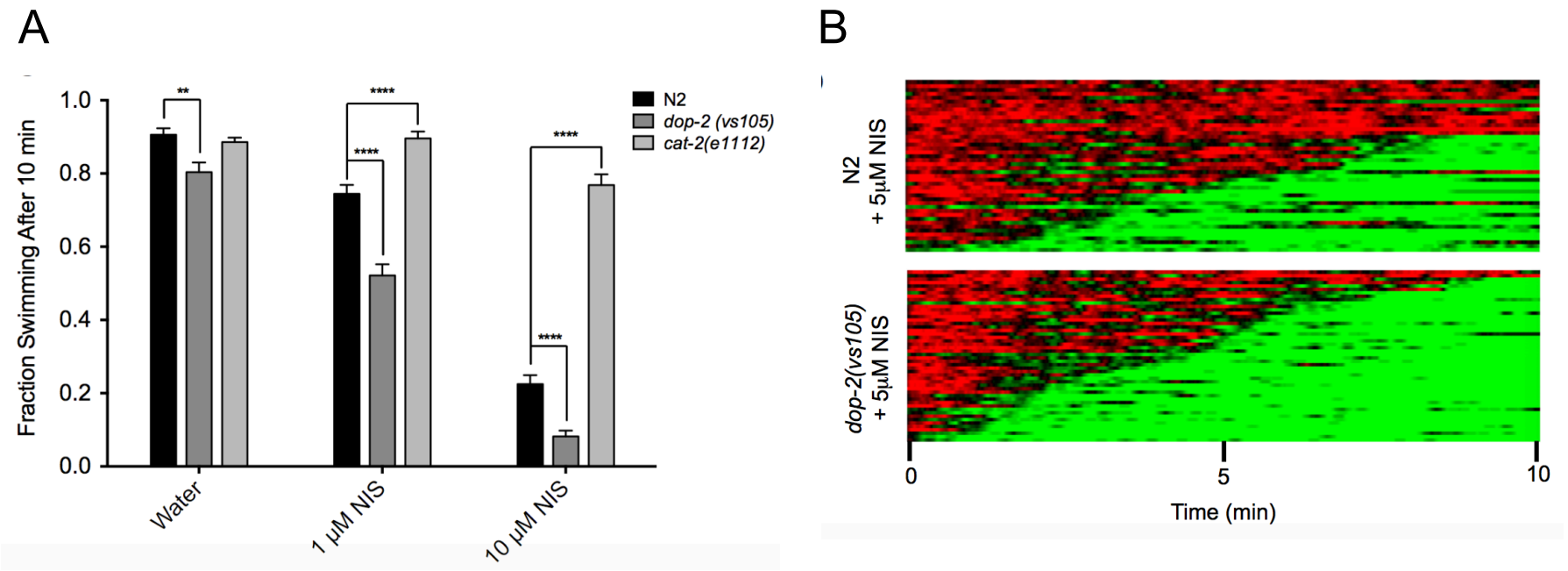

Figure 36 - NIS-induced Swip is enhanced by loss of *dop-2.* (a) *dop-2(vs105)* animals have subtle, yet significant increase in Swip compared to N2 in water, and a greater enhancement in 1 mM and 10 mM NIS. *cat-2(e1112)* animals have significantly less paralysis than N2 in both doses of NIS. Data was analyzed by two-way ANOVA with Bonferroni posttests comparing genotypes at each dose of NIS. ***P*<.01, ****P*<.0001. (b) Heat map analysis of animals in 5 mM NIS further demonstrates the increase in Swip in *dop-2(vs105)* mutants vs. N2. *dop-2(vs105)* showed a higher percentage of paralyzed animals (96.0% vs. 68.2% for N2), lower percentage of animals reverting to swimming (14.6% vs. 33.3% for N2) and significantly fewer average reversion events per paralyzed animal (2.14 ± 0.15 events vs. 4.40 ± 0.33 events for N2, P<.0001 two-tailed Student's t-test). n ≥ 44 for each condition.

afford insights into nervous system function. The model is also amenable to use of pharmacological agents, though the specificity and potency of these drugs does not always directly translate from studies of vertebrate targets. The AChE inhibitor aldicarb has proved the utility of agents that can act quickly to interfere with specific chemical signaling pathways, contributing to paradigms that can elucidate mechanisms by which mutations impact synaptic transmission. The findings presented in the current study make a case that NIS may provide a comparable tool for the dissection of components of DA signaling. Though a target of NET in mammalian systems, initial *in vitro* studies demonstrated NIS to be a potent inhibitor of DAT-1 mediated DA uptake (Jayanthi et al., 1998). Here, we show that low μM concentrations of NIS trigger Swip upon acute application, effects that are lost in animals that cannot produce DA (*cat-2*) and in animals that cannot support inhibitory DA signaling to motor neurons (*dop-3*). Furthermore, additivity experiments indicate that the behavioral effects of NIS are mediated through *dat-1*. The latter findings stand in contrast to those obtained with MPH, which appears to exert its Swip effects in a DA-independent manner. Our findings with MPH are reminiscent of the effects we reported with high dose imipramine, a tricyclic antidepressant that can induce DA-dependent Swip at low concentrations but also has potent actions at the serotonin transporter MOD-5 (Ranganathan et al., 2001). These actions at MOD-5 likely leads to the suppression of Swip observed at higher concentrations of imipramine, as detected in *dat-1(ok157)* animals (Hardaway et al., 2014). Cocaine, a nonspecific biogenic amine antagonist has also been used in *C. elegans*. We initially detected cocaine inhibition of DAT-1 in transfected mammalian cells, though at a potency orders of magnitude lower than seen with nisoxetine

(Jayanthi et al., 1998). Nonetheless, Musselman and colleagues detected an ability of cocaine to support chemosensory cue conditioning, with effects lost in mutants impacting DA synthesis and release (Musselman et al., 2012). In keeping, however, with the lack of specificity of cocaine in vertebrate preparations, cocaine also targets the serotonin transporter (MOD-5) (Ranganathan et al., 2001). These actions induce activation of ionotropic serotonin receptors that leads to movement inhibition independent of DA signaling (Ward et al., 2009). AMPH can trigger Swip upon acute application, though some of these actions are mediated by targets besides DAT-1 (Carvelli et al., 2010; Safratowich et al., 2013). Altogether, NIS appears to be the most specific drug to target DAT-1 *in vivo* to generate a robust and specific behavioral response.

While the use of a mammalian NET-specific drug to study DA signaling may seem counterintuitive, its utility here is based on its ability to create a context (elevated DA) in which the impact of other genes on DA signaling can be revealed. To this end, we showed that the Swip behavior generated by NIS treatment can be bidirectionally modified by genetic ablation of positive and negative presynaptic regulators of DA signaling. The acid-sensing channel ASIC-1 has been identified as a positive presynaptic regulator of DA release, and we found that mutation of *asic-1* could suppress Swip induced by NIS, classifying *asic-1(ok415)* animals as RID (**R**esistant to **I**nhibitors of **D**AT-1) mutants. Because loss of *asic-1* results in a **hypo**dopaminerigic state, we did not observe a Swip effect in *asic-1* mutants in the absence of NIS, highlighting the opportunity to reveal the effects of DA signaling mutants that may not have detectible behavioral effects on their own. We also demonstrated that NIS can

reveal the actions of a negative regulator of DA release, exemplified by *dop-2*. The DOP-2 receptor is expressed in DA neurons, and we show here for the first time to our knowledge that restoration of expression of *dop-2* in DA neurons significantly rescues a DA-dependent behavior, consistent with inhibitory autoreceptor action. Moreover, we showed that whereas loss of DOP-2 results in a barely detectable Swip phenotype on its own, a robust enhancement of paralysis is induced when a *dop-2* mutation is tested in combination with NIS treatments. While these observations are reminiscent of the effects that loss of *dop-2* has on Swip in *dat-1* mutants, the use of NIS to induce paralysis obviates the need for time-consuming genetic crosses and rescue experiments to provide evidence for DA signaling-dependent effects. Given that *asic-1* and *dop-2* have orthologs in mammals that appear to play conserved roles in regulating DA signaling (Ford, 2014; Pidoplichko and Dani, 2006), we suggest the use of NIS may be a significant aid to efforts to exploit the worm model for the identification of novel and conserved regulators of DA signaling.

CONCLUSIONS

We demonstrate that the mammalian NET-specific antagonist NIS induces Swip in *C. elegans*, a phenotype that our studies indicate as arising from high-affinity DAT-1 antagonism, leading to excess DA signaling at extrasynaptic D2-type DA receptors. The NIS-induced Swip phenotype can be used to probe the state of DA signaling in various genetic backgrounds. Unlike other drugs used by the field to induce this behavior, NIS effects are DA-specific, and its use can reveal states of both hyper- and hypodopaminergia based on enhancement or suppression of the Swip phenotype. By

analogy with the AChE aldicarb, NIS can be used to probe the molecular mechanics of synaptic transmission, as well as for more targeted analysis of candidate genes that support DA signaling.

REFERENCES

Abe, M.K., Kahle, K.T., Saelzler, M.P., Orth, K., Dixon, J.E., Rosner, M.R., 2001. ERK7 is an autoactivated member of the MAPK family. J Biol Chem 276, 21272-21279.

Abe, M.K., Kuo, W.L., Hershenson, M.B., Rosner, M.R., 1999. Extracellular signal-regulated kinase 7 (ERK7), a novel ERK with a C-terminal domain that regulates its activity, its cellular localization, and cell growth. Mol Cell Biol 19, 1301-1312.

Abe, M.K., Saelzler, M.P., Espinosa, R., 3rd, Kahle, K.T., Hershenson, M.B., Le Beau, M.M., Rosner, M.R., 2002. ERK8, a new member of the mitogen-activated protein kinase family. J Biol Chem 277, 16733-16743.

Adams, R.N., Conti, J., Marsden, C.A., Strope, E., 1978. The measurement of dopamine and 5-hydroxytryptamine release in CNS of freely moving unanaesthetised rats [proceedings]. Br J Pharmacol 64, 473P-471P.

Adams, R.N., Murrill, E., McCreery, R., Blank, L., Karolczak, M., 1972. 6-Hydroxydopamine, a new oxidation mechanism. Eur J Pharmacol 17, 287-292.

Allen, A.T., Maher, K.N., Wani, K.A., Betts, K.E., Chase, D.L., 2011. Coexpressed D1- and D2-like dopamine receptors antagonistically modulate acetylcholine release in Caenorhabditis elegans. Genetics 188, 579-590.

Alyea, R.A., Watson, C.S., 2009. Nongenomic mechanisms of physiological estrogen-mediated dopamine efflux. BMC Neurosci 10, 59.

Anden, N.E., Carlsson, A., Dahlstroem, A., Fuxe, K., Hillarp, N.A., Larsson, K., 1964. Demonstration and Mapping out of Nigro-Neostriatal Dopamine Neurons. Life Sci 3, 523-530.

Annamalai, B., Mannangatti, P., Arapulisamy, O., Shippenberg, T.S., Jayanthi, L., Ramamoorthy, S., 2011. Tyrosine Phosphorylation of the Human Serotonin Transporter: A Role in the Transporter Stability and Function. Mol Pharmacol.

Apparsundaram, S., Galli, A., DeFelice, L.J., Hartzell, H.C., Blakely, R.D., 1998. Acute regulation of norepinephrine transport: I. protein kinase C-linked muscarinic receptors influence transport capacity and transporter density in SK-N-SH cells. J Pharmacol Exp Ther 287, 733-743.

Arstikaitis, P., Gauthier-Campbell, C., 2006. BARS at the synapse: PICK-1 lipid binding domain regulates targeting, trafficking, and synaptic plasticity. J Neurosci 26, 6909-6910.

Bannon, M.J., Xue, C.H., Shibata, K., Dragovic, L.J., Kapatos, G., 1990. Expression of a human cocaine-sensitive dopamine transporter in Xenopus laevis oocytes. J Neurochem 54, 706-708.

Bany, I.A., Dong, M.Q., Koelle, M.R., 2003. Genetic and cellular basis for acetylcholine inhibition of Caenorhabditis elegans egg-laying behavior. J Neurosci 23, 8060-8069.

Batchelor, M., Schenk, J.O., 1998. Protein kinase A activity may kinetically upregulate the striatal transporter for dopamine. J Neurosci 18, 10304-10309.

Battaini, f., Pascale, A., Paoletti, R., Govoni, S., 1997. The role of anchoring protein RACK1 in PKC activation in the ageing brain. Trends in Neuroscience 20, 410-415.

Baudry, A., Mouillet-Richard, S., Schneider, B., Launay, J.M., Kellermann, O., 2010. miR-16 targets the serotonin transporter: a new facet for adaptive responses to antidepressants. Science 329, 1537-1541.

Bauman, A.L., Apparsundaram, S., Ramamoorthy, S., Wadzinski, B.E., Vaughan, R.A., Blakely, R.D., 2000. Cocaine and antidepressant-sensitive biogenic amine transporters exist in regulated complexes with protein phosphatase 2A. J Neurosci 20, 7571-7578.

Beaulieu, J.M., Gainetdinov, R.R., 2011. The physiology, signaling, and pharmacology of dopamine receptors. Pharmacol Rev 63, 182-217.

Beom, S., Cheong, D., Torres, G., Caron, M.G., Kim, K.M., 2004. Comparative studies of molecular mechanisms of dopamine D2 and D3 receptors for the activation of extracellular signal-regulated kinase. J Biol Chem 279, 28304-28314.

Bermingham, D.P., Hardaway, J.A., Snarrenberg, C.L., Robinson, S.B., Folkes, O.M., Salimando, G.J., Jinnah, H., Blakely, R.D., 2016. Acute blockade of the Caenorhabditis elegans dopamine transporter DAT-1 by the mammalian norepinephrine transporter inhibitor nisoxetine reveals the influence of genetic modifications of dopamine signaling in vivo. Neurochem Int.

Bertler, A., Rosengren, E., 1959. Occurrence and distribution of dopamine in brain and other tissues. Experientia 15, 10-11.

Birkmayer, W., Hornykiewicz, O., 1961. [The L-3,4-dioxyphenylalanine (DOPA)-effect in Parkinson-akinesia]. Wien Klin Wochenschr 73, 787-788.

Bjerggaard, C., Fog, J.U., Hastrup, H., Madsen, K., Loland, C.J., Javitch, J.A., Gether, U., 2004. Surface targeting of the dopamine transporter involves discrete epitopes in the distal C terminus but does not require canonical PDZ domain interactions. J Neurosci 24, 7024-7036.

Bolan, E.A., Kivell, B., Jaligam, V., Oz, M., Jayanthi, L.D., Han, Y., Sen, N., Urizar, E., Gomes, I., Devi, L.A., Ramamoorthy, S., Javitch, J.A., Zapata, A., Shippenberg, T.S., 2007. D2 receptors regulate dopamine transporter function via an extracellular signal-regulated kinases 1 and 2-dependent and phosphoinositide 3 kinase-independent mechanism. Mol Pharmacol 71, 1222-1232.

Boudanova, E., Navaroli, D.M., Melikian, H.E., 2008. Amphetamine-induced decreases in dopamine transporter surface expression are protein kinase C-independent. Neuropharmacology 54, 605-612.

Bowton, E., Saunders, C., Erreger, K., Sakrikar, D., Matthies, H.J., Sen, N., Jessen, T., Colbran, R.J., Caron, M.G., Javitch, J.A., Blakely, R.D., Galli, A., 2010. Dysregulation of dopamine transporters via dopamine D2 autoreceptors triggers anomalous dopamine efflux associated with attention-deficit hyperactivity disorder. J Neurosci 30, 6048-6057.

Brenner, S., 1974. The genetics of *Caenorhabditis elegans*. Genetics 77, 71-94.

Cardozo, D.L., Bean, B.P., 1995. Voltage-dependent calcium channels in rat midbrain dopamine neurons: modulation by dopamine and GABAB receptors. J Neurophysiol 74, 1137-1148.

Carlsson, A., Lindqvist, M., Magnusson, T., 1957. 3,4-Dihydroxyphenylalanine and 5-hydroxytryptophan as reserpine antagonists. Nature 180, 1200.

Carlsson, A., Lindqvist, M., Magnusson, T., Waldeck, B., 1958. On the presence of 3-hydroxytyramine in brain. Science 127, 471.

Carlsson, A., Waldeck, B., 1958. A fluorimetric method for the determination of dopamine (3-hydroxytyramine). Acta Physiol Scand 44, 293-298.

Carneiro, A., Blakely, R.D., 2004. A regulated association of the LIM domain protein HIC-5 with the antidepressant-sensitive serotonin transporter (SERT) in native tissues. Society for Neuroscience abstract.

Carneiro, A.M., Blakely, R.D., 2006. Serotonin, protein kinase C and HIC-5 associated redistribution of the platelet serotonin transporter. J Biol Chem 281, 24769-24780.

Carneiro, A.M., Ingram, S.L., Beaulieu, J.M., Sweeney, A., Amara, S.G., Thomas, S.M., Caron, M.G., Torres, G.E., 2002. The multiple LIM domain-containing adaptor protein Hic-5 synaptically colocalizes and interacts with the dopamine transporter. J Neurosci 22, 7045-7054.

Carvelli, L., Matthies, D.S., Galli, A., 2010. Molecular mechanisms of amphetamine actions in Caenorhabditis elegans. Mol Pharmacol 78, 151-156.

Carvelli, L., McDonald, P.W., Blakely, R.D., DeFelice, L.J., 2004. Dopamine transporters depolarize neurons by a channel mechanism. Proc Natl Acad Sci U S A 101, 16046-16051.

Carvelli, L., Moron, J.A., Kahlig, K.M., Ferrer, J.V., Sen, N., Lechleiter, J.D., Leeb-Lundberg, L.M., Merrill, G., Lafer, E.M., Ballou, L.M., Shippenberg, T.S., Javitch, J.A., Lin, R.Z., Galli, A., 2002. PI 3-kinase regulation of dopamine uptake. J Neurochem 81, 859-869.

Cervinski, M.A., Foster, J.D., Vaughan, R.A., 2005. Psychoactive substrates stimulate dopamine transporter phosphorylation and down regulation by cocaine sensitive and protein kinase C dependent mechanisms. J Biol Chem 280, 40442-40449.

Chang, M., Lee, S.-H., Kim, J.-H., Lee, K.-H., Kim, Y.-S., Son, H., Lee, Y.-S., 2001. Protein kinase C-mediated functional regulation of dopamine transporter is not achieved by direct phosphorylatin of the dopamine transporter protein. J. of Neurochem. 77, 754-761.

Chase, D.L., Pepper, J.S., Koelle, M.R., 2004a. Mechanism of extrasynaptic dopamine signaling in Caenorhabditis elegans. Nat Neurosci 7, 1096-1103.

Chase, D.L., Pepper, J.S., Koelle, M.R., 2004b. Mechanism of extrasynaptic dopamine signaling in Caenorhabditis elegans. Nat Neurosci 7, 1096-1103.

Chen, N.H., Reith, M.E., Quick, M.W., 2004. Synaptic uptake and beyond: the sodium- and chloride-dependent neurotransmitter transporter family SLC6. Pflugers Arch 447, 519-531.

Chen, R., Daining, C.P., Sun, H., Fraser, R., Stokes, S.L., Leitges, M., Gnegy, M.E., 2013. Protein kinase Cbeta is a modulator of the dopamine D2 autoreceptor-activated trafficking of the dopamine transporter. J Neurochem 125, 663-672.

Choy, R.K., Thomas, J.H., 1999. Fluoxetine-resistant mutants in C. elegans define a novel family of transmembrane proteins. Mol Cell 4, 143-152.

Ciliax, B.J., Drash, G.W., Staley, J.K., Haber, S., Mobley, C.J., Miller, G.W., Mufson, E.J., Mash, D.C., Levey, A.I., 1999. Immunocytochemical localization of the dopamine transporter in human brain. J Comp Neurol 409, 38-56.

Colecchia, D., Rossi, M., Sasdelli, F., Sanzone, S., Strambi, A., Chiariello, M., 2015. MAPK15 mediates BCR-ABL1-induced autophagy and regulates oncogene-dependent cell proliferation and tumor formation. Autophagy 11, 1790-1802.

Colecchia, D., Strambi, A., Sanzone, S., Iavarone, C., Rossi, M., Dall'Armi, C., Piccioni, F., Verrotti di Pianella, A., Chiariello, M., 2012. MAPK15/ERK8 stimulates autophagy by interacting with LC3 and GABARAP proteins. Autophagy 8, 1724-1740.

Conti, J.C., Strope, E., Adams, R.N., Marsden, C.A., 1978. Voltammetry in brain tissue: chronic recording of stimulated dopamine and 5-hydroxytryptamine release. Life Sci 23, 2705-2715.

Copeland, B.J., Vogelsberg, V., Neff, N.H., Hadjiconstantinou, M., 1996. Protein kinase C activators decrease dopamine uptake into striatal synaptosomes. The Journal of Pharmacology and Experimental Therapeutics 277, 1527-1532.

Cowell, R.M., Kantor, L., Hewlett, G.H., Frey, K.A., Gnegy, M.E., 2000. Dopamine transporter antagonists block phorbol ester-induced dopamine release and dopamine transporter phosphorylation in striatal synaptosomes. Eur J Pharmacol 389, 59-65.

Cremona, M.L., Matthies, H.J., Pau, K., Bowton, E., Speed, N., Lute, B.J., Anderson, M., Sen, N., Robertson, S.D., Vaughan, R.A., Rothman, J.E., Galli, A., Javitch, J.A., Yamamoto, A., 2011. Flotillin-1 is essential for PKC-triggered endocytosis and membrane microdomain localization of DAT. Nat Neurosci.

Daniels, G.M., Amara, S.G., 1999. Regulated trafficking of the human dopamine transporter. Clathrin-mediated internalization and lysosomal degradation in response to phorbol esters. J Biol Chem 274, 35794-35801.

Davis, M.W., Hammarlund, M., Harrach, T., Hullett, P., Olsen, S., Jorgensen, E.M., 2005. Rapid Single Nucleotide Polymorphism Mapping in C. elegans. BMC Genomics 6, 118.

De Mei, C., Ramos, M., Iitaka, C., Borrelli, E., 2009. Getting specialized: presynaptic and postsynaptic dopamine D2 receptors. Curr Opin Pharmacol 9, 53-58.

Derbez, A.E., Mody, R.M., Werling, L.L., 2002. Sigma(2)-receptor regulation of dopamine transporter via activation of protein kinase C. J Pharmacol Exp Ther 301, 306-314.

Doolen, S., Zahniser, N.R., 2001. Protein Tyrosine Kinase Inhibitors Alter Human Dopamine Transporter Activity in Xenopus Oocytes. J Pharmacol Exp Ther 296, 931-938.

Duerr, J.S., Frisby, D.L., Gaskin, J., Duke, A., Asermely, K., Huddleston, D., Eiden, L.E., Rand, J.B., 1999. The cat-1 gene of Caenorhabditis elegans encodes a vesicular monoamine transporter required for specific monoamine-dependent behaviors. J Neurosci 19, 72-84.

Dwyer, D.S., Aamodt, E., Cohen, B., Buttner, E.A., 2014. Drug elucidation: invertebrate genetics sheds new light on the molecular targets of CNS drugs. Front Pharmacol 5, 177.

Erickson, J.D., Eiden, L.E., Hoffman, B.J., 1992. Expression cloning of a reserpine-sensitive vesicular monoamine transporter. Proc Natl Acad Sci U S A 89, 10993-10997.

Fog, J.U., Khoshbouei, H., Holy, M., Owens, W.A., Vaegter, C.B., Sen, N., Nikandrova, Y., Bowton, E., McMahon, D.G., Colbran, R.J., Daws, L.C., Sitte, H.H., Javitch, J.A., Galli, A., Gether, U., 2006. Calmodulin kinase II interacts with the dopamine transporter C terminus to regulate amphetamine-induced reverse transport. Neuron 51, 417-429.

Ford, C.P., 2014. The role of D2-autoreceptors in regulating dopamine neuron activity and transmission. Neuroscience 282C, 13-22.

Foster, J.D., Adkins, S.D., Lever, J.R., Vaughan, R.A., 2008. Phorbol ester induced trafficking-independent regulation and enhanced phosphorylation of the dopamine transporter associated with membrane rafts and cholesterol. J Neurochem 105, 1683-1699.

Foster, J.D., Pananusorn, B., Cervinski, M.A., Holden, H.E., Vaughan, R.A., 2003. Dopamine transporters are dephosphorylated in striatal homogenates and in vitro by protein phosphatase 1. Brain Res Mol Brain Res 110, 100-108.

Foster, J.D., Vaughan, R.A., 2011. Palmitoylation controls dopamine transporter kinetics, degradation, and protein kinase C-dependent regulation. J Biol Chem 286, 5175-5186.

Foster, J.D., Yang, J.W., Moritz, A.E., Challasivakanaka, S., Smith, M.A., Holy, M., Wilebski, K., Sitte, H.H., Vaughan, R.A., 2012. Dopamine transporter phosphorylation site threonine 53 regulates substrate reuptake and amphetamine-stimulated efflux. J Biol Chem 287, 29702-29712.

Gabriel, L.R., Wu, S., Kearney, P., Bellve, K.D., Standley, C., Fogarty, K.E., Melikian, H.E., 2013. Dopamine transporter endocytic trafficking in striatal dopaminergic neurons: differential dependence on dynamin and the actin cytoskeleton. J Neurosci 33, 17836-17846.

Garcia, B.G., Wei, Y., Moron, J.A., Lin, R.Z., Javitch, J.A., Galli, A., 2005. Akt is essential for insulin modulation of amphetamine-induced human dopamine transporter cell-surface redistribution. Mol Pharmacol 68, 102-109.

Gerstein, M.B., Lu, Z.J., Van Nostrand, E.L., Cheng, C., Arshinoff, B.I., Liu, T., Yip, K.Y., Robilotto, R., Rechtsteiner, A., Ikegami, K., Alves, P., Chateigner, A., Perry, M., Morris, M., Auerbach, R.K., Feng, X., Leng, J., Vielle, A., Niu, W., Rhrissorrakrai, K., Agarwal, A., Alexander, R.P., Barber, G., Brdlik, C.M., Brennan, J., Brouillet, J.J., Carr, A.,

Cheung, M.S., Clawson, H., Contrino, S., Dannenberg, L.O., Dernburg, A.F., Desai, A., Dick, L., Dose, A.C., Du, J., Egelhofer, T., Ercan, S., Euskirchen, G., Ewing, B., Feingold, E.A., Gassmann, R., Good, P.J., Green, P., Gullier, F., Gutwein, M., Guyer, M.S., Habegger, L., Han, T., Henikoff, J.G., Henz, S.R., Hinrichs, A., Holster, H., Hyman, T., Iniguez, A.L., Janette, J., Jensen, M., Kato, M., Kent, W.J., Kephart, E., Khivansara, V., Khurana, E., Kim, J.K., Kolasinska-Zwierz, P., Lai, E.C., Latorre, I., Leahey, A., Lewis, S., Lloyd, P., Lochovsky, L., Lowdon, R.F., Lubling, Y., Lyne, R., MacCoss, M., Mackowiak, S.D., Mangone, M., McKay, S., Mecenas, D., Merrihew, G., Miller, D.M., 3rd, Muroyama, A., Murray, J.I., Ooi, S.L., Pham, H., Phippen, T., Preston, E.A., Rajewsky, N., Ratsch, G., Rosenbaum, H., Rozowsky, J., Rutherford, K., Ruzanov, P., Sarov, M., Sasidharan, R., Sboner, A., Scheid, P., Segal, E., Shin, H., Shou, C., Slack, F.J., Slightam, C., Smith, R., Spencer, W.C., Stinson, E.O., Taing, S., Takasaki, T., Vafeados, D., Voronina, K., Wang, G., Washington, N.L., Whittle, C.M., Wu, B., Yan, K.K., Zeller, G., Zha, Z., Zhong, M., Zhou, X., mod, E.C., Ahringer, J., Strome, S., Gunsalus, K.C., Micklem, G., Liu, X.S., Reinke, V., Kim, S.K., Hillier, L.W., Henikoff, S., Piano, F., Snyder, M., Stein, L., Lieb, J.D., Waterston, R.H., 2010. Integrative analysis of the Caenorhabditis elegans genome by the modENCODE project. Science 330, 1775-1787.

Giros, B., Jaber, M., Jones, S.R., Wightman, R.M., Caron, M.G., 1996. Hyperlocomotion and indifference to cocaine and amphetamine in mice lacking the dopamine transporter. Nature 379, 606-612.

Gonon, F., Cespuglio, R., Ponchon, J.L., Buda, M., Jouvet, M., Adams, R.N., Pujol, J.F., 1978. [In vivo continuous electrochemical determination of dopamine release in rat neostriatum]. C R Acad Sci Hebd Seances Acad Sci D 286, 1203-1206.

Gorentla, B.K., Moritz, A.E., Foster, J.D., Vaughan, R.A., 2009. Proline-directed phosphorylation of the dopamine transporter N-terminal domain. Biochemistry 48, 1067-1076.

Gorentla, B.K., Vaughan, R.A., 2005. Differential effects of dopamine and psychoactive drugs on dopamine transporter phosphorylation and regulation. Neuropharmacology 49, 759-768.

Granas, C., Ferrer, J., Loland, C.J., Javitch, J.A., Gether, U., 2003. N-terminal truncation of the dopamine transporter abolishes phorbol ester- and substance P receptor-stimulated phosphorylation without impairing transporter internalization. J Biol Chem 278, 4990-5000.

Hahn, M.K., Blakely, R.D., 2007. The Functional Impact of SLC6 Transporter Genetic Variation. Annu Rev Pharmacol Toxicol 47, 401-441.

Hall, D.H., Russell, R.L., 1991. The posterior nervous system of the nematode Caenorhabditis elegans: serial reconstruction of identified neurons and complete pattern of synaptic interactions. J Neurosci 11, 1-22.

Hardaway, J.A., Hardie, S.L., Whitaker, S.M., Baas, S.R., Zhang, B., Bermingham, D.P., Lichtenstein, A.J., Blakely, R.D., 2012. Forward genetic analysis to identify determinants

of dopamine signaling in Caenorhabditis elegans using swimming-induced paralysis. G3 (Bethesda) 2, 961-975.

Hardaway, J.A., Sturgeon, S.M., Snarrenberg, C.L., Li, Z., Xu, X.Z., Bermingham, D.P., Odiase, P., Spencer, W.C., Miller, D.M., 3rd, Carvelli, L., Hardie, S.L., Blakely, R.D., 2015. Glial Expression of the Caenorhabditis elegans Gene swip-10 Supports Glutamate Dependent Control of Extrasynaptic Dopamine Signaling. J Neurosci 35, 9409-9423.

Hardaway, J.A., Wang, J., Fleming, P.A., Fleming, K.A., Whitaker, S.M., Nackenoff, A., Snarrenberg, C.L., Hardie, S.L., Zhang, B., Blakely, R.D., 2014. An open-source analytical platform for analysis of C. elegans swimming-induced paralysis. J Neurosci Methods 232, 58-62.

Hardaway, J.A., Whitaker, S.M., Blakely, R.D., 2010. Media osmolarity modulates dopamine-dependent, swimming induced paralysis (SWIP). The Worm Breeder's Gazette 18.

Hare, E.E., Loer, C.M., 2004. Function and evolution of the serotonin-synthetic bas-1 gene and other aromatic amino acid decarboxylase genes in Caenorhabditis. BMC Evol Biol 4, 24.

Harikrishnan, K.N., Bayles, R., Ciccotosto, G.D., Maxwell, S., Cappai, R., Pelka, G.J., Tam, P.P., Christodoulou, J., El-Osta, A., 2010. Alleviating transcriptional inhibition of the norepinephrine slc6a2 transporter gene in depolarized neurons. J Neurosci 30, 1494-1501.

Henrich, L.M., Smith, J.A., Kitt, D., Errington, T.M., Nguyen, B., Traish, A.M., Lannigan, D.A., 2003. Extracellular signal-regulated kinase 7, a regulator of hormone-dependent estrogen receptor destruction. Mol Cell Biol 23, 5979-5988.

Hills, T., Brockie, P.J., Maricq, A.V., 2004. Dopamine and glutamate control area-restricted search behavior in Caenorhabditis elegans. J Neurosci 24, 1217-1225.

Holton, K.L., Loder, M.K., Melikian, H.E., 2005. Nonclassical, distinct endocytic signals dictate constitutive and PKC-regulated neurotransmitter transporter internalization. Nat Neurosci 8, 881-888.

Hong, W.C., Amara, S.G., 2013. Differential targeting of the dopamine transporter to recycling or degradative pathways during amphetamine- or PKC-regulated endocytosis in dopamine neurons. Faseb J 27, 2995-3007.

Hoover, B.R., Everett, C.V., Sorkin, A., Zahniser, N.R., 2007. Rapid regulation of dopamine transporters by tyrosine kinases in rat neuronal preparations. J Neurochem 101, 1258-1271.

Hornykiewicz, O., 1966. Dopamine (3-hydroxytyramine) and brain function. Pharmacol Rev 18, 925-964.

Horvitz, H.R., Chalfie, M., Trent, C., Sulston, J.E., Evans, P.D., 1982. Serotonin and octopamine in the nematode Caenorhabditis elegans. Science 216, 1012-1014.

Hu, Z., Cooper, M., Crockett, D.P., Zhou, R., 2004. Differentiation of the midbrain dopaminergic pathways during mouse development. J Comp Neurol 476, 301-311.

Huff, R.A., Vaughan, R.A., Kuhar, M.J., Uhl, G.R., 1997. Phorbol esters increase dopamine transporter phosphorylation and decrease transport V_{max}. The Journal of Neurochemistry 68, 225-232.

Iavarone, C., Acunzo, M., Carlomagno, F., Catania, A., Melillo, R.M., Carlomagno, S.M., Santoro, M., Chiariello, M., 2006. Activation of the Erk8 mitogen-activated protein (MAP) kinase by RET/PTC3, a constitutively active form of the RET proto-oncogene. J Biol Chem 281, 10567-10576.

Iwasaki, K., Staunton, J., Saifee, O., Nonet, M., Thomas, J.H., 1997. *aex-3* encodes a novel regulator of presynaptic activity in C.elegans. Neuron 18, 613-622.

Izquierdo, P.G., Calahorro, F., Ruiz-Rubio, M., 2013. The dopamine reuptake inhibitor methylphenidate causes swimming- induced paralysis in C. elegans. The Worm Breeder's Gazette 19.

Jaber, M., Jones, S., Giros, B., Caron, M.G., 1997. The dopamine transporter: a crucial component regulating dopamine transmission. Mov Disord 12, 629-633.

Jayanthi, L.D., Apparsundaram, S., Malone, M.D., Ward, E., Miller, D.M., Eppler, M., Blakely, R.D., 1998. The Caenorhabditis elegans gene T23G5.5 encodes an antidepressant- and cocaine-sensitive dopamine transporter. Mol Pharmacol 54, 601-609.

Jayanthi, L.D., Samuvel, D.J., Ramamoorthy, S., 2004. Regulated internalization and phosphorylation of the native norepinephrine transporter in response to phorbol esters:

Evidence for localization in lipid rafts and lipid raft mediated internalization. J Biol Chem 279, 19315-19326.

Jorgensen, E.M., Hartwieg, E., Schuske, K., Nonet, M.L., Jin, Y., Horvitz, H.R., 1995. Defective recycling of synaptic vesicles in synaptotagmin mutants of Caenorhabditis elegans. Nature 378, 196-199.

Jovanovic, J.N., Czernik, A.J., Fienberg, A.A., Greengard, P., Sihra, T.S., 2000. Synapsins as mediators of BDNF-enhanced neurotransmitter release. Nat Neurosci 3, 323-329.

Kannan, N., Neuwald, A.F., 2004. Evolutionary constraints associated with functional specificity of the CMGC protein kinases MAPK, CDK, GSK, SRPK, DYRK, and CK2alpha. Protein Sci 13, 2059-2077.

Khoshbouei, H., Sen, N., Guptaroy, B., Johnson, L., Lund, D., Gnegy, M.E., Galli, A., Javitch, J.A., 2004. N-terminal phosphorylation of the dopamine transporter is required for amphetamine-induced efflux. PLoS Biol 2, E78.

Kilty, J.E., Lorang, D., Amara, S.G., 1991. Cloning and expression of a cocaine-sensitive rat dopamine transporter. Science 254, 578-579.

Kimura, K.D., Fujita, K., Katsura, I., 2010. Enhancement of odor avoidance regulated by dopamine signaling in Caenorhabditis elegans. J Neurosci 30, 16365-16375.

Kindt, K.S., Quast, K.B., Giles, A.C., De, S., Hendrey, D., Nicastro, I., Rankin, C.H., Schafer, W.R., 2007. Dopamine mediates context-dependent modulation of sensory plasticity in C. elegans. Neuron 55, 662-676.

Kitayama, S., Dohi, T., Uhl, G., 1994. Phorbol esters alter functions of the expressed dopamine transporter. European Journal of Pharmacology 268, 115-119.

Kivell, B., Uzelac, Z., Sundaramurthy, S., Rajamanickam, J., Ewald, A., Chefer, V., Jaligam, V., Bolan, E., Simonson, B., Annamalai, B., Mannangatti, P., Prisinzano, T.E., Gomes, I., Devi, L.A., Jayanthi, L.D., Sitte, H.H., Ramamoorthy, S., Shippenberg, T.S., 2014. Salvinorin A regulates dopamine transporter function via a kappa opioid receptor and ERK1/2-dependent mechanism. Neuropharmacology 86, 228-240.

Kopin, I.J., 1985. Catecholamine metabolism: basic aspects and clinical significance. Pharmacol Rev 37, 333-364.

Koushika, S.P., Nonet, M.L., 2000. Sorting and transport in C. elegans: aA model system with a sequenced genome. Curr Opin Cell Biol 12, 517-523.

Kurian, M.A., Gissen, P., Smith, M., Heales, S., Jr., Clayton, P.T., 2011. The monoamine neurotransmitter disorders: an expanding range of neurological syndromes. Lancet Neurol 10, 721-733.

Kushner, S.A., Elgersma, Y., Murphy, G.G., Jaarsma, D., van Woerden, G.M., Hojjati, M.R., Cui, Y., LeBoutillier, J.C., Marrone, D.F., Choi, E.S., De Zeeuw, C.I., Petit, T.L., Pozzo-Miller, L., Silva, A.J., 2005. Modulation of presynaptic plasticity and learning by

the H-ras/extracellular signal-regulated kinase/synapsin I signaling pathway. J Neurosci 25, 9721-9734.

Lacey, M.G., Mercuri, N.B., North, R.A., 1987. Dopamine acts on D2 receptors to increase potassium conductance in neurones of the rat substantia nigra zona compacta. J Physiol 392, 397-416.

Lee, F.J., Liu, F., Pristupa, Z.B., Niznik, H.B., 2001. Direct binding and functional coupling of a-synuclein to the dopamine transporters accelerate dopamine-induced apoptosis. Faseb J 15, 916-926.

Lee, K.H., Kim, M.Y., Kim, D.H., Lee, Y.S., 2004. Syntaxin 1A and receptor for activated C kinase interact with the N-terminal region of human dopamine transporter. Neurochem Res 29, 1405-1409.

Li, L., Su, Y., Zhao, C., Zhao, H., Liu, G., Wang, J., Xu, Q., 2006a. The role of Ret receptor tyrosine kinase in dopaminergic neuron development. Neuroscience 142, 391-400.

Li, W., Feng, Z., Sternberg, P.W., Xu, X.Z., 2006b. A C. elegans stretch receptor neuron revealed by a mechanosensitive TRP channel homologue. Nature 440, 684-687.

Lin, Z., Zhang, P.W., Zhu, X., Melgari, J.M., Huff, R., Spieldoch, R.L., Uhl, G.R., 2003. Phosphatidylinositol 3-Kinase, Protein Kinase C, and MEK1/2 Kinase Regulation of Dopamine Transporters (DAT) Require N-terminal DAT Phosphoacceptor Sites. J Biol Chem 278, 20162-20170.

Lints, R., Emmons, S.W., 1999. Patterning of dopaminergic neurotransmitter identity among Caenorhabditis elegans ray sensory neurons by a TGFbeta family signaling pathway and a Hox gene. Development 126, 5819-5831.

Liu, K.S., Sternberg, P.W., 1995. Sensory regulation of male mating behavior in Caenorhabditis elegans. Neuron 14, 79-89.

Loder, M.K., Melikian, H.E., 2003. The dopamine transporter constitutively internalizes and recycles in a protein kinase C-regulated manner in stably transfected PC12 cell lines. J Biol Chem 278, 22168-22174.

Loer, C.M., Kenyon, C.J., 1993. Serotonin-deficient mutants and male mating behavior in the nematode Caenorhabditis elegans. J Neurosci 13, 5407-5417.

Loonam, T.M., Noailles, P.A., Yu, J., Zhu, J.P., Angulo, J.A., 2003. Substance P and cholecystokinin regulate neurochemical responses to cocaine and methamphetamine in the striatum. Life Sci 73, 727-739.

Marti, M.J., James, C.J., Oo, T.F., Kelly, W.J., Burke, R.E., 1997. Early developmental destruction of terminals in the striatal target induces apoptosis in dopamine neurons of the substantia nigra. J Neurosci 17, 2030-2039.

Mazei-Robison, M.S., Bowton, E., Holy, M., Schmudermaier, M., Freissmuth, M., Sitte, H.H., Galli, A., Blakely, R.D., 2008. Anomalous dopamine release associated with a human dopamine transporter coding variant. J Neurosci 28, 7040-7046.

McDonald, P.W., Hardie, S.L., Jessen, T.N., Carvelli, L., Matthies, D.S., Blakely, R.D., 2007. Vigorous motor activity in Caenorhabditis elegans requires efficient clearance of dopamine mediated by synaptic localization of the dopamine transporter DAT-1. J Neurosci 27, 14216-14227.

McDonald, P.W., Jessen, T., Field, J.R., Blakely, R.D., 2006a. Dopamine Signaling Architecture in Caenorhabditis elegans. Cell Mol Neurobiol 26, 591-616.

McDonald, P.W., Jessen, T., Field, J.R., Blakely, R.D., 2006b. Dopamine signaling architecture in Caenorhabditis elegans. Cell Mol Neurobiol 26, 593-618.

Melikian, H., Buckley, K., 1999. Membrane trafficking regulates the activity of the human dopamine transporter. J. Neuroscience 19, 7699-7710.

Mercuri, N.B., Saiardi, A., Bonci, A., Picetti, R., Calabresi, P., Bernardi, G., Borrelli, E., 1997. Loss of autoreceptor function in dopaminergic neurons from dopamine D2 receptor deficient mice. Neuroscience 79, 323-327.

Mergy, M.A., Gowrishankar, R., Gresch, P.J., Gantz, S.C., Williams, J., Davis, G.L., Wheeler, C.A., Stanwood, G.D., Hahn, M.K., Blakely, R.D., 2014. The rare DAT coding variant Val559 perturbs DA neuron function, changes behavior, and alters in vivo responses to psychostimulants. Proc Natl Acad Sci U S A 111, E4779-4788.

Mijatovic, J., Patrikainen, O., Yavich, L., Airavaara, M., Ahtee, L., Saarma, M., Piepponen, T.P., 2008. Characterization of the striatal dopaminergic neurotransmission in MEN2B mice with elevated cerebral tissue dopamine. J Neurochem 105, 1716-1725.

Miller, K.G., Alfonso, A., Nguyen, M., Crowell, J.A., Johnson, C.D., Rand, J.B., 1996. A genetic selection for *Caenorhabditis elegans* synaptic transmission mutants. Proc Natl Acad Sci 93, 12593-12598.

Miranda, M., Wu, C.C., Sorkina, T., Korstjens, D.R., Sorkin, A., 2005. Enhanced ubiquitylation and accelerated degradation of the dopamine transporter mediated by protein kinase C. J Biol Chem 280, 35617-35624.

Miyatake, K., Kusakabe, M., Takahashi, C., Nishida, E., 2015. ERK7 regulates ciliogenesis by phosphorylating the actin regulator CapZIP in cooperation with Dishevelled. Nat Commun 6, 6666.

Montagu, K.A., 1957. Catechol compounds in rat tissues and in brains of different animals. Nature 180, 244-245.

Moron, J.A., Zakharova, I., Ferrer, J.V., Merrill, G.A., Hope, B.T., Lafer, E.M., Lin, Z.C., Wang, J.B., Javitch, J.A., Galli, A., Shippenberg, T.S., 2003. Mitogen-Activated protein kinase regulates dopamine transporter surface expression and dopamine transport capacity. The Journal of Neuroscience 23, 8480-8488.

Mortensen, O.V., Larsen, M.B., Prasad, B.M., Amara, S.G., 2008. Genetic complementation screen identifies a mitogen-activated protein kinase phosphatase, MKP3, as a regulator of dopamine transporter trafficking. Mol Biol Cell 19, 2818-2829.

Mullen, G.P., Mathews, E.A., Vu, M.H., Hunter, J.W., Frisby, D.L., Duke, A., Grundahl, K., Osborne, J.D., Crowell, J.A., Rand, J.B., 2007. Choline transport and de novo

choline synthesis support acetylcholine biosynthesis in Caenorhabditis elegans cholinergic neurons. Genetics 177, 195-204.

Musselman, H.N., Neal-Beliveau, B., Nass, R., Engleman, E.A., 2012. Chemosensory cue conditioning with stimulants in a Caenorhabditis elegans animal model of addiction. Behav Neurosci 126, 445-456.

Nagatsu, T., Levitt, M., Udenfriend, S., 1964. Conversion of L-tyrosine to 3,4-dihydroxyphenylalanine by cell-free preparations of brain and sympathetically innervated tissues. Biochem Biophys Res Commun 14, 543-549.

Nass, R., Hall, D.H., Miller, D.M., 3rd, Blakely, R.D., 2002. Neurotoxin-induced degeneration of dopamine neurons in Caenorhabditis elegans. Proc Natl Acad Sci U S A 99, 3264-3269.

Navaroli, D.M., Stevens, Z.H., Uzelac, Z., Gabriel, L., King, M.J., Lifshitz, L.M., Sitte, H.H., Melikian, H.E., 2011. The Plasma Membrane-Associated GTPase Rin Interacts with the Dopamine Transporter and Is Required for Protein Kinase C-Regulated Dopamine Transporter Trafficking. The Journal of Neuroscience 31, 13.

Nonet, M.L., Staunton, J.E., Kilgard, M.P., Fergestad, T., Hartwieg, E., Horvitz, H.R., Jorgensen, E.M., Meyer, B.J., 1997. Caenorhabditis elegans rab-3 mutant synapses exhibit impaired function and are partially depleted of vesicles. J Neurosci 17, 8061-8073.

O'Neill, C.M., Ball, S.G., Vaughan, P.F., 1994. Effects of ischaemic conditions on uptake of glutamate, aspartate, and noradrenaline by cell lines derived from the human nervous system. J Neurochem 63, 603-611.

Olson, P.A., Tkatch, T., Hernandez-Lopez, S., Ulrich, S., Ilijic, E., Mugnaini, E., Zhang, H., Bezprozvanny, I., Surmeier, D.J., 2005. G-protein-coupled receptor modulation of striatal CaV1.3 L-type Ca2+ channels is dependent on a Shank-binding domain. J Neurosci 25, 1050-1062.

Omura, D.T., Clark, D.A., Samuel, A.D., Horvitz, H.R., 2012. Dopamine signaling is essential for precise rates of locomotion by C. elegans. PLoS One 7, e38649.

Opazo, F., Schulz, J.B., Falkenburger, B.H., 2010. PKC links G(q)-coupled receptors to DAT-mediated dopamine release. J Neurochem.

Owens, W.A., Williams, J.M., Saunders, C., Avison, M.J., Galli, A., Daws, L.C., 2012. Rescue of dopamine transporter function in hypoinsulinemic rats by a D2 receptor-ERK-dependent mechanism. J Neurosci 32, 2637-2647.

Page, G., Barc-Pain, S., Pontcharraud, R., Cante, A., Piriou, A., Barrier, L., 2004. The up-regulation of the striatal dopamine transporter's activity by cAMP is PKA-, CaMK II- and phosphatase-dependent. Neurochem Int 45, 627-632.

Page, G., Peeters, M., Najimi, M., Maloteaux, J.M., Hermans, E., 2001. Modulation of the neuronal dopamine transporter activity by the metabotropic glutamate receptor mGluR5 in rat striatal synaptosomes through phosphorylation mediated processes. J Neurochem 76, 1282-1290.

Pan, J., You, Y., Huang, T., Brody, S.L., 2007. RhoA-mediated apical actin enrichment is required for ciliogenesis and promoted by Foxj1. J Cell Sci 120, 1868-1876.

Park, T.J., Mitchell, B.J., Abitua, P.B., Kintner, C., Wallingford, J.B., 2008. Dishevelled controls apical docking and planar polarization of basal bodies in ciliated epithelial cells. Nat Genet 40, 871-879.

Perez-Polo, J.R., Tiffany-Castiglioni, E., Ziegler, M.G., Werrbach-Perez, K., 1982. Effect of nerve growth factor on catecholamine metabolism in a human neuroblastoma clone (SY5Y). Dev Neurosci 5, 418-423.

Peter, D., Liu, Y., Sternini, C., de Giorgio, R., Brecha, N., Edwards, R.H., 1995. Differential expression of two vesicular monoamine transporters. J Neurosci 15, 6179-6188.

Pidoplichko, V.I., Dani, J.A., 2006. Acid-sensitive ionic channels in midbrain dopamine neurons are sensitive to ammonium, which may contribute to hyperammonemia damage. Proc Natl Acad Sci U S A 103, 11376-11380.

Pizzo, A.B., Karam, C.S., Zhang, Y., Ma, C.L., McCabe, B.D., Javitch, J.A., 2014. Amphetamine-induced behavior requires CaMKII-dependent dopamine transporter phosphorylation. Mol Psychiatry 19, 279-281.

Portig, P.J., Vogt, M., 1969. Release to the cerebral ventricles of substances with possible transmitter function in the caudate nucleus. J Physiol 204, 687-715.

Prasad, H.C., Zhu, C.B., McCauley, J.L., Samuvel, D.J., Ramamoorthy, S., Shelton, R.C., Hewlett, W.A., Sutcliffe, J.S., Blakely, R.D., 2005. Human serotonin transporter variants display altered sensitivity to protein kinase G and p38 mitogen-activated protein kinase. Proc Natl Acad Sci U S A 102, 11545-11550.

Pristupa, Z.B., McConkey, F., Liu, F., Man, H.Y., Lee, F.J., Wang, Y.T., Niznik, H.B., 1998. Protein kinase-mediated bidirectional trafficking and functional regulation of the human dopamine transporter. Synapse 30, 79-87.

Quick, M.W., Hu, J., Wang, D., Zhang, H.Y., 2004. Regulation of a gamma -aminobutyric acid (GABA) transporter by reciprocal tyrosine and serine phosphorylation. J Biol Chem 279, 15961-15967.

Rand, J.B., 2007. Acetylcholine, WormBook,WormBook.

Rand, J.B., Duerr, J.S., Frisby, D.L., 1998. Using Caenorhabditis elegans to study vesicular transport. Methods Enzymol 296, 529-547.

Ranganathan, R., Sawin, E.R., Trent, C., Horvitz, H.R., 2001. Mutations in the Caenorhabditis elegans serotonin reuptake transporter MOD-5 reveal serotonin-dependent and -independent activities of fluoxetine. J Neurosci 21, 5871-5884.

Ringstad, N., Abe, N., Horvitz, H.R., 2009. Ligand-gated chloride channels are receptors for biogenic amines in C. elegans. Science 325, 96-100.

Rizo, J., Xu, J., 2015. The Synaptic Vesicle Release Machinery. Annu Rev Biophys 44, 339-367.

Roeper, J., 2013. Dissecting the diversity of midbrain dopamine neurons. Trends Neurosci 36, 336-342.

Rossi, M., Colecchia, D., Iavarone, C., Strambi, A., Piccioni, F., Verrotti di Pianella, A., Chiariello, M., 2011. Extracellular signal-regulated kinase 8 (ERK8) controls estrogen-related receptor alpha (ERRalpha) cellular localization and inhibits its transcriptional activity. J Biol Chem 286, 8507-8522.

Rossi, M., Colecchia, D., Ilardi, G., Acunzo, M., Nigita, G., Sasdelli, F., Celetti, A., Strambi, A., Staibano, S., Croce, C.M., Chiariello, M., 2016. MAPK15 upregulation promotes cell proliferation and prevents DNA damage in male germ cell tumors. Oncotarget.

Rothman, R.B., Dersch, C.M., Carroll, F.I., Ananthan, S., 2002. Studies of the biogenic amine transporters. VIII: identification of a novel partial inhibitor of dopamine uptake and dopamine transporter binding. Synapse 43, 268-274.

Sacchetti, P., Mitchell, T.R., Granneman, J.G., Bannon, M.J., 2001. Nurr1 enhances transcription of the human dopamine transporter gene through a novel mechanism. J Neurochem 76, 1565-1572.

Saelzler, M.P., Spackman, C.C., Liu, Y., Martinez, L.C., Harris, J.P., Abe, M.K., 2006. ERK8 down-regulates transactivation of the glucocorticoid receptor through Hic-5. J Biol Chem 281, 16821-16832.

Safratowich, B.D., Hossain, M., Bianchi, L., Carvelli, L., 2014. Amphetamine potentiates the effects of beta-phenylethylamine through activation of an amine-gated chloride channel. J Neurosci 34, 4686-4691.

Safratowich, B.D., Lor, C., Bianchi, L., Carvelli, L., 2013. Amphetamine activates an amine-gated chloride channel to generate behavioral effects in Caenorhabditis elegans. J Biol Chem 288, 21630-21637.

Sakrikar, D., Mazei-Robison, M.S., Mergy, M.A., Richtand, N.W., Han, Q., Hamilton, P.J., Bowton, E., Galli, A., Veenstra-Vanderweele, J., Gill, M., Blakely, R.D., 2012. Attention deficit/hyperactivity disorder-derived coding variation in the dopamine transporter disrupts microdomain targeting and trafficking regulation. J Neurosci 32, 5385-5397.

Samuvel, D.J., Jayanthi, L.D., Bhat, N.R., Ramamoorthy, S., 2005. A role for p38 mitogen-activated protein kinase in the regulation of the serotonin transporter: evidence for distinct cellular mechanisms involved in transporter surface expression. J Neurosci 25, 29-41.

Sanyal, S., Wintle, R.F., Kindt, K.S., Nuttley, W.M., Arvan, R., Fitzmaurice, P., Bigras, E., Merz, D.C., Hebert, T.E., van der Kooy, D., Schafer, W.R., Culotti, J.G., Van Tol, H.H., 2004. Dopamine modulates the plasticity of mechanosensory responses in Caenorhabditis elegans. Embo J 23, 473-482.

Sawin, E.R., Ranganathan, R., Horvitz, H.R., 2000. *C. elegans* locomotory rate is modulated by the environment through a dopaminergic pathway and by experience through a serotonergic pathway. Neuron 26, 619-631.

Schafer, W.R., Kenyon, C.J., 1995. A calcium-channel homologue required for adaptation to dopamine and serotonin in Caenorhabditis elegans. Nature 375, 73-78.

Schmid, T., Snoek, L.B., Frohli, E., van der Bent, M.L., Kammenga, J., Hajnal, A., 2015. Systemic Regulation of RAS/MAPK Signaling by the Serotonin Metabolite 5-HIAA. PLoS Genet 11, e1005236.

Shimada, S., Kitayama, S., Lin, C., Patel, A., Nanthakumar, E., Gregor, P., Kuhar, M., Uhl, G., 1991. Cloning and expression of a cocaine-sensitive dopamine transporter complementary DNA. Science 254, 576-577.

Simon, J.R., Bare, D.J., Ghetti, B., Richter, J.A., 1997. A possible role for tyrosine kinases in the regulation of the neuronal dopamine transporter in mouse striatum. Neurosci.Lett. 224, 201-205.

Sorkina, T., Miranda, M., Dionne, K.R., Hoover, B.R., Zahniser, N.R., Sorkin, A., 2006. RNA interference screen reveals an essential role of Nedd4-2 in dopamine transporter ubiquitination and endocytosis. J Neurosci 26, 8195-8205.

Speed, N., Saunders, C., Davis, A.R., Owens, W.A., Matthies, H.J., Saadat, S., Kennedy, J.P., Vaughan, R.A., Neve, R.L., Lindsley, C.W., Russo, S.J., Daws, L.C., Niswender, K.D., Galli, A., 2011. Impaired striatal Akt signaling disrupts dopamine homeostasis and increases feeding. PLoS One 6, e25169.

Speed, N.K., Matthies, H.J., Kennedy, J.P., Vaughan, R.A., Javitch, J.A., Russo, S.J., Lindsley, C.W., Niswender, K., Galli, A., 2010. Akt-dependent and isoform-specific regulation of dopamine transporter cell surface expression. ACS Chem Neurosci 1, 476-481.

Spencer, W.C., Zeller, G., Watson, J.D., Henz, S.R., Watkins, K.L., McWhirter, R.D., Petersen, S., Sreedharan, V.T., Widmer, C., Jo, J., Reinke, V., Petrella, L., Strome, S., Von Stetina, S.E., Katz, M., Shaham, S., Ratsch, G., Miller, D.M., 3rd, 2011. A spatial and temporal map of C. elegans gene expression. Genome Res 21, 325-341.

Steiner, J.A., Carneiro, A.M., Wright, J., Matthies, H.J., Prasad, H.C., Nicki, C.K., Dostmann, W.R., Buchanan, C.C., Corbin, J.D., Francis, S.H., Blakely, R.D., 2009. cGMP-dependent protein kinase Ialpha associates with the antidepressant-sensitive serotonin transporter and dictates rapid modulation of serotonin uptake. Mol Brain 2, 26.

Steinkellner, T., Mus, L., Eisenrauch, B., Constantinescu, A., Leo, D., Konrad, L., Rickhag, M., Sorensen, G., Efimova, E.V., Kong, E., Willeit, M., Sotnikova, T.D., Kudlacek, O., Gether, U., Freissmuth, M., Pollak, D.D., Gainetdinov, R.R., Sitte, H.H., 2014. In vivo amphetamine action is contingent on alphaCaMKII. Neuropsychopharmacology 39, 2681-2693.

Steinkellner, T., Yang, J.W., Montgomery, T.R., Chen, W.Q., Winkler, M.T., Sucic, S., Lubec, G., Freissmuth, M., Elgersma, Y., Sitte, H.H., Kudlacek, O., 2012. Ca(2+)/calmodulin-dependent protein kinase IIalpha (alphaCaMKII) controls the activity of the dopamine transporter: implications for Angelman syndrome. J Biol Chem 287, 29627-29635.

Subramanian, J., Morozov, A., 2011. Erk1/2 inhibit synaptic vesicle exocytosis through L-type calcium channels. J Neurosci 31, 4755-4764.

Sucic, S., El-Kasaby, A., Kudlacek, O., Sarker, S., Sitte, H.H., Marin, P., Freissmuth, M., 2011. The serotonin transporter is an exclusive client of the COPII component SEC24C. J Biol Chem.

Sugiura, M., Fuke, S., Suo, S., Sasagawa, N., Van Tol, H.H., Ishiura, S., 2005. Characterization of a novel D2-like dopamine receptor with a truncated splice variant and a D1-like dopamine receptor unique to invertebrates from Caenorhabditis elegans. J Neurochem 94, 1146-1157.

Sulston, J., Dew, M., Brenner, S., 1975. Dopaminergic neurons in the nematode Caenorhabditis elegans. J Comp Neurol 163, 215-226.

Suo, S., Sasagawa, N., Ishiura, S., 2002. Identification of a dopamine receptor from Caenorhabditis elegans. Neurosci Lett 319, 13-16.

Suo, S., Sasagawa, N., Ishiura, S., 2003. Cloning and characterization of a Caenorhabditis elegans D2-like dopamine receptor. J Neurochem 86, 869-878.

Tian, Y., Kapatos, G., Granneman, J.G., Bannon, M.J., 1994. Dopamine and g-aminobutyric acid transporters: Differential regulation by agents that promote phosphorylation. Neuroscience Letters 173, 143-146.

Tkachenko, E., Sabouri-Ghomi, M., Pertz, O., Kim, C., Gutierrez, E., Machacek, M., Groisman, A., Danuser, G., Ginsberg, M.H., 2011. Protein kinase A governs a RhoA-RhoGDI protrusion-retraction pacemaker in migrating cells. Nat Cell Biol 13, 660-667.

Tong, J., Li, L., Ballermann, B., Wang, Z., 2016. Phosphorylation and Activation of RhoA by ERK in Response to Epidermal Growth Factor Stimulation. PLoS One 11, e0147103.

Torres, G.E., Carneiro, A., Seamans, K., Fiorentini, C., Sweeney, A., Yao, W.D., Caron, M.G., 2003. Oligomerization and trafficking of the human dopamine transporter. Mutational analysis identifies critical domains important for the functional expression of the transporter. J Biol Chem 278, 2731-2739.

Torres, G.E., Yao, W.D., Mohn, A.R., Quan, H., Caron, M.G., 2000. Specific interaction between the dopamine transporter and the PDZ domain-containg protein pick1, Society for Neurocience. Vol. 26, New Orleans, LA, p. 17.13.

Tsao, C.W., Lin, Y.S., Cheng, J.T., Lin, C.F., Wu, H.T., Wu, S.R., Tsai, W.H., 2008. Interferon-alpha-induced serotonin uptake in Jurkat T cells via mitogen-activated protein kinase and transcriptional regulation of the serotonin transporter. J Psychopharmacol 22, 753-760.

Usdin, T.B., Mezey, E., Chen, C., Brownstein, M.J., Hoffman, B.J., 1991. Cloning of the cocaine-sensitive bovine dopamine transporter. Proc Natl Acad Sci 88, 11168-11171.

Vara, H., Onofri, F., Benfenati, F., Sassoe-Pognetto, M., Giustetto, M., 2009. ERK activation in axonal varicosities modulates presynaptic plasticity in the CA3 region of the hippocampus through synapsin I. Proc Natl Acad Sci U S A 106, 9872-9877.

Vaughan, R.A., Huff, R.A., Uhl, G.R., Kuhar, M.J., 1997. Protein kinase C-mediated phosphorylation and functional regulation of dopamine transporters in striatal synaptosomes. The Journal of Biological Chemistry 272, 15541-15546.

Vidal-Gadea, A.G., Davis, S., Becker, L., Pierce-Shimomura, J.T., 2012. Coordination of behavioral hierarchies during environmental transitions in. Worm 1, 5-11.

Voglis, G., Tavernarakis, N., 2008. A synaptic DEG/ENaC ion channel mediates learning in C. elegans by facilitating dopamine signalling. Embo J 27, 3288-3299.

Vuorenpaa, A., Jorgensen, T.N., Newman, A.H., Madsen, K.L., Scheinin, M., Gether, U., 2016. Differential Internalization Rates and Postendocytic Sorting of the Norepinephrine and Dopamine Transporters Are Controlled by Structural Elements in the N Termini. J Biol Chem 291, 5634-5651.

Walkinshaw, G., Waters, C.M., 1994. Neurotoxin-induced cell death in neuronal PC12 cells is mediated by induction of apoptosis. Neuroscience 63, 975-987.

Ward, A., Walker, V.J., Feng, Z., Xu, X.Z., 2009. Cocaine modulates locomotion behavior in C. elegans. PLoS One 4, e5946.

Ward, S., Thomson, N., White, J.G., Brenner, S., 1975. Electron microscopical reconstruction of the anterior sensory anatomy of the nematode Caenorhabditis elegans.?2UU. J Comp Neurol 160, 313-337.

Weatherspoon, J.K., Werling, L.L., 1999. Modulation of amphetamine-stimulated [3H]dopamine release from rat pheochromocytoma (PC12) cells by sigma type 2 receptors. J Pharmacol Exp Ther 289, 278-284.

Wei, Y., Williams, J.M., Dipace, C., Sung, U., Javitch, J.A., Galli, A., Saunders, C., 2007. Dopamine transporter activity mediates amphetamine-induced inhibition of Akt through a Ca2+/calmodulin-dependent kinase II-dependent mechanism. Mol Pharmacol 71, 835-842.

Weinshenker, D., Garriga, G., Thomas, J.H., 1995. Genetic and pharmacological analysis of neurotransmitters controlling egg laying in C. elegans. J Neurosci 15, 6975-6985.

Wheeler, D.S., Underhill, S.M., Stolz, D.B., Murdoch, G.H., Thiels, E., Romero, G., Amara, S.G., 2015. Amphetamine activates Rho GTPase signaling to mediate dopamine transporter internalization and acute behavioral effects of amphetamine. Proc Natl Acad Sci U S A.

White, J.G., Southgate, E., Thomson, J.N., Brenner, S., 1986. The structure of the nervous system of the nematode Caenorhabditis elegans. Philos Trans R Soc Lond B Biol Sci 314, 1-340.

Whitty, C.J., Paul, M.A., Bannon, M.J., 1997. Neurokinin receptor mRNA localization in human midbrain dopamine neurons. J Comp Neurol 382, 394-400.

Wintle, R.F., Van Tol, H.H., 2001. Dopamine signaling in Caenorhabditis elegans-potential for parkinsonism research. Parkinsonism Relat Disord 7, 177-183.

Wu, S., Bellve, K.D., Fogarty, K.E., Melikian, H.E., 2015a. Ack1 is a dopamine transporter endocytic brake that rescues a trafficking-dysregulated ADHD coding variant. Proc Natl Acad Sci U S A 112, 15480-15485.

Wu, S., Bellve, K.D., Fogarty, K.E., Melikian, H.E., 2015b. Ack1 is a dopamine transporter endocytic brake that rescues a trafficking-dysregulated ADHD coding variant. Proc Natl Acad Sci U S A.

Yang, S.W., Huang, H., Gao, C., Chen, L., Qi, S.T., Lin, F., Wang, J.X., Hou, Y., Xing, F.Q., Sun, Q.Y., 2013. The distribution and possible role of ERK8 in mouse oocyte meiotic maturation and early embryo cleavage. Microsc Microanal 19, 190-200.

Yu, H.S., Kim, S.H., Park, H.G., Kim, Y.S., Ahn, Y.M., 2011. Intracerebroventricular administration of ouabain, a Na/K-ATPase inhibitor, activates tyrosine hydroxylase through extracellular signal-regulated kinase in rat striatum. Neurochem Int 59, 779-786.

Zapata, A., Kivell, B., Han, Y., Javitch, J.A., Bolan, E.A., Kuraguntla, D., Jaligam, V., Oz, M., Jayanthi, L.D., Samuvel, D.J., Ramamoorthy, S., Shippenberg, T.S., 2007. Regulation of dopamine transporter function and cell surface expression by D3 dopamine receptors. J Biol Chem 282, 35842-35854.

Zhu, C., Hewlett, W., Feoktistov, I., Biaggioni, I., Blakely, R.D., 2004. Adenosine receptor, protein kinase G, and p38 mitogen-activated protein kinase-dependent up-regulation of serotonin transporters involves both transporter trafficking and activation. Mol Pharmacol 65, 1462-1474.

Zhu, C.B., Carneiro, A.M., Dostmann, W.R., Hewlett, W.A., Blakely, R.D., 2005. p38 MAPK activation elevates serotonin transport activity via a trafficking-independent, protein phosphatase 2A-dependent process. J Biol Chem 280, 15649-15658.

Zhu, S., Zhao, C., Wu, Y., Yang, Q., Shao, A., Wang, T., Wu, J., Yin, Y., Li, Y., Hou, J., Zhang, X., Zhou, G., Gu, X., Wang, X., Bustelo, X.R., Zhou, J., 2015. Identification of a Vav2-dependent mechanism for GDNF/Ret control of mesolimbic DAT trafficking. Nat Neurosci 18, 1084-1093.

Zhu, S.J., Kavanaugh, M.P., Sonders, M.S., Amara, S.G., Zahniser, N.R., 1997. Activation of protein kinase C inhibits uptake, currents and binding associated with the human dopamine transporter expressed in *Xenopus* oocytes. J. Pharmacol. Exp. Ther. 282, 1358-1365.